

AMERICAN UNIVERSITY OF BEIRUT

ANTITUMOR EFFECT AND NANOPARTICLE DEVELOPMENT
OF THE ADAMANTYL RETINOID ST1926 IN ACUTE MYELOID
LEUKEMIA

by
Leeanna Ali El-Houjeiri

A thesis
submitted in partial fulfillment of the requirements
for the degree of Master of Science
to the Department of Biochemistry and Molecular Genetics
of the Faculty of Medicine
at the American University of Beirut

Beirut, Lebanon
December 2015

AMERICAN UNIVERSITY OF BEIRUT

ANTITUMOR EFFECT AND NANOPARTICLE DEVELOPMENT
OF THE ADAMANTYL RETINOID ST1926 IN ACUTE MYELOID
LEUKEMIA


by
Leeanna Ali El-Houjeiri

Approved by:

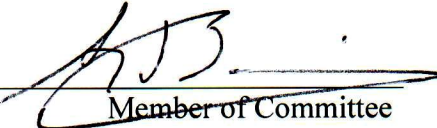
Dr. Nadine Darwiche, Professor
Department of Biochemistry and Molecular Genetics


Advisor


Dr. Hiba El-Hajj, Assistant Professor
Departments of Internal Medicine
and Experimental Pathology, Immunology, and Microbiology


Co-Advisor

Dr. Ayad Jaffa, Professor
Department of Biochemistry and Molecular Genetics


Member of Committee

Dr. Walid Saad, Assistant Professor
Department of Chemical Engineering


Member of Committee

Date of thesis defense: December 16, 2015

AMERICAN UNIVERSITY OF BEIRUT

THESIS, DISSERTATION, PROJECT RELEASE FORM

Student Name: El-Hayjiri Leanna Ali
Last First Middle

Master's Thesis

Master's Project

Doctoral Dissertation

I authorize the American University of Beirut to: (a) reproduce hard or electronic copies of my thesis, dissertation, or project; (b) include such copies in the archives and digital repositories of the University; and (c) make freely available such copies to third parties for research or educational purposes.

I authorize the American University of Beirut, **three years after the date of submitting my thesis, dissertation, or project**, to: (a) reproduce hard or electronic copies of it; (b) include such copies in the archives and digital repositories of the University; and (c) make freely available such copies to third parties for research or educational purposes.

Signature

Date

Leanna Hayjiri 25/1/2016

ACKNOWLEDGEMENTS

This thesis marks the end of a long and eventful journey for which there are many people that I would like to acknowledge for their support along the way. I apologize to all those not mentioned by name, your help and support is really appreciated.

First and foremost, I would like to express my deepest gratitude to my advisor Dr. Nadine Darwiche for her guidance, caring, patience, and especially for her confidence in me. I would like to thank her for providing me with an excellent atmosphere for conducting research. I attribute the level of my Master degree to her encouragement and effort where without her, this thesis would not have been completed. One simply could not wish for a better or friendlier advisor, she is by far a great inspiration and example to pursue.

I would also like to take this opportunity to express my profound gratitude and deep regard to my one and only co-advisor Dr. Hiba El Hajj, for her exemplary guidance, valuable feedback and constant encouragement throughout the duration of this project. Her valuable suggestions, perceptive criticism, and beautiful smile were of immense help throughout my project work. Working under her supervision was an extremely knowledgeable experience for me.

Besides my advisors, I would like to thank the rest of my thesis committee members: Prof. Ayad Jaffa and Dr. Walid Saad for taking the time to read my thesis and for their insightful feedback and encouragement.

I have to thank my parents for their love and support throughout my life. Thank you both for giving me strength and in believing me, for this and much more, I am forever in your debt. My sisters, Loubna and Lama and my brother Mohamad, you deserve my wholehearted gratitude as well.

Next, I need to thank all my fellow labmates who created such a good atmosphere in our Blue lab; Dr. Rana, Houda, Zainab S, Melody, Zaynab J, Berthe and Raed. A special thanks goes to my dearest friend and colleague Patrick Aouad for all the stimulating discussions, the sleepless nights we had working together before deadlines, and for all the fun we have had in the past 2 years.

I would also like to thank my colleague Nadim Tawil for his support and guidance throughout this project especially the *in vivo* part. Many thanks go to Martin Karam and Ali Jalloul for all their help and support. Thank you all and I wish you the best of luck in your future endeavors.

Lastly, I would like to thank my dearest friends Rola Hammoud and Zeina Azrak for always being there for me through thick and thin. Thank you for all your support, encouragement, and believing in me.

This thesis is only a beginning of my journey...

AN ABSTRACT OF THE THESIS OF

Leeanna El-Houjeiri for Master of Science
Major: Biochemistry

Title: Antitumor Effect and Nanoparticle Development of the Adamantyl Retinoid ST1926 in Acute Myeloid Leukemia

Acute myeloid leukemia (AML) is a clinically and genetically heterogeneous disorder of hematopoietic progenitor cells, which have lost their normal ability to differentiate. AML represents one of the most complex types of leukemias. Clinical treatment of AML subtypes is highly dependent on the patients' karyotype. Until today, there is no standard regimen to treat AML patients.

Retinoids regulate a wide range of biological processes, including development, differentiation, proliferation, and cell death, especially in hematopoietic cells. Differentiation therapy using the natural retinoid all-*trans* retinoic acid (ATRA) became the paradigm for the treatment of acute promyelocytic leukemia (APL), an AML subtype. However, in non-APL AML patients, ATRA is only effective on those presenting with *nucleophosmin-1* mutations, and was often linked with acquired resistance and disease relapse. Therefore, synthetic retinoids, specifically the adamantyl ST1926, emerged as potent anticancer agent. However, ST1926 development in clinic was limited due to its rapid glucuroconjugation resulting in low plasma concentrations. Nanomedicine has recently gained widespread attention, where it enables more efficient drug delivery, increasing stability, bioavailability, and reducing drug toxicity. Therefore, we aimed at investigating the antitumor effect of ST1926 using human non-APL AML *in vitro* models, developing nanoparticle formulations of the drug, and reproducing an AML xenograft mouse models for preclinical drug assessment.

We used representative human non-APL AML cell lines harboring different genetic mutations and representing several AML karyotypes. We showed that sub-micromolar concentrations of ST1926 inhibited the proliferation of all tested AML cell lines and primary AML patient cells in an irreversible manner. ST1926 induced apoptosis as evidenced by the accumulation of treated cells in the preG1 region of the cell cycle, Annexin V positivity, PARP cleavage, and mitochondrial membrane dissipation. Furthermore, ST1926 increased the expression levels of p53 and γ H2AX whilst decreasing that of retinoic acid receptors (RAR) α and RAR γ . Interestingly, the ST1926 antitumor effect was shown to be p53 and RAR independent but was reversed upon the addition of DNA damage inhibitors. Polymer stabilized ST1926 nanoparticles were developed using Flash NanoPrecipitation, and were shown to have comparable anti-growth activities to the naked drug *in vitro*.

In conclusion, our studies highlight the use of ST1926 and its nanoparticle formulation as promising anticancer drugs for further preclinical investigation in AML therapy.

CONTENTS

	Page
ACKNOWLEDGEMENTS.....	v
ABSTRACT.....	vi
LIST OF ILLUSTRATIONS.....	xi
TABLES.....	xiii
LIST OF ABBREVIATIONS.....	vii

Chapter

I. INTRODUCTION

A. Cancer: A General Background.....	1
B. Hematological Malignancies: Leukemia.....	3
1. Normal hematopoiesis to leukemia.....	4
2. Leukemia: Four major types.....	5
C. Acute Myeloid Leukemia.....	6
1. An overview.....	6
2. Diagnostic tools.....	7
3. Prognosis.....	9
4. Frontline treatment options and consequences.....	10
D. Retinoids.....	12
1. An overview.....	12
2. ATRA in leukemia.....	13
3. Drawbacks of ATRA in cancer therapy.....	14
E. Retinoid Related Molecules.....	15
1. An overview.....	15

2. The adymental retinoid ST1926	16
F. ST1926 in APL	17
G. Optimizing ST1926 Drug Formulations: Nanoparticle-Based Systems	18
1. Nanotechnology: An overview	18
2. Nanomedicine	18
3. Nanomedicine in cancer applications	19
4. Retinoids in cancer nanomedicine	20
5. Flash Nanoprecipitation	21
H. Xenograft Models: Preclinical assessment of anticancer drug development	22
I. Aim of the Study	24

II. MATERIALS AND METHODS

A. AML Cell Lines Characterization	25
B. Cell Culture	28
C. ST1926 and ATRA Preparation	29
D. Cell Growth Assay	29
E. Cell Viability Assay	30
F. Microscopic Imaging	30
G. Drug Reversibility Assay	30
H. Caffeine Preparation and Treatment	31
I. Pan-RAR Inverse Agonist BMS493 Preparation and Treatment	31
J. Cell Cycle Analysis	32
K. Annexin V/PI Assay	33
L. Mitochondrial Membrane Dissipation Assay	34

M. Western Blotting	35
N. Nanoparticle Formulation	36
O. Dynamic Light Scattering	37
P. Generation of the AML Xenografted Mouse Model	37
Q. Statistical Analysis	38

III. RESULTS

A. ST1926 inhibits the proliferation of AML cells at sub-micromolar concentration as evident by the MTT proliferation assay	39
B. ST1926 inhibits the viability of AML cell lines and primary patient cells at sub-micromolar concentration as evident by trypan blue exclusion assay	44
C. ST1926-induced growth-inhibitory effect on AML cells is irreversible.....	44
D. ST1926 induces the accumulation of treated AML cells in the pre-G ₁ region of the cell cycle as assessed by PI-based flow cytometric analysis	46
E. ST1926 induces apoptosis in AML cells.....	47
1. Effect of ST1926 on AML cell morphology and confluence	50
2. ST1926 induces early apoptosis in AML cells as evident by the Annexin V/PI.....	51
3. ST1926 treatment of AML cells results in loss of mitochondrial membrane potential as assessed by Rhodamine-123 efflux.....	55
4. ST1926 induces PARP cleavage in AML-treated cells.....	58
5. ST1926 treatment in AML cells increases total p53 protein levels.....	59
6. ST1926 treatment of AML cells induces early accumulation of γ H ₂ AX, an indication of DNA damage.....	60

F. ST1926 induced growth-inhibitory effect on AML cells is reversed by the DNA damage inhibitor Caffeine	61
G. ST1926 treatment of AML cells results in RAR γ and RXR α downregulation	61
H. ST1926 growth-inhibitory effect is independent of the RAR signaling pathways	63
I. ST1926 at sub-micromolar concentrations re-sensitizes ATRA-resistant THP-1 cells to ATRA	66
J. Nanoparticle formulation of ST1926	69
K. ST1926- exhibited similar growth-inhibitory effect in AML cells as its nanoparticle formulation	70
L. Generation of AML xenograft mouse model	72
IV. DISCUSSION	74
REFERENCES	84

ILLUSTRATIONS

Figure	Page
1. Hallmarks of cancer.....	3
2. Formation of blood cells from a pluripotent stem cell.....	5
3. Cytogenetic risk groups and molecular abnormalities in AML.....	10
4. AML treatments in development.....	11
5. Chemical structure of ATRA.....	13
6. Chemical structures of the RRM: CD347 and ST1926.....	16
7. Schematic presentation of the EPR effect.....	20
8. Flash Nanoprecipitation Technique.....	22
9. Schematic demonstration of Annexin V/PI assay.....	35
10. Effect of ST1926 on the proliferation of AML cells.....	40
11. Effect of ST1926 on the viability of AML cells.....	42
12. Effect of ST1926 on the viability of patient cells.....	43
13. Irreversible effect of ST1926 on AML cell growth.....	45
14. Effect of ST1926 on different cell cycle phases.....	48
15. Representative histograms of the cell cycle distribution and progression in ST1926 treated AML cells.....	49
16. Effect of ST1926 on the morphology of AML cells in culture.....	50
17. Annexin V/PI compensation controls.....	52
18. Early apoptosis induction in ST1926 treated THP-1 cells as evident by the Annexin V FITC-positivity.....	53
19. Early apoptosis induction in ST1926 treated- MOLM-13 cells as evident by the Annexin V FITC positivity.....	54
20. The percentage change in the mitochondrial membrane dissipation in	

ST1926-treated AML cells.....	56
21. Loss of the mitochondrial membrane potential after ST1926 treatment of AML cells.....	57
22. Induction of PARP cleavage after ST1926 treatment in AML cells.....	58
23. Increase of total p53 protein levels after ST1926 treatment of AML cells.....	60
24. Early accumulation of γ H2AX following ST1926 treatment of AML cells.....	61
25. ST1926-induced growth inhibition in AML cells is reversed upon the abrogation of DNA damage.....	62
26. RAR γ and RXR α downregulation following ST1926 treatment of AML cells.....	63
27. ST1926-induced growth inhibition effect is independent of the retinoid receptor signaling pathway.....	65
28. ATRA-induced growth inhibition in the C8166 is reversed by the pan-RAR inverse agonist BMS493.....	66
29. ST1926 at sub-micromolar concentrations re-sensitizes ATRA-resistant AML cells.....	68
30. Intensity-based particle size distribution of the formulated ST1926 nanoparticles.....	70
31. Effect of ST1926 and its nanoparticle formulation on the proliferation of AML cells using MTT assay.....	71
32. Survival graph of the generated AML xenografted mouse models.....	73

TABLES

Table	Page
1. The French-American-British (FAB) classification of AML.....	8
2. WHO classification of acute myeloid leukemia	8
3. Summarized description of the AML cell lines used	27

ABBREVIATIONS

ATRA	all- <i>trans</i> retinoic acid
APL	acute promyelocytic leukemia
ATL	adult T-cell leukemia/lymphoma
AML	acute myeloid leukemia
ALL	acute lymphoblastic leukemia
BM	bone marrow
9c-RA	9- <i>cis</i> retinoic acid
CD437	6-[3-(1-adamantyl)-4-hydroxyphenyl] -2-naphthalene carboxylic acid
CML	chronic myeloid leukemia
CLL	chronic lymphoblastic leukemia
CR	complete remission
CSC	cancer stem cell
HSC	hematopoietic stem cell
DMSO	dimethylsulfoxide
DNA	deoxyribonucleic acid
DSB	double-strand breaks
EDTA	ethylene-diamineteraacetic acid
EPR	enhanced permeability and retention
FAB	French-American-British
FBS	fetal bovine serum

FDA	US Food and Drug Administration
FNP	Flash NanoPrecipitation
FLT-3	FMS-like tyrosine kinase-3
GAPDH	glyceraldehyde-3-phosphate dehydrogenase
h	hour
ITD	internal tandem duplication
IRB	Institutional Review Board
JNK	Jun N-terminal kinase
K	cytokeratin
LSC	leukemic stem cells
μM	micromolar
MAP	mitogen-activated protein
MDS	myelodysplastic syndromes
min	minute
MPD	myeloproliferative disorders
MLL	Mixed-lineage leukemia
NP	nanoparticle
NPM-1	nucleophosmin-1
OD	optical density
PAGE	polyacrylamide gel electrophoresis
PARP	Poly (ADP-ribose) polymerase
PBS	phosphate-buffered saline
PI	propidium iodide

PML-RAR α	promyelocytic leukemia-retinoic acid receptor alpha
RA	retinoic acid
RAR	retinoic acid receptor
RARE	retinoic acid response element
RXR	retinoid X receptor
SCID	Severe combined immunodeficiency
SD	standard deviation
SDS	sodium dodecyl sulfate
SEM	standard error of the mean
ST1926	E-4-(4'-hydroxy-3'-adamantyl biphenyl-4-yl) acrylic acid
USA	United States of America
WHO	World Health Organization

CHAPTER I

INTRODUCTION

A. Cancer: A General Background

Cancer is a leading cause of death in the Western world and accounts for a quarter of all mortalities, where it is expected to surpass cardiovascular diseases as the leading cause of death in the next few years (Siegel 2015). According to the United States of America (USA) National Cancer Institute, the National Program of Cancer Registries, and the North American Association of Central Cancer Registries, cancer is currently considered as a major health problem in the world where a total of 1,658,370 new cancer cases and 589,430 cancer deaths are projected to occur in 2015 (Siegel 2015). Nevertheless, cancer death rates have been continuously declining over the past two decades where the risk of dying from cancer has decreased by 22% between 1991 and 2011 (Siegel 2015). For this reason, cancer research is one of the largest and fastest developing and, thus, best-funded area of the biomedical sciences (DeSantis 2011).

Cancer is a class of more than 200 diseases characterized by several complex and interrelated traits that govern the transformation of normal cells into abnormal cancerous ones. These traits or “hallmarks” have been clearly briefed by Hanahan and Weinberg 15 years ago, and they constitute essential multistep alterations in the cell physiology that ultimately render normal cells cancerous (Hanahan 2000). The hallmarks include; maintaining the proliferative capacity through self-sufficiency in cellular growth, insensitivity to anti-growth signals, evading growth suppressors, resisting cell death, limitless replicative potential, induction of angiogenesis, and activation of tissue invasion and metastasis signals. Recently, two additional hallmarks have

been added to list that include reprogramming of energy metabolism and evading immune destruction (Figure 1) (Hanahan 2011).

Cancer cells are characterized by genetic instability that involves a series of mutations, where the first mutation that occurs provides a selective growth advantage to the cell. The developing tumor then acquires mutations in oncogenes (genes that normally help cells grow), or tumor suppressors (genes that halt cell division, repair DNA damage, and induce apoptosis) and/or stability genes (genes that control the rate of mutations), all of which contribute to the tumor progression as well as the development of the resistance to chemotherapeutic drugs. In the last two decades, many genes responsible for the genesis of various cancers have been discovered, their mutations precisely identified, and the pathways through which they act characterized (Vogelstein 2004).

In addition to the genetic alterations, recent advancements in the rapidly evolving field of cancer epigenetics have shown extensive reprogramming of several components of the epigenetic machinery in cancer including DNA methylation, nucleosome positioning, histone modifications, non-coding RNAs, and microRNA expression (Sharma 2010). Cancer may, therefore, be considered a multifactorial disease, resulting from the combined influence of many genetic and epigenetic factors, acting in concert along with several environmental insults (ultraviolet radiation, pollution, smoking, and viruses) (Vogelstein 2013).



Figure 1. Hallmarks of cancer. Adapted from: Hanahan 2011. The hallmarks of cancer. *Cell* 144: 646 - 674.

B. Hematological Malignancies: Leukemia

One group of cancers that usually begins in the bone marrow and results in a high number of white blood cells is called “leukemia” (formed from the two Greek words leukos, meaning "white", and haima, meaning "blood"). Leukemia is the leading cause of cancer death in those aged younger than 40 years (Seigel 2015). In females, it is the leading cause of cancer death in children and adolescents (Seigel 2014). Currently, the average five-year survival rate of leukemia patients is 59% in the USA, and more dramatically, it ranges in children between 60 to 85%, depending on the type of leukemia (Seigel 2015).

1. Normal hematopoiesis to leukemia

Hematopoiesis is a highly orchestrated process of blood cell production that maintains homeostasis by producing billions of red blood cells, white blood cells, and platelets on daily basis (Smith 2003) (Figure 2). The blood components proliferate and differentiate from multipotent hematopoietic stem cells (HSCs); which represent a small population of long-lived, quiescent, and undifferentiated cells characterized by the capacity of self-renewal, high proliferative potential, and the ability of multilineage differentiation into all blood cell types (Huang 2007). On average, a healthy adult person produces 10^{11} to 10^{12} new blood cells daily in order to maintain steady state levels in the peripheral circulation (Smith 2003). Understanding of the normal hierarchical path for an undifferentiated HSC to a fully differentiated and committed progenitor cell is a prerequisite to gain insight to cancer development. HSCs initially differentiate into myeloid and lymphoid progenitor cells; wherein the latter differentiate into natural killer cells and lymphocytes (B and T cells). Myeloid progenitors differentiate into four different cell classes: erythrocytes, mast cells, megakaryocytes, and myeloblasts. Myeloblasts in turn differentiate into basophils, neutrophils, eosinophils, and monocytes. Such process is a highly controlled and regulated process where any dysregulation may result in an excess or a lack of certain blood cell types, leading to immune system disorders, anemia, coagulopathy, or cancer (Griseri 2012).

One hallmark of cancer is the unlimited self-renewal capacity, which is also a characteristic of normal stem cells. Given that, it has been proposed that leukemia may be initiated by multiple transforming events at the level of HSCs or at the level of more committed progenitors, caused by mutations or selective expressions of genes that enhance their limited self-renewal abilities (Horton 2012).

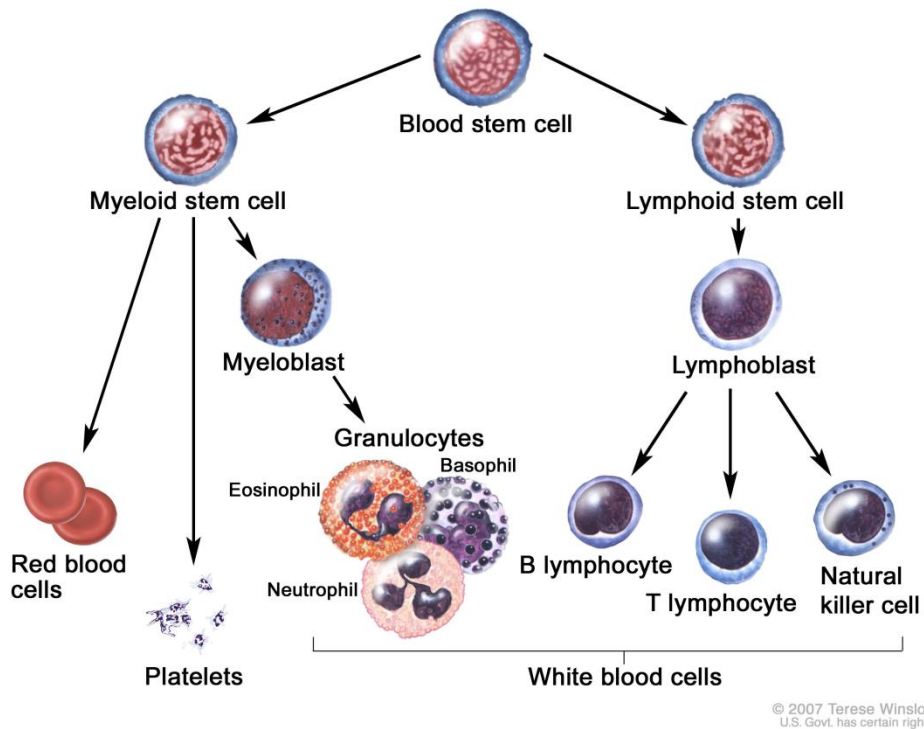


Figure 2. Formation of blood cells from a pluripotent stem cell. Adapted from *Terese Winslow*, USA. Govt. 2008

2. *Leukemia: Four major types*

There are over a dozen different types of leukemia that vary significantly in terms of their morphological, cytogenic, immunophenotypic, and molecular features (Bain 2010). These features reflect the differences in the biological alterations that occur during the malignant process, or the stage of the HSCs where the transformation occurs. Nevertheless, clinically and pathologically, leukemia can be divided into either acute or chronic forms. Acute leukemia is characterized by a rapid increase in the number of immature hematopoietic cells and can overrun the body within a few weeks or months. By contrast, chronic leukemia is slow growing and progressively worsens over years, where the affected blood cells are relatively mature but still abnormal. Furthermore, leukemia is also classified according to the cell type, where it can be

subdivided into lymphoblastic or myeloid types. In lymphoblastic forms, the cancerous change takes place in the infection-fighting immune cells (B and T cells), however, in the myeloid forms such change occurs in the types of cells that normally form red blood cells, some other types of white blood cells, and platelets. Combining these two classifications provides a total of four main categories: chronic lymphoblastic leukemia (CLL), acute lymphoblastic leukemia (ALL), chronic myeloid leukemia (CML), and acute myeloid leukemia (AML). In this study, we focused our research on AML.

C. Acute Myeloid Leukemia

1. An overview

AML represents 10-15% of leukemias diagnosed in childhood and is the most common type of acute leukemia diagnosed in adults (Hoffbrand 2011). The American Cancer Society estimates that 20,830 new cases of AML (12,730 in men, 8100 in women) are expected to occur in the USA in 2015, accounting for 32% of all leukemia cases in adults who are 20 years of age and older (Smith 2015).

AML is the most frequent hematological malignancy in adults with a median age of presentation in the late 60s. AML accounts for 30% of leukemias and 44% of leukemia-related deaths (Jemal 2010). It is a clinically and genetically heterogeneous clonal disorder of hematopoietic progenitor cells (Nakanishi 1999), which lost the ability to differentiate normally and to respond to normal proliferation regulators (Lowenberg 1999). It is characterized by a significant increase in the number of myeloid cells in the bone marrow and an arrest in their maturation, commonly resulting in hematopoietic insufficiency (granulocytopenia, thrombocytopenia, or anemia) (McPherson 2011).

2. *Diagnostic tools*

The diagnostic procedures used to classify AML include: morphologic assessment of bone marrow specimens and blood smears, identification of chromosomal findings by means of conventional cytogenetic testing analysis of the expression of cell surface or cytoplasmic markers by flow cytometry, and more recently, screening for selected molecular genetic lesions (Döhner 2015).

The diversity and heterogeneity of AML is due to the fact that leukemic transformation can occur at different steps along the myeloid cell differentiation pathway. Hence, many systems have been used to classify AML into its subtypes: the French-American-British (FAB) classification (Bennett 1976) and the more recent World Health Organization (WHO) classification (Vardiman 2002). FAB system divides AML into subtypes M0 through M7, solely based upon the morphology of cells from which the leukemia developed and the extent of cell maturation (Table 1). However, the WHO published a newer system where the classification of different AML subtypes includes morphology, cytogenetics, molecular genetics and immunologic markers, and such classification is more universally applicable and valid in terms of prognosis (Jaffe 2001) (Table 2).

Table 1. The French-American-British (FAB) classification of AML

FAB Subtype	Name	Adult AML patient (%)
M0	Undifferentiated acute myeloblastic leukemia	5
M1	Acute myeloblastic leukemia with minimal maturation	15
M2	Acute myeloblastic leukemia with maturation	25
M3	Acute promyelocytic leukemia	10
M4	Acute myelomonocytic leukemia	20
M4eos	Acute myelomonocytic leukemia with eosinophilia	5
M5	Acute monocytic leukemia	10
M6	Acute erythroid leukemia	5
M7	Acute megakaryocytic leukemia	5

Table 2. WHO classification of acute myeloid leukemia

AML with recurrent genetic abnormalities	<ul style="list-style-type: none"> • AML with t(8;21)(q22;q22) • AML with abnormal BM* eosinophils and inv(16)(p13q22) or t(16;16)(p13;q22) • Acute promyelocytic leukemia with t(15;17)(q22;q12), (PML-RARα)* and variants • AML with 11q23 (MLL)* abnormalities
AML with multilineage dysplasia	<ul style="list-style-type: none"> • Following MDS* or MDS/MPD* • Without antecedent MDS or MDS/MPD, but with dysplasia in at least 50% of the cells
AML and MDS, therapy related	<ul style="list-style-type: none"> • Alkylating agent/radiation-related type • Topoisomerase II inhibitor-related type • Others
AML, not otherwise categorized	<ul style="list-style-type: none"> • AML minimally differentiated • AML without maturation • AML with maturation • Acute myelomonocytic leukemia • Acute monoblastic leukemia • Acute erythroid leukemia • Acute basophilic leukemia • Myeloid sarcoma • Acute panmyelosis

*BM: Bone marrow; MDS: Myelodysplastic syndromes; MPD: Myeloproliferative disorders; PML-RAR α : promyelocytic leukemia-retinoic acid receptor alpha; MLL: Mixed-lineage leukemia

3. Prognosis

Prognostic factors can be subdivided into categories that are either related to the patient or the disease. Patient-associated factors include; increasing age, coexisting conditions, and poor performance status, and they commonly predict treatment-related early death. Disease related factors include the white cell count, leukemic cell genetic changes, and prior myelodysplastic syndrome or cytotoxic therapy for another disorder. These factors predict resistance to current standard therapy (Döhner 2015).

In addition to the classifications listed above, evaluation of the molecular genetic lesions in the patients allows the segregation of patients with AML into three broad categories or risk groups of: favorable, intermediate, and unfavorable with very different cure rates (Martens 2010) (Figure 3). In fact, more than half of AML patients have abnormal karyotype and this can be highly predictive of their treatment response. Approximately 25% of patients have favorable cytogenetics, where the mutations include $t(15; 17)(q22;q21)$, $inv(16)$, $t(16;16)$, and $t(8;21)(q22;q22)$. These patients have a 65-80% five-year disease free survival. Around 10% of patients have adverse cytogenetics that include $(-7;-5-5q)$, abnormalities of 3q or a complex karyotype. These patients have a 10-20% five-year survival. The remaining patients have intermediate risk cytogenetics, many of them with a normal karyotype, and their prognosis is determined by specific genetic alterations particularly *NPM-1* mutation and *FMS-like tyrosine kinase-3 (FLT-3)* internal tandem duplication (ITD) (Martelli 2013). These patients have a 30 to 40% five-year survival.

ITD mutations of *FLT-3* have been found in 15-30% of cases of AML. Such mutations result in dimerization and constitutive activation of the tyrosine kinase receptor leading to abnormal downstream activation of signaling pathways of cell proliferation and survival (Yokota 1997).

Subgroup	Cytogenetics	Molecular genetics
Favorable	t(15;17)(q22;q21)	<i>PML-RARA</i>
	t(8;21)(q22;q22)	<i>RUNX1-RUNX1T1</i>
	inv(16)(p13.1q22) or t(16;16)(p13.1;q22)	<i>CBFB-MYH11</i>
	Normal karyotype	Mutated <i>NPM1</i> without <i>FLT3</i> -ITD
	Normal karyotype	Mutated <i>CEBPA</i>
Intermediate-1	Other normal karyotypes	
Intermediate-2	t(9;11)(p22;q23)	<i>MLL3-MLL</i>
	Other non-adverse non-favorable abns.	
Adverse	t(6;9)(p23;q34)	<i>DEK-NUP214</i>
	inv(3)(q21q26.2) or t(3;3)(q21;q26.2)	<i>RPN1-EVI1</i>
	t(v;11q23)	<i>MLL</i> rearranged
	-5, del(5q), -7	
	17p abns.	
	Complex karyotype (3+ abns.)	

Figure 3. Cytogenetic risk groups and molecular abnormalities in AML.

Taken from: Döhner, H 2010. Diagnosis and management of acute myeloid leukemia in adults. *Blood*, 115(3), 453-474.

4. Frontline AML treatment options and consequences

Even though multiple efforts have been put towards characterizing AML and identifying the most common mutations it possesses, its treatment can still be challenging as it varies according to the age, health of the patient, and to the specific subtype of AML (Grimwad 1998; Slovak 2000). Current induction chemotherapy regimens employing a backbone of cytarabine combined with an anthracycline have remained largely unchanged since 1973 (Burnett 2011). In patients with normal diploid karyotype, *NPM-1* mutation, when present in the absence of *FLT3*-ITD, confers a major survival advantage and lower risk of relapse (Schnittger 2005; Verhaak 2005; Thiede 2006). In general, the standard treatment of AML is commonly referred to as “7+3”,

where all FAB subtypes except M3 are given 7 days of standard-dose cytarabine and 3 days of anthracycline (Venditti 2000). The goal of such treatment is to reach complete remission (CR) and lower the risk of disease resistance through drug combination therapy. To prevent disease recurrence, such treatment is often consolidated with repetition or intensification chemotherapy with additional drugs. These Drugs include nucleoside analogues, FLT3 inhibitors, demethylating agents, and others (Figure 4). Consequently, it has been reported that approximately 70 to 80% of patients < 60 years of age will achieve CR rate, however, they will ultimately relapse with treatment-resistant disease with an overall five-year survival rate of 40 to 45% (Fernandez 2009; Mandelli 2009). Survival is worse among patients > 60 years of age, where 40 to 50% can achieve CR, and the cure rates are 10% with a median survival of only one year (Burnett 2010). This relatively poor outcome emphasizes a perceived lack of progress in the standard treatment of AML and calls for more research and newer, more potent or targeted therapies.

Parameter	Treatment
Nucleoside analogues	Clofarabine, sapacytibine, elacytarabine
FLT3 inhibitors	Midostaurin, leustaurinib, sorafenib, AC220
Antibody based	Gemtuzumab ozogamicin, CLS123
Demethylation agents	Azacitidine, decitabine
Other agents	Aurora kinase inhibitor/Aminopeptidase inhibitor Tosedostat/mTOR inhibitor voreloxin/amonofide/ceplene

Abbreviations: *FLT3*, *FMS*-like tyrosine kinase 3; mTOR, mammalian target of rapamycin.

Figure 4. AML treatments in development. Reviewed in: Burnett 2011. Attempts to optimize induction and consolidation treatment in acute myeloid leukemia. *Journal of clinical Oncology*, 28(4), 586-595.

D. Retinoids

I. An overview

Retinoids are a family of molecules comprising both natural and synthetic analogues of vitamin A (retinol). These compounds regulate a wide range of biological processes, including development, differentiation, proliferation, and apoptosis (Lippman 2000; Tang 2011). In addition, retinoids regulate the growth and differentiation of various types of tumor cells (Lee 2000; Freemantle 2003; Collins 2008). Importantly, natural retinoids control HSC development and help regulate granulocytic differentiation (Chanda 2013). Retinoids mediate their effects by binding and activating one or more of the closely related retinoic acid receptors (RAR α , β , and γ) that function as ligand-dependent transcriptional regulators (Asson-Batres 2014). These receptors form heterodimers with retinoid x receptors (RXR α , β , and γ) and bind to retinoic acid responsive response elements (RAREs) located in the promoter region of retinoid target genes to stimulate gene transcription in coordination with coactivators and/or corepressors. In the absence of retinoids, RARs repress their target genes through recruiting co-repressors that may result in histone deacetylation, chromatin compaction, and gene silencing (Altucci 2001).

All-*trans* retinoic acid (ATRA) (Figure 5) and 9-*cis* retinoic acid (9-c RA) are two biologically active stereoisomers of RA that bind to RARs with high affinity (Germain 2006, Tang 2011, di Masi 2015). Similar to other nuclear receptors, ATRA was also shown to function *via* non-genomic pathways independent of the classical mechanism of nuclear receptor action where it can effectively modulate the activities of proteins involved in signal transduction in a manner that is highly cell type specific (Tanoury 2013).

ATRA has been used widely as an anticancer drug, where it was shown to block proliferation and induce differentiation in several types of tumor cells including various

leukemias, lymphomas, colon, ovarian, breast, lung, skin and prostate (Fontana 2002; Maeda 2008; Lee 2000; Alizadeh 2014; di Masi 2015).

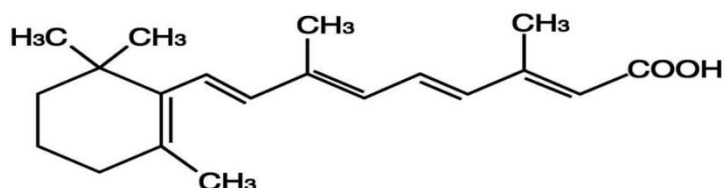


Figure 5. Chemical structure of ATRA

2. ATRA in leukemia

The ability of retinoids to regulate normal hematopoietic differentiation has made them powerful and promising agents in the treatment of several leukemias and lymphomas (Collins 2002).

ATRA alone or in combination with other drugs is established as the primary treatment of choice for patients suffering from acute promyelocytic leukemia (APL), an AML M3 subtype (de Thé 2010). APL is characterized by t(15;17) which results in a chimeric promyelocytic leukemia/retinoic acid receptor-alpha (PML-RAR α) fusion protein being formed (di Masi 2015). ATRA specifically induces promyelocytes with t(15;17) to differentiate into mature granulocytes *in vitro* and *in vivo* with CR obtained in more than 90% of APL patients treated with ATRA alone (Cassinat 2001; Fenaux 2001).

Arsenic alone or combined to other agents is emerging as an efficient treatment against leukemia. In APL, ATRA/arsenic combination treatment induces degradation of PML/RAR α through distinct pathways. Their combination cures APL in mice (Ablain 2014; Lallemand-

Breitenbach 1999; Nasr 2008) and patients (Lo-Coco 2013; Ravandi 2009; Shen 2004). In more details, ATRA/arsenic synergizes to clear leukemia stem cells LSCs through cooperative PML-RAR α degradation (Nasr 2008) with retinoic acid targeting the RAR α moiety and arsenic targeting the PML moiety.

In AML patients, some studies suggested that addition of ATRA to conventional chemotherapy improves survival, selectively in AML patients with *NPM-1* mutation (Schlenk 2009). More recent studies have demonstrated that arsenic and RA synergistically induced proteasome-mediated degradation of mutant NPM-1, resulting in differentiation, growth arrest and apoptosis, selectively in *NPM-1* mutant AML cells (El Hajj 2015; Martelli 2015). The ATRA/arsenic combination significantly reduced leukemic blasts in BM of *NPM-1*-mutant AML patients and restored nucleolar localization of NPM-1 and PML NBs both *ex vivo* and *in vivo* (El Hajj 2015).

In adult T-cell leukemia (ATL), ATRA induced growth inhibition in several human T-lymphotropic virus (HTLV)-1-positive cell lines (Miyatake 1997), but resistance was observed in others (Darwiche 2004, Dawiche 2011). In addition, treatment of ATRA in several patients showed different responses where some of them developed resistance (Maeda 1996). ATRA was also evaluated in 20 ATL patients and showed partial response in 40% of them (Maeda 2008).

3. Drawbacks of ATRA in cancer therapy

Non-APL AML types respond poorly to ATRA and this is because the target genes that are important to the ATRA-driven differentiation pathway are not properly transcriptionally activated. It has been widely accepted that effective differentiation of APL cells by ATRA is only observed in cells that harbor the PML-RAR α oncogene (PML-RAR α) (Cassinat 2001).

Furthermore, the clinical usage of ATRA in many cancers including APL was linked to toxic secondary effects known as RA syndrome (Frankel 1992) and alterations in the retinoid receptor signaling pathway leading to resistance to cell death, and ultimate disease relapse (De The 1996; Darwiche 1996; di Masi 2015). Such drawbacks in ATRA treatment of AML emphasize the interest of identification of novel strategies to facilitate cancerous cells to undergo cell death with increased specificity and decreased toxicity.

E. Retinoid Related Molecules

1. An overview

Among novel apoptosis-based approaches, atypical retinoids, also known as retinoid-related molecules, exhibit significant potential as therapeutic agents in tumor treatment (Fontana 2002; Yim 2014). Out of the tested atypical retinoids, CD437 ([3-(1-adamantyl)-4-hydroxyl phenyl]-2-naphthalene carboxylic acid) (Fontana, 2000) (Figure 6A) and its analogue ST1926 (E-3-(4'-hydroxy-3'-adamantylbiphenyl-4-yl) acrylic acid) (Cincinelli 2003) (Figure 6B), were shown to be potent inducers of apoptosis with promising potential in antitumor therapy that show no cross resistance with other chemotherapeutics (Cincinelli 2003).

CD437 exerts its effects through retinoid receptor-dependent and -independent pathways inducing apoptosis and tumor growth arrest (Parrella 2006). It binds selectively to RAR β and RAR γ , and minimally to RAR α (Bernard 1992; Dawson 1998). CD437-induced apoptosis activates Jun N-terminal kinase (JNK), which is required for maximal induction of apoptosis and membrane depolarization (Bushue 2010). Furthermore, CD437 was shown to induce cell cycle arrest at different stages of the tumor development depending on the cancer cell type (Zhang 2000).

2. The adamantyl retinoid ST1926

Despite the promising anti-neoplastic properties that CD437 held in different tumor types, it showed to have a narrow window between its therapeutic and toxic doses with relatively low pharmacokinetic profile. Hence, ST1926, a more specific, stable, and less toxic analogue to CD437, was synthesized (Cincinelli 2003; Garattini 2004; Parella 2006). ST1926 can be administered orally and was shown to be effective against several solid and hematological tumor cells that are resistant to ATRA (Cincinelli 2003; Garattini 2004; El Hajj 2014; Nasr 2015; Basma 2015). ST1926 biodistribution in mouse was found to be favorable, as micromolar (μM) concentrations of the compound were achievable in the plasma of mice, with a significant extravascular distribution of the compound (Basma 2015). Moreover, ST1926 was effective *in vivo* in several leukemia models including; APL (Garattini 2004), in ATL SCID mouse models (El Hajj 2014), and in a bone marrow retroviral transduction/transplantation model of CML (Nasr 2015).

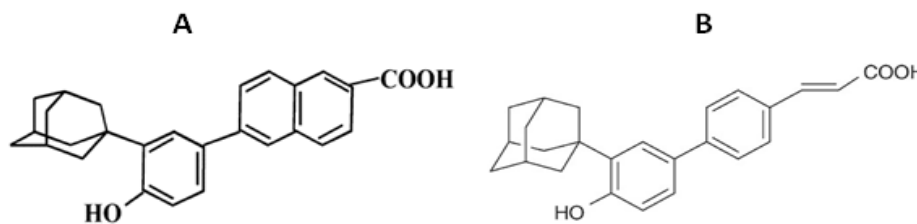


Figure 6. Chemical structures of the retinoid related molecules: CD347 (A) and ST1926 (B).

F. ST1926 in APL

In AML cells, namely the APL subtype, ST1926 was found to be able to trans-activate RAR γ , to induce the phosphorylation of p38 and JNK, and to down-regulate the expression of many genes necessary for tumor progression (Garattini 2004). Moreover, it was shown to cause an immediate increase in the cytosolic level of calcium that is directly related to apoptosis (Garattini 2004). Interestingly, ST1926 was shown to mediate its mechanism of action independent of the retinoid receptor pathway (Valli 2008). Additionally, ST1926 induces phase-specific DNA double-strand breaks (DSB) and cell death through mitochondrial pathways of apoptosis, with maximal DSB occurring during the S-phase of the cell cycle (Valli 2008). Remarkably, a concentration of ST1926 (0.1 μ M) caused a delay in the growth of APL cell lines with almost pure cytostatic effect. Mechanistically, histone H2A.Z was identified as a protein capable of specifically binding to ST1926 (Fratelli 2013).

Despite the success of ST1926 in several cancer models, there are some drawbacks of the drug that limits its development in clinical trials (Sala 2009). Solubility and bioavailability problems are both major reasons for many drug candidates to fail in preclinical development, and appropriate measures need to be taken to address these issues. ST1926 is a highly hydrophobic drug that was found to undergo major glucuro-conjugation leading to its poor bioavailability and rapid excretion by the liver (Sala 2009). Despite all the efforts in synthesizing derivatives of ST1926 that do not get glucuronidated, they all appeared to revert fast and act as prodrugs of their parent molecule (Giannini 2012).

Recently, nanotechnology and nanomedicine have proven to be a promising alternative, with several drug-loaded nanocarriers approved to be used in clinic (Chow 2012).

G. Optimizing ST1926 Drug Formulations: Nanoparticle-Based Systems

1. Nanotechnology: An overview

Nanotechnology is defined as the engineering and manufacturing of materials at the atomic and molecular scale (Drexler 1987). The National Nanotechnology Initiative refers to nanotechnology as structures roughly in the 1-100 nm size window in at least one dimension (Roco 2007). Despite this size restriction, nanotechnology commonly passes for structures that are up to several hundred nanometers in size and that are developed by top-down or bottom-up engineering of individual components. Currently, nanotechnology is emerging as a powerful tool in various fields of medicine, including cardiology, immunology, ophthalmology, oncology, endocrinology, and in highly specialized areas such as gene delivery, brain targeting and oral vaccine formulation (Svenson 2012).

2. Nanomedicine

Using nanotechnology in medicine has several advantages as it is widely expected to change the landscape of pharmaceutical and biotechnology industries in the foreseeable future (Bhattacharyya 2009; Malakar 2012; Lamba 2006; Svenson 2012). These advantages include; improving the delivery of water-insoluble drugs, targeting drugs to specific cells or tissues, overpassing the tight epithelial and endothelial barrier that hinders the efficient delivery of most drugs, carrying large macromolecules to specific intracellular site of action, co-delivering two or more drugs which is applicable for combination therapy, visualizing the drug's body circulation and site of delivery when combined with several imaging modalities, and a real-time analysis on the *in vivo* efficacy of the drugs (Ferrari 2005).

3. *Nanomedicine in cancer applications*

In cancer applications, as tumors reach 150–200 μm in size, they start developing their own blood supply and become dependent on neovasculature for their nutritional and oxygen demand (Folkman 1990). These newly formed and poorly aligned tumor vessels are usually abnormal in form and architecture, with wide fenestrations lacking a smooth muscle layer and an effective lymphatic drainage (Pepper 2001; Padera 2002). All these factors lead to the enhanced permeability and retention (EPR) effect, which promotes the selective accumulation of nanosize agents in tumor tissues (Torchilin 2012) (Figure 7). This is referred to as passive targeting of nanodrugs into the desired tumor and can occur without any specific ligand being attached to the surface of the nanocarrier.

Nanomedicine has been applied in several cancer applications where the FDA has approved some, and some are still undergoing clinical trials. Doxil (doxorubicin hydrochloride liposome injection, Orthobiotech) was the first FDA approved nanodrug used to treat metastatic ovarian cancer and Kaposi's sarcoma, where it improved the balance between the efficacy and the toxicity of the treatment (Barenholz 2012). In addition to that, the well-known paclitaxel (Taxol, Bristol-Myers Squibb) was formulated into nanoparticles, where it resulted in enhanced cytotoxicity *in vitro* and enhanced therapeutic efficacy *in vivo* (Jong 2008). Interestingly, the albumin bound nanoparticle formulation of paclitaxel, Abraxane (Bioscience, Astra), is currently approved in the clinic against metastatic breast, pancreatic, and non-small cell lung cancer (Langer 2007; Walker 2013). In adenocarcinomas, the nanoparticle formulations of Lipoplatin (Regulon) significantly lowered its free drug's side effects and currently it is in phase III clinical trials. Formulating ThermoDox (Celsion) in nanoparticles concentrated the drug up to 25 times

more in the treatment area and was found to be superior in reducing the tumor volume compared to the naked drug.

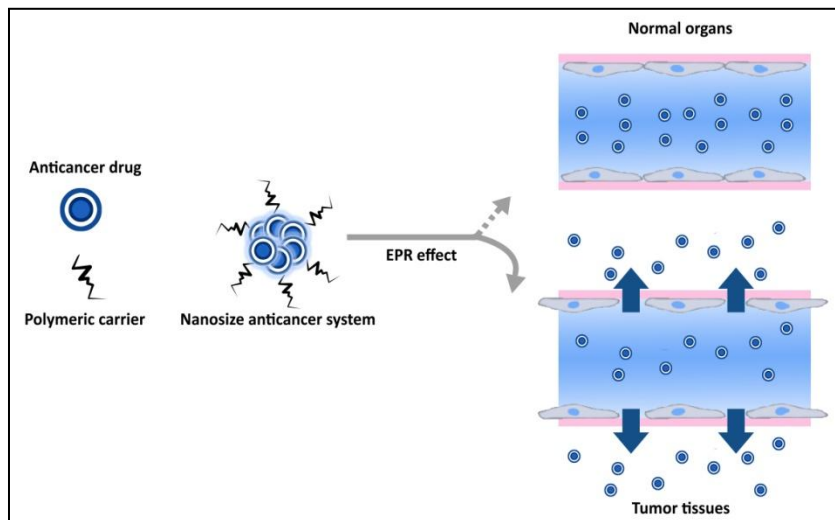


Figure 7. Schematic presentation of the enhanced permeability and retention (EPR) effect in normal *versus* tumor cells.

4. Retinoids in cancer nanomedicine

The administration of retinoids in nanocarriers is evident in several applications including anti-aging, anti-acne, anti-microbial, and cancer therapy (Brannon-Peppas 2012). In cancer applications, a high-density lipoprotein nanoparticle formulation of the synthetic retinoid, fenretinide, was proven to have high encapsulation efficiency with a 2-fold lower IC_{50} value when compared to the native drug in neuroblastoma cells (Sabnis 2013). The natural retinoid ATRA have also been formulated into nanoparticles where it showed similar anticancer activities *in vitro* as the free drug and was shown to be more potent *in vivo* in a pulmonary metastatic model of CT26 colorectal cancer cells (Jeong 2013). In cervical cancer, ATRA-poly (ethylene glycol)-thiol gold nanoparticle formulations were found to be of a better potency than the naked

drug (Ye 2015). In APL, ATRA loaded in polymer poly (lactide-coglycolide) nanoparticles were shown to reverse the malignant cell growth and induces cell differentiation and apoptosis *in vitro* models (Simon 2012). Moreover, this latter formulation was also shown to increase its anticancer activity in human liver carcinoma cells, and bioavailability in *in vivo* relative to free ATRA (Li 2009).

5. Flash Nanoprecipitation

There are several methods for formulating nanoparticles, including attrition, pyrolysis, and hydrothermal synthesis. In our work, we made use of the Flash Nanoprecipitation (FNP) experimental technique for producing polymer-protected nanoparticles with narrow size distributions through self-assembly (Liu 2008). FNP is a process where, through rapid mixing, particles of an insoluble low molecular weight compound are stabilized with an amphiphilic polymer (Figure 8). Many factors need to be taken into consideration to fully exploit the potential of FNP including particle structure, size, and stability. Typically, amphiphilic diblock copolymers are used for nanoparticles stabilization, and the more hydrophobic the drug they encapsulate, the higher the efficacy of the technique. The hydrophilic block used was polyethylene glycol (PEG) where it has been shown to prolong the nanoparticles circulation time *in vivo* (Zhang 2008), which is crucial for the cancer application considered here. To formulate the nanoparticles, the hydrophobic drug and stabilizing polymer are dissolved in a water-miscible organic solvent. The obtained solution is mixed through a confined impingement jet (CIJ) mixer with a stream of water, at a high velocity, causing precipitation of the drug, and simultaneous particle surface stabilization by the polymer due to the supersaturation condition produced in the CIJ mixing cell (Figure 8).

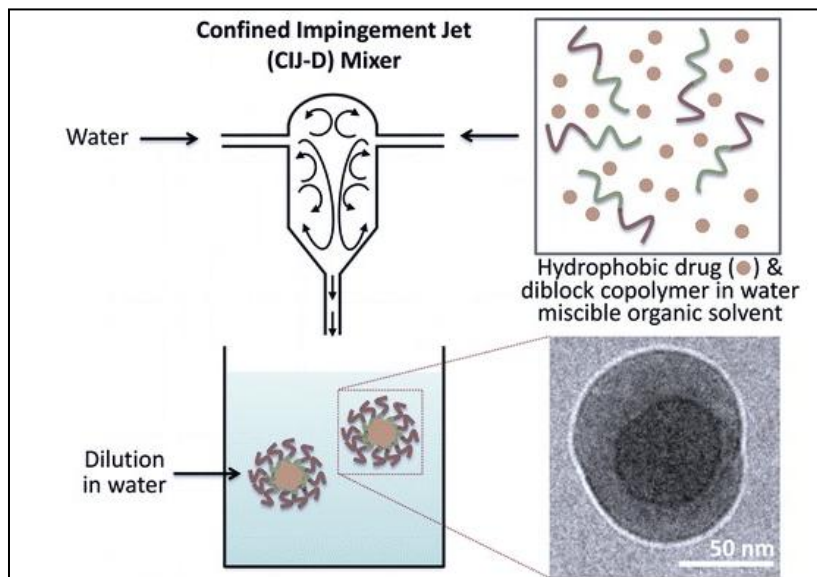


Figure 8. Flash Nanoprecipitation Technique. Adapted from: Pustulka 2013. Flash nanoprecipitation: particle structure and stability. *Molecular Pharmaceutics* 10: 4367-4377

H. Xenograft Models: Preclinical assessment of anticancer drug development

Using human cell lines can be useful in drug screening; however, it is poorly defined at the genotypic level where it fails to engage the microenvironment, and more specially the immune one, that has a significant role in cancer progression. As such, *in vitro* models are not sufficient for predicting the drug's mode of action in patients. Animal models have been used as the front line in predicting efficacy and finding toxicities for cancer chemotherapeutic agents before reaching the clinic (Cheon 2011). In particular, one of the most widely used models is the human tumor xenograft. In this model, human tumor cells are transplanted, either subcutaneously or into the organ type in which the tumor originated in immunocompromised mice that do not reject human cells (Morton 2007). Depending on the number of cells injected,

or the size of the tumor transplanted, the cancer profile will develop over 1-8 weeks, and the response to appropriate therapeutic regimes can be studied *in vivo*.

In AML, many xenograft mouse models were generated by inoculation of AML cell lines such as HL-60, HL-60 cy, U937, THP-1, MOLM-13, and OCI-AML3 into immunocompromised mice (SCID and NOD SCID mice) (Blair 1998; Rombouts 2000; Lumkul 2002; Marx 2003). These xenografted animals showed significant weight loss, development of scruffy coats, buffalo head, hind limb paralysis, and presence of palpable tumors and developed the same features of AML as in patients. In addition, these mice die after a period of time ranging between 4 and 5 weeks according to the xenografted cell line, which allows successful measurement of survival specially in studies aiming at testing the beneficial potential effect of targeted therapies or new drugs against AML (Cesano 1992; Quentmeier 2005).

Data accumulated to date suggest that one of the most severely immunocompromised mice, the NOG (NOD-*scid* IL2 γ^{null}) mouse model, is the best recipient for humanized tissue and human cell engraftment in mice (Brehm 2010). Therefore, optimization and standardization of animal models can enhance the predictability of anticancer drugs response and can be used as a good tool for their preclinical assessment.

I. Aims of the Study

Previous studies in our laboratory have demonstrated the anticancer effects of ST1926 on several cancer models, including ATL, CML, colon, rhabdomyosarcoma, breast, and prostate cancer cells (El Hajj 2014; Nasr 2014; Darwiche 2014; Basma 2015; and unpublished data).

In this study, using an *in vitro* and *ex vivo* ATRA-resistant AML models, we examined the antitumor activities of the synthetic retinoid ST1926. The effects of ST1926 on proliferation, viability, cell cycle, cell death mechanisms, DNA damage, and retinoid signaling were investigated. Furthermore, given the potential of nanotechnology in cancer therapeutics, we aimed to enhance ST1926 bioavailability and efficacy by formulating it into polymer-encapsulated nanoparticles using FNP technique. In order to translate the effects of ST1926 observed in cells into *in vivo* models, we generated and optimized an AML xenografted mouse model which will be used for future preclinical experiments.

This study supports the potential therapeutic role of ST1926 in ATRA-resistant AML cells, and deciphering its mechanism of action will help us understand how ST1926 is eradicating the blast cells while sparing the normal ones. Additionally, we highlighted the use of ST1926 and its nanoparticle formulation as promising lead anticancer drug candidates for further preclinical investigation in AML therapy, where two AML xenografted mouse models using two AML cell lines were successfully reproduced and optimized.

CHAPTER II

MATERIALS AND METHODS

A. AML Cell Lines Characterization

For this study, five ATRA-resistant AML cell lines were used; HEL (DSM ACC 11), THP-1 (DSM ATCC 16), KG1- α (ATCC CCL246.1), MOLM-13 (DSM ACC 554), and ML-2 (DSM ACC15), harboring different genetic mutations and corresponding to many AML karyotypes. They were kindly provided as a gift from F. Mazurier. Detailed description of each cell line is shown in Table 3.

HEL cell line was established from the peripheral blood of a 30-year old male with erythroleukemia (AML M6) in relapse (after treatment for Hodgkin lymphoma) in 1980 (Martin P 1982); cells were described to be capable of spontaneous and induced globin synthesis. They are round single cells in suspension and show macrophage-like features, with a doubling time of 36 hours.

THP-1 cell line was derived from the peripheral blood of a 1-year-old male with acute monocytic leukemia (AML M5) (Tsuchiya 1980). THP-1 cells can be induced to differentiate into monocytes/macrophages but not cells of other hematopoietic lineages, and are considered as the leukemic “counterpart” of blood monocytes. They are round, colony-forming cells in suspension, with a doubling time of 26 hours.

KG-1 cell line was derived from the bone marrow of a 59-year-old man with erythroleukemia (AML M6) who developed into AML. KG1- α is a sub-clone of KG-1 cell line and is described as its "undifferentiated variant" that was isolated by Koefler (1983). KG-1 α

cells are morphologically, and functionally less mature than the parental KG-1. They are round, single cells in suspension and show macrophage-like features, with a doubling time of 30 hours.

MOLM-13 cell lines was derived from the peripheral blood of a 20-year-old man with AML M5 who relapsed in 1995 after initial myelodysplastic syndromes (MDS, refractory anemia with excess of blasts, RAEB) (Quentmeier 2003). This cell line carries ITD of FLT-3 protein where the protein is not expressed. Most cells are round growing in suspension, and have a doubling time of 50 hours.

ML-2 cell line was derived from the peripheral blood of a 26-year-old man with AML M4 (following T-non-Hodgkin lymphoma and T-ALL) in 1978. ML-2 cells carry a t(6;11) (q27;q23) leading to MLL-AF6 fusion gene (Ohyashiki 1989) and are round single cells in suspension, with a doubling time of 40 hours.

Moreover, primary AML cells from the bone marrow of two patients (patients 1 and 2) were extracted following Ficoll separation (as described by El Hajj 2014). These samples were collected after approval by the Institutional Review Board (IRB) at the American University of Beirut and after patients provided informed consent in accordance with the Declaration of Helsinki.

Table 3. Summarized description of the AML cell lines used

AML Cell Line	Description	Origin & source	Morphology	p21 status	P53 status	FLT-3 status	NPM-1 status
HEL	Acute erythroid leukemia (AML M6 in relapse after treatment for Hodgkin's disease)	Peripheral blood Male, 30 yo	Macrophage-like	wt	Mutant**	wt	wt
THP-1	Acute monocytic leukemia	Peripheral blood Male, 1 yo	Large, round, single-cell morphology	wt	Mutant*	wt	wt
KG1-α	Acute erythroid leukemia	Bone marrow aspirate, Male, 59 yo	Large, round, single-cell morphology myeloblastic	wt	Mutant**	wt	wt
MOLM-13	Acute monoblastic/monocytic leukemia	Peripheral blood, Male, 20 yo	Large, round, colony-forming morphology	wt	wt	Mutant ^(?)	wt
ML-2	Hematopoietic neoplasm, Acute myeloid leukemia	Peripheral blood, Male, 26 yo	myelo-monoblastoid appearance	wt	wt	wt	wt

*Heterozygous, **Homozygous, ^(?)Unknown, wt: wild type

B. Cell Culture

HEL, THP-1, KG1- α , MOLM-13, and ML-2 were all maintained in RPMI 1640 medium (Lonza) containing 10-20% heat inactivated fetal bovine serum (FBS) (Gibco) and 50 U/ml penicillin-streptomycin antibiotics (Lonza). All cells were maintained under standard incubator conditions (humidified atmosphere, 21% O₂, 5% CO₂, 37°C). The cells were passaged and maintained every two to three days depending on their growth status. Typically, when the confluence of the cells reached 70-80%, they were centrifuged for 5 min at 900 rpm and the pellet was resuspended in fresh media and transferred into new 75 cm² cell culture flasks for maintenance. Prior to any experiment, the number of cells was expanded by the addition of fresh media to the pellet of the freshly suspended cells. Moreover, primary AML cells, obtained from the bone marrow of 2 patients, were cultured and maintained in Minimum Essential Medium- α (MEM- α) supplemented with 20% FBS and antibiotics.

Using trypan blue dye exclusion assay (0.4% trypan blue solution), cell count was done by a hemocytometer according to the formula: cells/ml=average number of cells x dilution factor x volume of suspension x 10⁴. For experiments, cells were seeded at the concentration of 2 x 10⁵ cells/ml.

C. ST1926 and ATRA Preparation

ST1926 was kindly provided by Biogem SCARL (Ariano Irpino-Martiri, Italy), prepared as stock solution, dissolved in dimethyl sulfoxide (DMSO) at 1 x 10⁻² M, and stored in amber tubes at -80°C. For experiments, an aliquot of ST1926 was applied either directly on the cells, for concentration of 5 μ M, or serially diluted in DMSO to obtain concentrations ranging from

0.05 μM to 1 μM . ST1926 was applied to the cells while the visible light inside the cell culture cabinet was turned off.

ATRA is commercially available and was purchased from Sigma Chemical Co. ATRA was dissolved in DMSO under yellow light to obtain a stock concentration of $3.3 \times 10^{-2} \text{ M}$, aliquoted into amber tubes, and stored at -80°C . For experiments, ATRA was diluted in DMSO to obtain concentrations of 0.5 μM , 1 μM , and 3 μM . All experiments with ATRA were performed under yellow light to prevent photoisomerization.

The final DMSO concentration never exceeded 0.1% and this concentration was shown to have no effect on the proliferation of all studied AML cells.

D. Cell Growth Assay

To test for the anti-proliferative effects of ST1926 and ATRA, AML cells were treated with 0.1% DMSO or varying concentrations of ST1926 or its nanoparticle formulation (0.05 μM , 0.075 μM , 0.1 μM , 0.5 μM , 1 μM and 5 μM), or ATRA (0.5 μM , 1 μM and 3 μM), or combination of both, then seeded into 96-well plates at a concentration of 2×10^5 cells/ml. Cell growth at 24, 48 or 72 hours post-treatment was assayed using MTT ([3-(4, 5-dimethylthiazol-2-yl)-2, 5-diphenyltetrazolium bromide]) CellTiter 96[®] non-radioactive cell proliferation assay kit. Such assay quantifies the metabolic activity in the mitochondria of the cells that converts tetrazolium salt into a blue formazan product, 3 to 4 hours post-addition of the dye. The formazan dye is then solubilized in an SDS-based stop solution and the absorbance of the blue color is assessed in triplicate wells by measuring the optical density (OD) at 595 nm using an ELISA microplate reader. The results were expressed as a percentage of control (0.1% DMSO) and they represent an average of up to three independent experiments \pm standard error (SE).

E. Cell Viability Assay

Cell growth was confirmed with trypan blue dye exclusion assay. AML cells or primary patient cells were treated with 0.1% DMSO or varying concentrations of ST1926 (0.05 μ M, 0.1 μ M, 0.5 μ M, 1 μ M and 5 μ M) then seeded into 96-well plates at a concentration of 2×10^5 cells/ml. Upon the retinoid addition (24, 48 or 72 hours post-treatment), trypan blue dye enters the disrupted membranes of the non-viable cells and causes the cells to turn blue in color which can be distinguished from the colorless viable ones under the light microscope. Cells were counted on the four corner chambers of a hemocytometer. The results were expressed as a percentage of control (0.1% DMSO) and they represent an average of up to three independent experiments (\pm SE).

F. Microscopic Imaging

AML cells were treated with 0.1% DMSO or 0.5 μ M ST1926 for up to 48 hours and representative bright field images were acquired using Zeiss axiovert light microscope and compared to their respective controls.

G. Drug Reversibility Assay

To check whether the effect of ST1926 on AML cells is reversible or not, 2×10^5 cells/ml were seeded in 25 mm² cell culture flasks and pre-treated with 0.1% DMSO or 0.5 μ M of ST1926 for 24 hours. The next day, the cells were centrifuged, washed twice with 1X calcium free- phosphate buffered saline (PBS), and resuspended in fresh drug-free media; this was recorded to be Day 0. Cell growth was then assayed at 24, 48 or 72 hours post-ST1926 removal

using MTT assay. The results were expressed as a percentage of control (0.1% DMSO) and they represent an average of up to three independent experiments (\pm SE).

H. Caffeine Preparation and Treatment

Caffeine was purchased from Sigma Chemical Co. Caffeine was dissolved in water to obtain a stock concentration of 100 μ M and stored at room temperature. For experiments, the drug was diluted in media to a final concentration of 2 μ M per treatment. THP-1 and MOLM-13 cells were pre-treated with 2 μ M Caffeine at a concentration of 2×10^5 cells/ml in 25 mm² cell culture flasks for 24 hours. The next day, and after washing and replenishing the media, cells were treated with 0.1% DMSO, 2 μ M Caffeine alone, 0.5 μ M of ST1926 alone, or both ST1926 and caffeine. Cells were then seeded into 96-well plates and their growth was assayed 48 hours post-treatment using MTT assay. The results were expressed as a percentage of control (0.1% DMSO) and they represent an average of up to three independent experiments (\pm SE).

I. Pan-RAR Inverse Agonist BMS493 Preparation and Treatment

The pan-RAR inverse agonist BMS493 was purchased from Santa Cruz Biotechnology, dissolved in 0.1% DMSO, stored at +4°C, and used at a final concentration of 1 μ M. THP-1 and MOLM-13 cells were pre-treated with 1 μ M BMS493 at a concentration of 2×10^5 cells/ml for 20 min, then cells were treated with 0.1% DMSO or varying concentrations of ST1926 (0.5 or 1 μ M). Cells were then seeded into 96-well plates and their growth was assayed 24 or 48 hours post-treatment using MTT assay. For a positive control, the growth of C8166 cells (ATL cell line sensitive to ATRA), was assayed with ATRA in the presence and absence of the inverse

agonist, 48 hours post-treatment. Results were expressed as a percentage of control (0.1% DMSO) and they represent an average of up to three independent experiments (\pm SE).

J. Cell Cycle Analysis

Cell cycle analysis was performed using the propidium iodide (PI) flow cytometric assay. PI (Ex/Em = 535/617 nm; Sigma) is a membrane impermeant dye that binds to double-stranded DNA through intercalating between the base pairs. For cell cycle analysis, 2×10^5 cells/ml were seeded in 25 mm² cell culture flasks and treated with 0.1% DMSO or 0.5 μ M of ST1926. Cells were then collected 24 or 48 hours post-treatment, washed twice with 1 x PBS, fixed with 80% ethanol and stored at -20 °C for up to 10 days. Fixing the cells with ethanol permeabilizes the membranes to take up the PI dye, and the DNA content can then be quantified and analyzed using flow cytometry. Next, the fixed cells were brought down to room temperature, centrifuged and then washed few times with 1X PBS to remove any traces of ethanol. Then the cell pellet was incubated with 200 μ g/ml DNase-free RNase A for an hour. After the RNase was washed off, the cells were resuspended in 1 x PBS and stained with 1 mg/ml PI (Sigma). Subsequently, cell cycle analysis was done using FACScan flow cytometer (FACScan, Becton Dickinson). A total of 10,000 gated events were acquired in order to assess the proportions of cells at different stages of the cell cycle. Results were expressed as percentages of elements detected in the different phases of the cell cycle, namely pre-G₁, G₀/G₁, S, and G₂/M, and are an average of at least three independent experiments (\pm SE).

K. Annexin V/PI Assay

In order to investigate whether ST1926 induced early apoptosis in AML cells, Annexin V/PI assay (Roche) was used. The rationale behind this protocol is that at early stages of apoptosis, phosphatidylserine (PS) gets translocated from the inner to the outer leaflet of the plasma membrane exposing it to the external cellular environment. Annexin V (Ex/Em = 488/512 nm; Roche) is a 35-36 kDa Ca^{2+} -dependent phospholipid-binding protein that has a high affinity for PS that can be conjugated to a fluorochromes including FITC. Its high affinity for PS serves as a sensitive probe for flow cytometric analysis of cells undergoing early apoptosis. Differentiation between early *versus* late stages of apoptosis can be done by accompanying Annexin V with the plasma membrane impermeant PI dye that binds exclusively to DNA of cells with disrupted membranes, indicating late apoptosis. As such, early apoptosis can be identified through PI-negative and Annexin V-positive flow cytometric analysis, whereas late apoptosis would normally show both PI and Annexin-positive reading. Cells that are negative to both dyes are alive and not undergoing apoptosis.

AML cells were seeded at a concentration of 2×10^5 cells/ml in 25 mm^2 cell culture flasks and treated with 0.1% DMSO or 0.5 μM of ST1926. Cells were then collected 12 and 24 hours post-ST1926 treatment, and washed with 1X PBS. Cells were then resuspended in 2 μL of the dyes and incubated for 15 minutes in the dark at room temperature. In addition to the treated cells, four controls were required to set up the compensation and quadrants by flow cytometry: unstained cells, cells stained with FITC Annexin V alone (no PI), cells stained with PI alone (no FITC Annexin V), and control cells stained with both dyes. To ensure both PI and Annexin V positive controls, cells were fixed with 80% ethanol at -20°C for 1 hour followed by vigorous vortexing. Then, 300 μL incubation buffer was added to all tubes which were analyzed

by flow cytometry using 488 nm excitation and a 515 nm band pass filter. Electronic compensation was done using the controls to exclude overlapping of the two emission spectra according to the manufacturer's instructions. Results are expressed as an average of three independent experiments (\pm SE). Figure 9 shows a schematic representation of the assay .

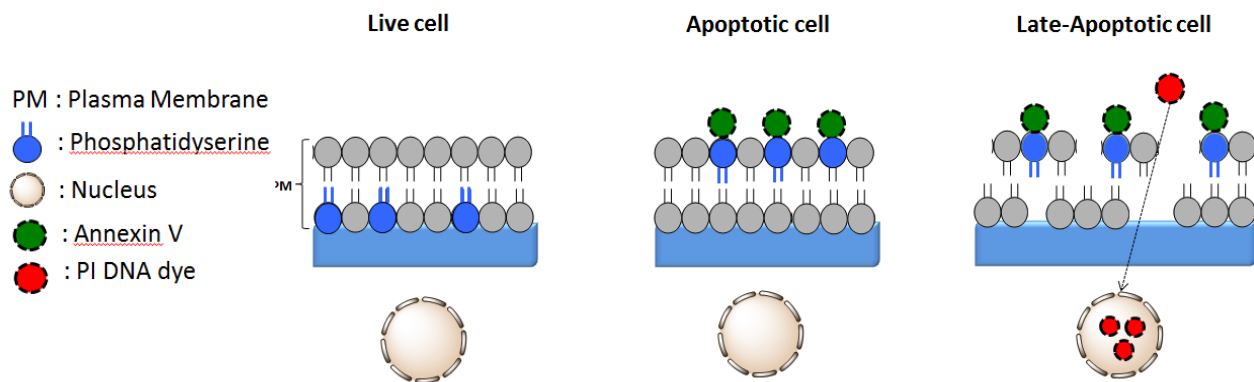


Figure 9. Schematic demonstration of Annexin V/PI assay

L. Mitochondrial Membrane Dissipation Assay

The mitochondrial membrane potential for AML cell lines after ST1926 treatment was monitored using Rhodamine-123 fluorescent dye (Ex/Em = 485 nm/535 nm; Sigma), a cell-permeable cationic dye, which preferentially enters into mitochondria due to the highly negative mitochondrial membrane potential ($\Delta\Psi_m$). Depolarization of $\Delta\Psi_m$ results in the loss of Rhodamine from the mitochondria and a decrease in intracellular fluorescence.

On the experiment day, 2×10^5 cells/ml were seeded in 25 mm² cell culture flasks and treated with 0.1% DMSO or 0.5 μ M of ST1926. Cells were then collected 24 or 48 hours post-treatment, washed, and resuspended in Rhodamine washing buffer. Then cells were incubated in the thermoshaker for 1 hour at 37°C in the dark with Rhodamine-123 dye at a final concentration

of 1 μM . Cells were then washed and resuspended with Rhodamine washing buffer, transferred into polystyrene round bottom tubes (Falcon) and the fluorescence was measured through FACScan flow cytometer.

M. Western Blotting

AML cells were seeded at a concentration of 2×10^5 cells/ml in 25 mm^2 cell culture flasks and treated with 0.1% DMSO or 0.5 μM of ST1926. Cells were then collected 24 or 48 hours post-treatment, and washed with 1 x PBS, followed by their lysis with 50-100 μl of 2X Laemmli Lysis Buffer (Bio-Rad) to extract the proteins. Proteins were then quantified using the NanoDrop-1000 (Thermo Scientific) through the Protein A280 method. Then, 5% β -mercaptoethanol was added to each sample to reduce the disulfide bonds in the proteins. Using Bio-Rad electrophoresis cell, a gel casting system was set according to the manufacturer's instructions. Subsequently, equal amount of the protein extracts was loaded into each well of the 10-15% sodium dodecyl sulfate (SDS)-polyacrylamide gel electrophoresis (PAGE), which was run at 80 V for around 2.5 hours using the Mini-PROTEAN II electrophoresis cell unit (Bio-Rad). After the run, the proteins were transferred into nitrocellulose membrane using the Bio-Rad Trans-Blot® Electrophoretic Transfer Cell (Bio-Rad) at 90 V for 1.5 hours. Following the transfer, the membranes were incubated with a blocking solution (10 mM tris-HCl pH 8.0, 150 mM NaCl, 0.05% Tween 20 with 5% dry milk (fat-free) or 5% BSA for 1 hour while shaking at room temperature. Then the membranes were incubated in primary antibodies dissolved in a blocking solution at $+4^\circ\text{C}$ overnight. The next morning, the membranes were washed briefly and incubated with a secondary antibody (Santa Cruz Biotechnology, horseradish peroxidase-conjugated anti-rabbit or anti-mouse) for 2 hours at room temperature while shaking.

Finally, membranes were washed and the proteins were detected by enhanced chemiluminescence using ECL system (Santa Cruz Biotechnology) in conjunction with horseradish peroxidase-conjugated secondary antibody. The membranes were then exposed to X-Ray films for various time points (2 sec-10 min) using the Xomat machine (Carestream®), or through chemiluminescence detection by the Chemidoc Touch Imager (Bio-Rad). The following antibodies were used: PARP (1:1000, Cell Signaling), p53 (1:500, Santa Cruz), γ H2AX (1:1000, Cell Signaling), RAR γ (1:250, Santa Cruz) and RXR α (1:250, Santa Cruz). The membranes were also probed with anti- glyceraldehyde-3-phosphate dehydrogenase (GAPDH) (1:1000, Cell Signaling) for assessment of equal protein loading.

N. Nanoparticle Formulation

Flash Nanoprecipitation (FNP) was used to formulate ST1926 into polymer-coated nanoparticles. The FNP setup required for the production and characterization of nanoparticles is already established and optimized in the laboratory of Dr. Walid Saad, Department of Chemical and Petroleum Engineering at the American University of Beirut. A multi-inlet vortex mixer (MIVM) was used in which streams of solution were mixed at high velocity in the small chamber to make an output of 1:9 tetrahydrofuran (THF):H₂O. Flow rates were controlled using Harvard apparatus PHD2000 syringe pumps.

The protocol for generating the nanoparticles using FNP has been optimized in Dr. Walid Saad's laboratory (Department of Chemical Engineering/American University of Beirut) (Zaynab Jaber MS. AUB, 2015). ST1926 was formulated into nanoparticles with a drug to polymer mass ratio of 1:5. 5 mg of ST1926 and 25 mg of polystyrene-b-poly(ethylene oxide) block copolymer (PS1.5-PEO2.4) with a polystyrene hydrophobic block size of 1,500 g/mole,

and a poly(ethylene oxide) block size of 2,400 g/mole (Polymer Source) were dissolved in 3 mL of THF. The resulting solution was mixed at 12 ml/min with water at 108 ml/min using the MIVM mixer and the nanoparticle suspension was directly collected at the mixer outlet.

O. Dynamic Light Scattering

The nanoparticle size was determined using dynamic light scattering (DLS) (Brookhaven Instruments, BI-200SM, Stonybrook, NY) following nanoparticle formation. The instrument was powered up at least 30 min in advance of measurements to allow the laser to stabilize. The temperature of the apparatus was maintained at 25°C, and the samples were left to equilibrate in the chamber for at least 5 min prior to taking a size measurement. The particle solution was then placed in Quartz cuvette inside the sample holder, where a coherent laser light (of wavelength of 532 nm) was directed at the particle solution, resulting in Doppler shifts in the frequency of light due to Brownian motion. These frequency changes are correlated to particle size. Three measurements were recorded for three min per sample. Number-weighted particle size distributions were calculated by the software and plotted.

P. Generation of the AML Xenografted Mouse Models

A preliminary experiment to reproduce xenografted AML mouse models following injection with MOLM-13 and THP-1 cell lines was approved by the Institutional Animal Care and Utilization Committee (IACUC) of the American University of Beirut. To expand our *in vivo* models and test therapies, the full proposal will be submitted for IACUC approval.

NOD-*scid* IL2 γ^{null} mice (6 weeks old; average weight of 20g, Jackson Laboratories, USA) were intraperitoneally injected with 5×10^6 MOLM-13 or THP-1 AML cells (5 mice for

MOLM-13 and 3 for THP-1, due to the availability of the mice). Animals were housed in a specific pathogen-free facility. The health status of the mice and the possible nodules formation around the abdomen region were monitored every other day, over a period of 4 weeks. Mice were humanely euthanized when moribund as defined by: weight loss >10-15%, lethargy, ruffled fur, slow motion, after deep anesthesia by isoflurane followed by cervical dislocation. Overall survival of the mice was recorded and plotted, and will be used as a standard for later experiments.

Q. Statistical Analysis

For the *in vitro* studies, data presented are the means \pm SE of three independent experiments. Statistical analysis was performed using Microsoft Excel 2010, and the significance of the data was analyzed using a Student's t-test. Statistical significance was reported when the P-value was < 0.05 (*, P < 0.05; **, P < 0.01; *** P < 0.001).

CHAPTER III

RESULTS

A. ST1926 inhibits the proliferation of AML cells at sub-micromolar concentration as evident by the MTT proliferation assay

First, we started by characterizing the anti-proliferative effect of ST1926 on the five ATRA-resistant AML cell lines (HEL, THP-1, KG1- α , MOLM-13, and ML-2) harboring different genetic mutations, thus corresponding to many AML karyotypes (Table 3). Cell growth was assayed using CellTiter non-radioactive cell MTT proliferation assay. The tested ST1926 concentrations ranged from 0.05 to 5 μM , wherein it has been shown that micromolar concentrations of ST1926 can be achieved physiologically (Basma 2015). Interestingly, we have shown that ST1926 significantly inhibits the growth of all the tested AML cell lines, even at concentrations as low as 0.1 μM in a time dependent manner (Figure 10); furthermore, all the cells showed a similar ST1926 growth-inhibitory profile with a threshold of 0.1-0.5 μM . In addition, an ST1926 concentration of 0.5 μM inhibited the growth all the AML cells by at least 50% after two days of treatment, demonstrating that the minimum inhibitory concentration (IC_{50}) is approximated to be 0.5 μM for all the tested cells. To our interest, it has been shown that 10 μM supra-physiological concentrations of ST1926 has no effect on normal, resting, and activated lymphocytes from the bone marrow of three normal donors (El Hajj 2014).

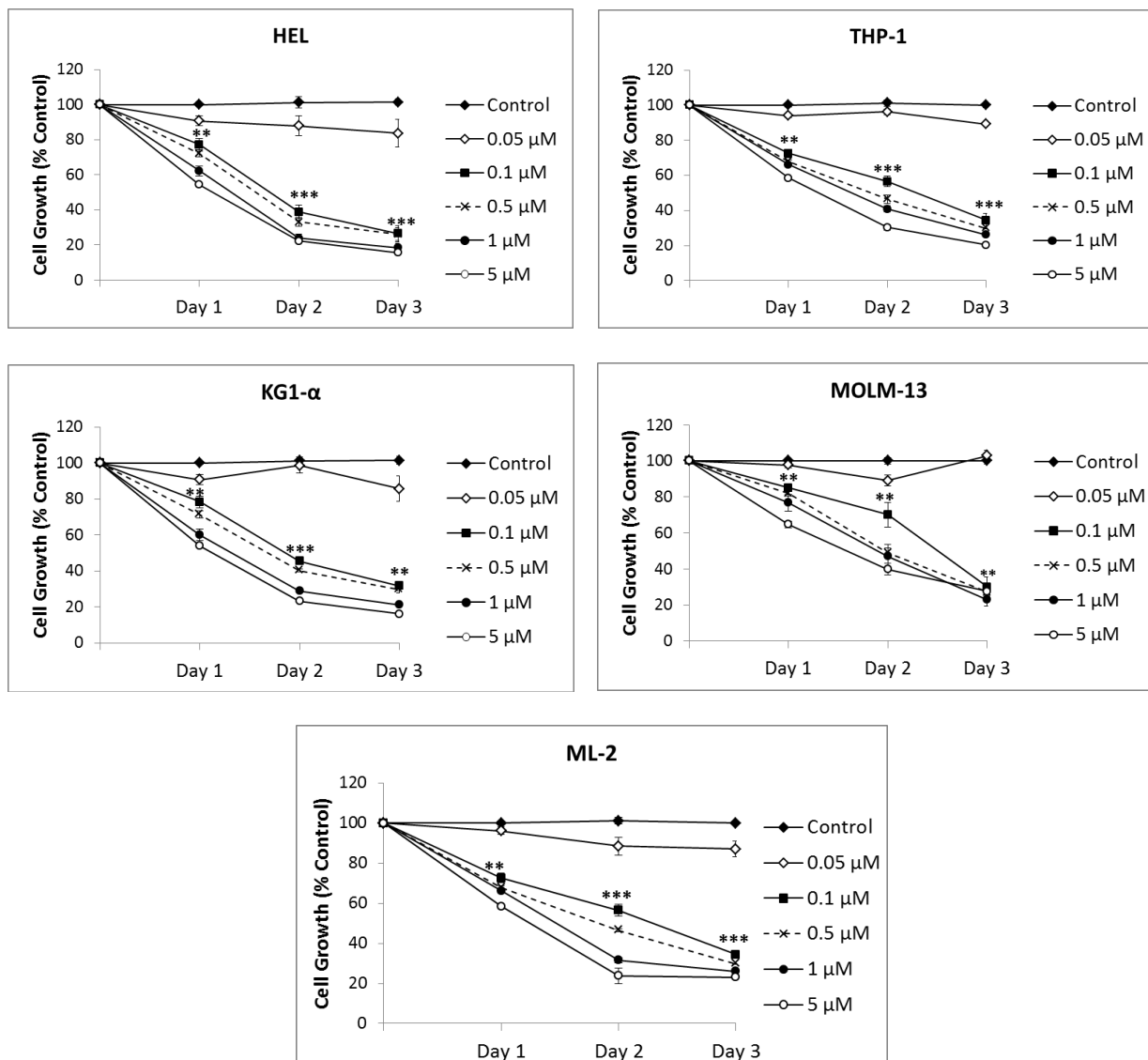


Figure 10. Effect of ST1926 on the proliferation of AML cells using MTT assay. HEL, THP-1, KG1- α , MOLM-13, and ML-2 were seeded at a concentration of 2×10^5 cells/ml and treated with 0.1% DMSO or indicated concentrations of ST1926 up to three days. Cell growth was assayed in triplicate wells using CellTiter non-radioactive cell MTT proliferation assay. Results are expressed as a percentage of control (0.1% DMSO) and they represent an average of three independent experiments (\pm SE) (*, $P < 0.05$; **, $P < 0.01$; *** $P < 0.001$).

B. ST1926 inhibits the viability of AML cell lines and primary patient cells at sub-micromolar concentration as evident by trypan blue exclusion assay

We also tested the effect of ST1926 on the viability of AML cells using trypan blue exclusion assay. Similar to MTT results, we have shown that ST1926 significantly inhibits the viability of all the tested AML cell lines at sub-micromolar concentrations (Figure 11), with an IC_{50} of 0.5 μ M at day two post-treatment, consistently with our MTT results.

Interestingly, we have tested ST1926 effect on ex-vivo cultured primary derived cells from two AML patients (Patient 1 and Patient 2), and we have shown that ST1926 reduces the viability of these primary cells, with an almost complete abolishment of proliferation after two days of the treatment with 0.5 μ M ST1926 (Figure 12). The patient samples were collected after approval by the Institutional Review Board (IRB) at the American University of Beirut, and after patients provided informed consent in accordance with the Declaration of Helsinki.

Based on the results of our MTT and trypan blue assays, 0.5 μ M was selected to be the working concentration to further decipher the mechanisms of growth suppression and cell death in ST1926-treated AML cells.

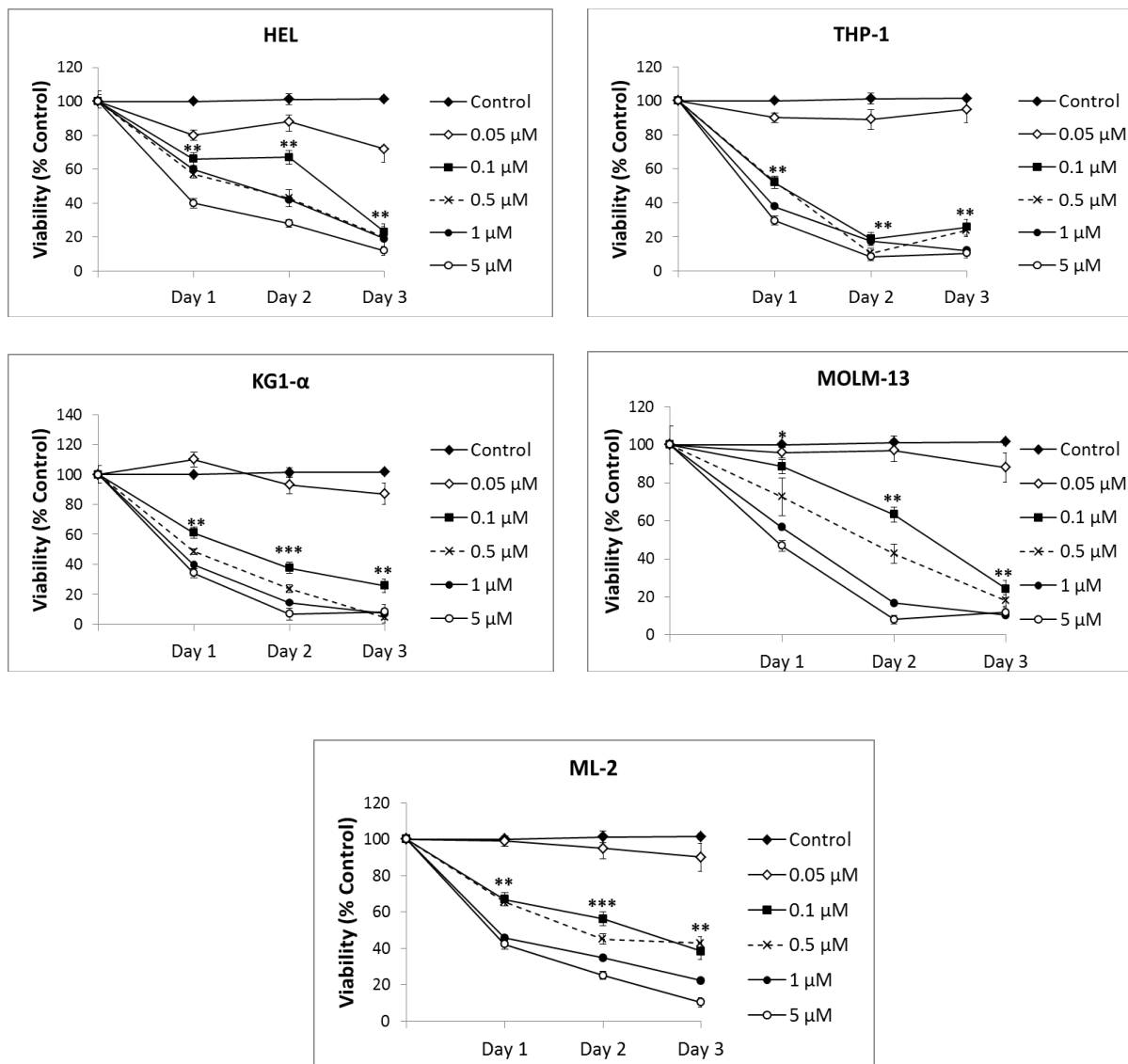


Figure 11. Effect of ST1926 on the viability of AML cells using trypan blue exclusion assay. HEL, THP-1, KG1- α , MOLM-13, and ML-2 were seeded at a concentration of 2×10^5 cells/ml and treated with 0.1% DMSO or indicated concentrations of ST1926 up to 72 hours. Cell growth was assessed in triplicate wells by trypan blue exclusion assay. The results are expressed as a percentage of control (0.1% DMSO) and they represent an average of up to three independent experiments (\pm SE) (*, $P < 0.05$; **, $P < 0.01$; *** $P < 0.001$).

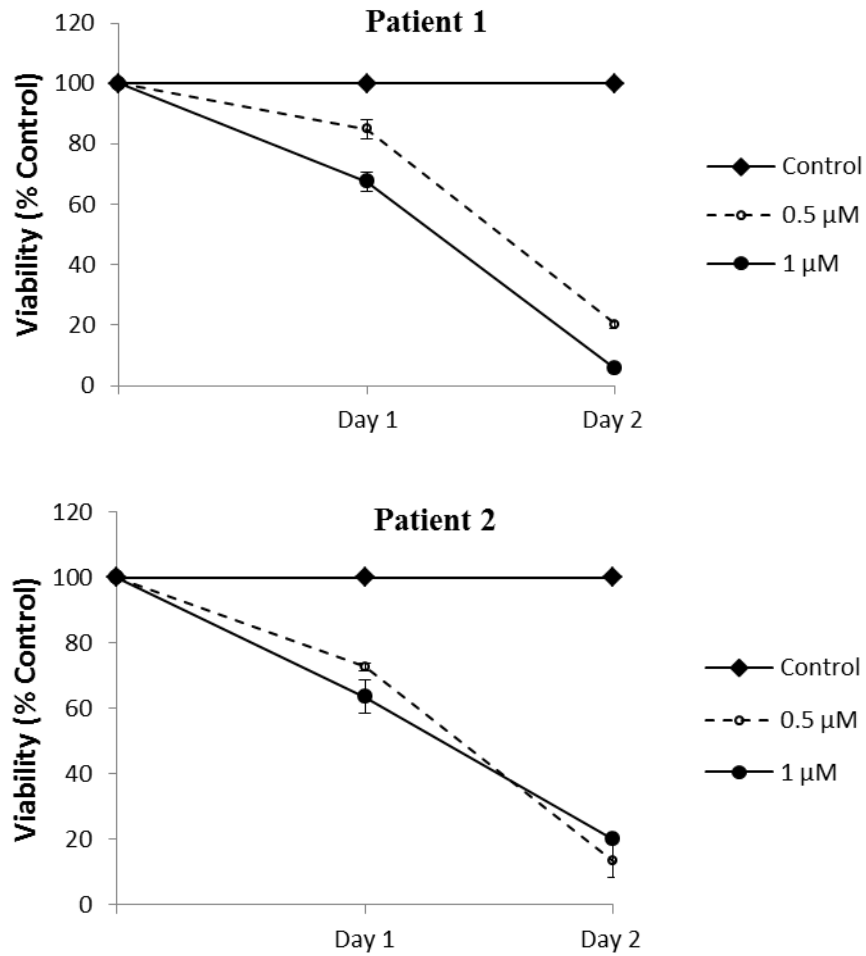


Figure 12. Effect of ST1926 on the viability of patient cells using trypan blue exclusion assay. Primary AML cells from the bone marrow of two patients (patients 1 and 2) were seeded at a concentration of 2×10^5 cells/ml and treated with 0.1% DMSO or indicated concentrations of ST1926 up to 48 hours. Cell growth was assessed in triplicate wells by trypan blue exclusion assay. Results are expressed as a percentage of control (0.1% DMSO) and they represent an average of triplicate wells \pm standard deviation (\pm SD).

C. ST1926-induced growth-inhibitory effect on AML cells is irreversible

The growth inhibitory effect of ST1926 has previously been shown to be irreversible on CML, colon, and breast cancer cell lines in our laboratory (unpublished data). To assess whether ST1926-growth inhibitory effect is also irreversible in AML cells, we have selected two AML cell lines, THP-1 having a p53 mutation and MOLM-13 having a FLT-3 mutation (Table 3), one of the most aggressive mutations in AML (Levis 2003). THP-1 and MOLM-13 cells were pretreated with 0.5 μ M ST1926. One day later, cells were washed and re-suspended in drug-free media. Using MTT assay, the growth of the cells was assessed up to three days of post removal of the drug. As shown in Figure 13, the inhibitory effect of ST1926 persisted after removal of the drug. Two days post-ST1926- treatment, THP-1 and MOLM-13 cell growth dropped to 30% and 40%, respectively; this growth inhibition persisted three days after removing the drug, underlining the irreversibility of ST1926-growth inhibitory effect in AML cells.

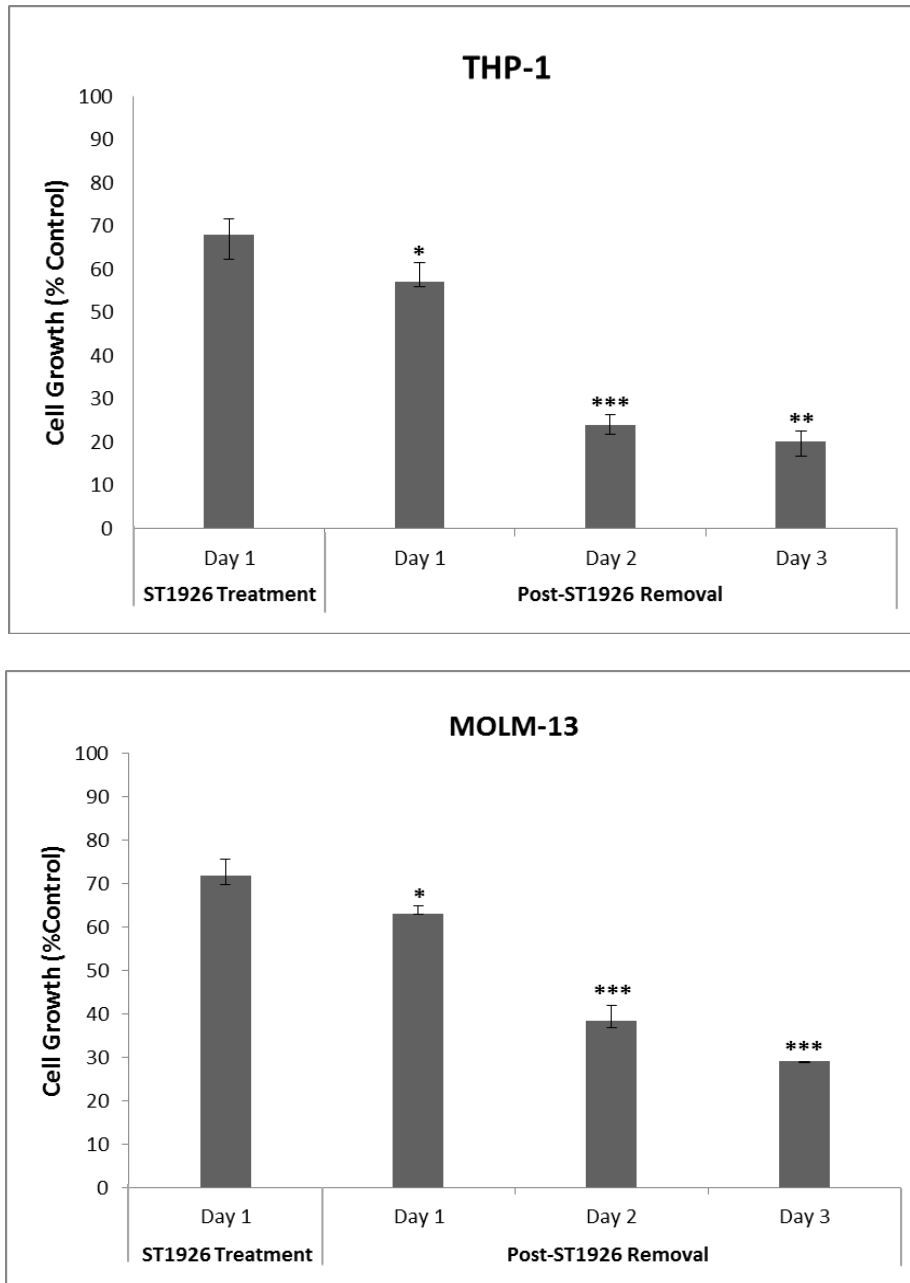


Figure 13. Irreversible effect of ST1926 on AML cell growth. THP-1 and MOLM-13 were seeded at a concentration of 2×10^5 cells/ml and treated with $0.5 \mu\text{M}$ ST1926. On day post treatment, the cells were collected, washed with PBS and resuspended in fresh drug-free media up to three days. Cell growth was assayed in triplicate wells by trypan blue exclusion assay. The results are expressed as a percentage of control (0.1% DMSO) and they represent an average of up to three independent experiments (\pm SE). (*, $P < 0.05$; **, $P < 0.01$; *** $P < 0.001$).

D. ST1926 induces the accumulation of treated AML cells in the pre-G₁ region of the cell cycle as assessed by PI-based flow cytometric analysis.

We next intended to study the mechanism through which ST1926 is exhibiting its growth inhibitory effects on the tested AML cells. After assessing the cell growth profiles of the treated AML cells, KG1- α and HEL cells exhibiting similar mutational background (Table 3), were shown to have relatively comparable profiles. Thus, we chose to proceed with our experiments using KG1- α as a representative of both cell lines.

Cell cycle analysis was performed on the four AML cell lines; THP-1, KG1- α , MOLM-13, and ML-2 which were treated with 0.5 μ M ST1926 for up to 48 hours. Control and treated cells were stained with PI (50 μ g/ml) and their cell cycle progression was assessed using PI-based flow cytometric analysis of DNA content. All of the ST1926 treated cell lines showed a significant accumulation of the cells in the pre-G₁ region of the cell cycle starting 24 hours post-ST1926-treatment; this accumulation further augmented after 48 hours (Figure 14A), specifically, in THP-1 cells where 70% to 80% of the cells accumulated in the pre-G₁ region after 24 and 48 hours of ST1926 treatment, respectively. Similarly, the number of cells in the pre-G₁ region in KG1- α cells increased from 30% to 40% region, in MOLM-13 from 50% to 70%, and lastly in ML-2 from 55% to 80%, after 24 and 48 hours of ST1926 treatment, respectively (Figure 14B). As for the cycling cells, we show a minor G₀/G₁ phase arrest for all, KG1- α , MOLM-13, and ML-2; and a minor S-phase arrest in the THP-1, after 24 hours of treatment.

Representative histograms of the cell cycle distribution of treated AML cells compared to their respective controls for 48 hours post-0.5 μ M ST1926 treatment are shown in Figure 15.

After assessing the effects of ST1926 on the cell cycle progression of the treated AML cells, ST1926 was shown to massively induce the accumulation of the AML cells in the pre-G₁ phase of the cell cycle. Pre-G₁ accumulation presumably indicates cell death by apoptosis, and this will be assessed next by different assays in order to be confirmed.

E. ST1926 induces apoptosis in AML cells

Apoptosis is a programmed cell death and can be characterized by many morphological and biochemical changes which can be tracked in several *in vitro* assays (Minton 2015). These changes include; cell shrinkage, membrane blebbing, PS externalization, DNA damage, loss of the mitochondrial membrane potential leading to subsequent downstream events including cleavage of PARP into its death-associated fragment, and upregulation of the tumor suppressor *p53* (Muller 2014)

To confirm apoptosis induction in ST1926-treated AML cells, we investigated the cellular response to the drug treatment using different cell death approaches and assays.

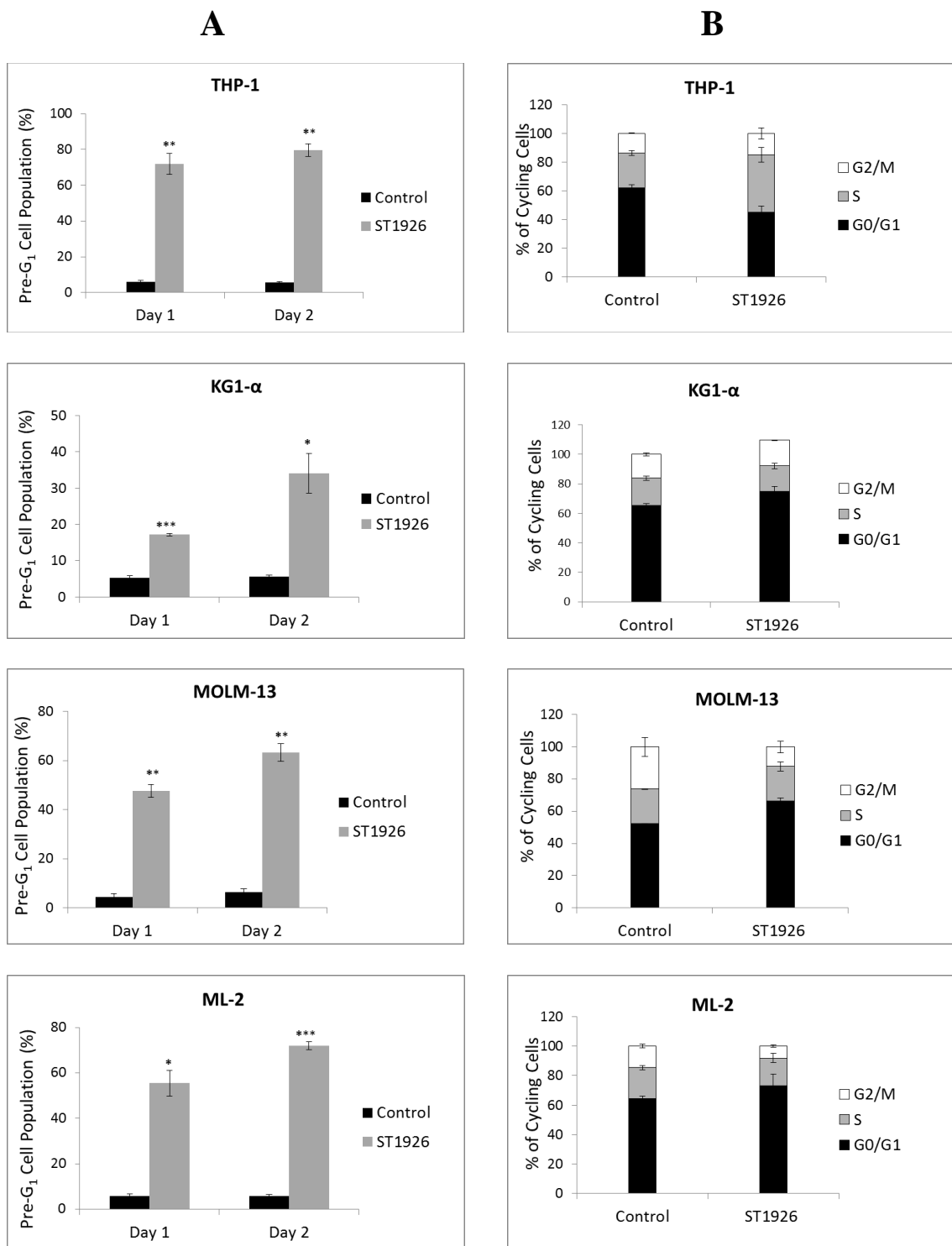


Figure 14. Effect of ST1926 on different cell cycle phases. THP-1, KG1- α , MOLM-13, and ML-2 cells were seeded at a concentration of 2×10^5 cells/ml and treated with $0.5 \mu\text{M}$ ST1926 for up to 48 hours. Cell cycle was assessed using PI-based flow cytometric analysis of DNA content. Panel A shows the effect of ST1926 on cell accumulation in pre-G₁ region, while panel B shows the change in the percentage of the cycling cells after 24 hours of ST1926 treatment. Results are reported as mean \pm SE of three or more independent experiments (*, $P < 0.05$; **, $P < 0.01$; ***, $P < 0.001$).

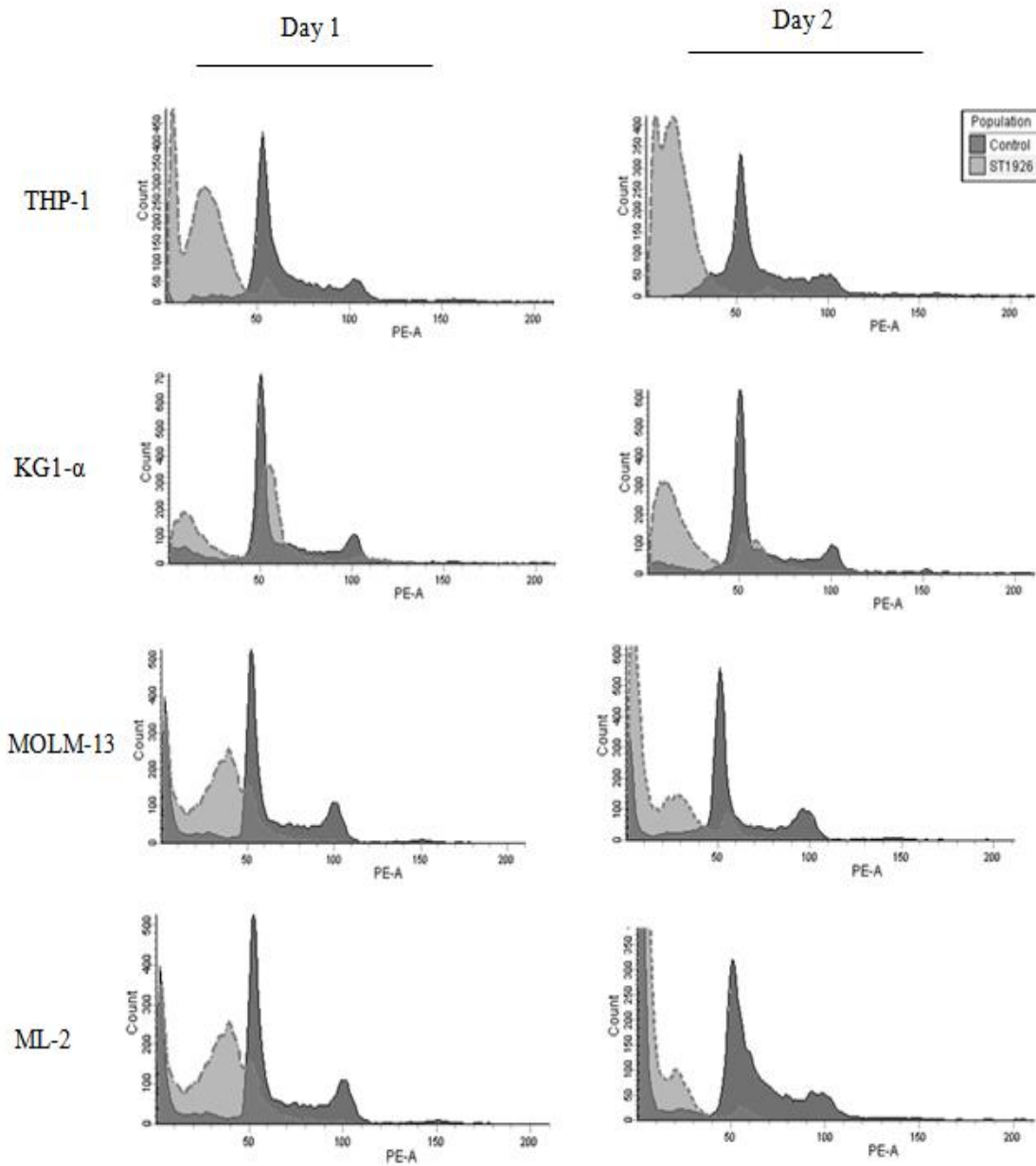


Figure 15. Representative histograms of the cell cycle distribution and progression in ST1926 treated AML cells. THP-1, KG1- α , MOLM-13, and ML-2 cells were seeded at a concentration of 2×10^5 cells/ml and treated with $0.5 \mu\text{M}$ ST1926 up to 48 hours. Cell cycle was assessed using PI-based flow cytometric analysis of DNA content. The histograms shown are representative of three independent experiments and they express an overlay of the treated (light grey) cells compared to the control (dark grey).

1. Effect of ST1926 on AML cell morphology and confluence

Initially, to test the effect of ST1926 on AML cell morphology and confluence, we worked on two representative cell lines THP-1 and MOLM-13. Bright-fielded images of these two cell lines were acquired using Zeiss axiovert light microscope. Cells treated with 0.5 μM for up to 48 hours showed a substantial decrease in confluence, in addition to their membrane shrinkage and inability to form colonies, when compared to their respective DMSO-treated controls (Figure 16).

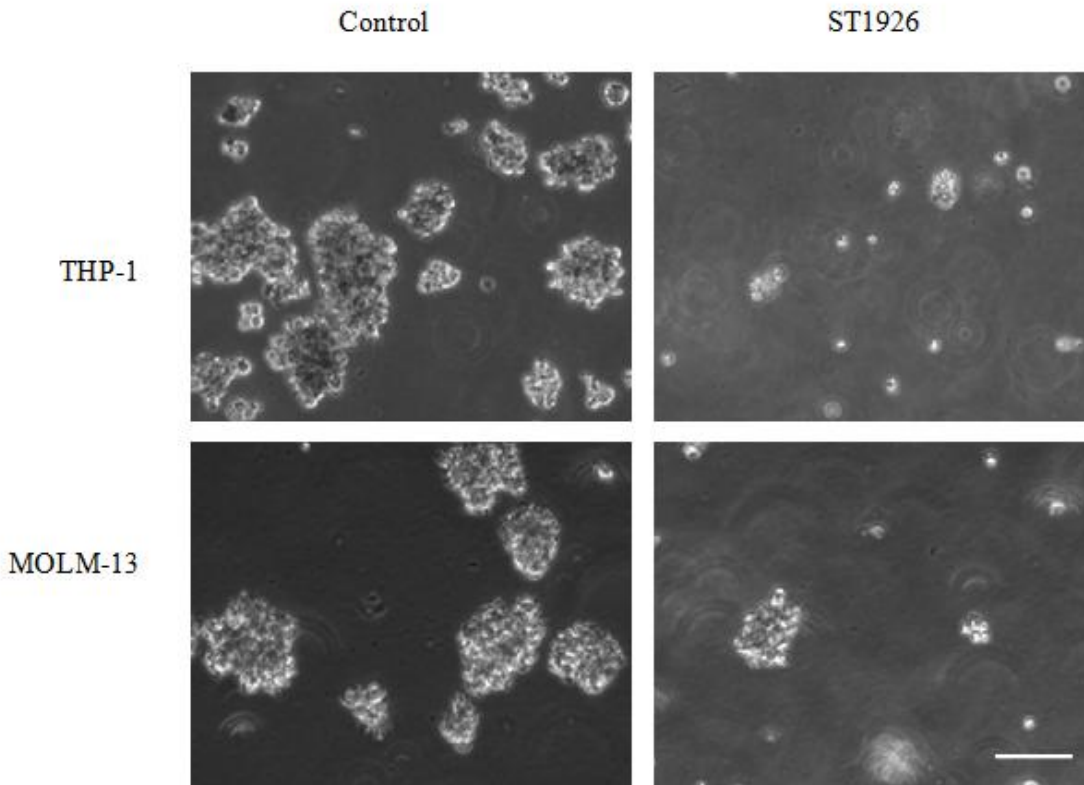


Figure 16. Effect of ST1926 on the morphology and the confluence of AML cells in culture. THP-1 and MOLM-13 cells were seeded at a concentration of 2×10^5 cells/ml treated with 0.1% DMSO (control) or 0.5 μM of ST1926 up to 48 hours. Representative bright field images were acquired using Zeiss axiovert light microscope (x10). Scale bar represents 50 μm .

2. ST1926 induces early apoptosis in AML cells as evident by the Annexin V/PI-based flow cytometric analysis

Next, we performed Annexin V/PI assay on the same two representative cell lines: THP-1 and MOLM-13. Not only does this assay detect apoptosis in cells, but also it can differentiate between its early and late stages. At early stages of apoptosis, PS gets translocated from the inner to the outer leaflet of the plasma membrane exposing it to the external cellular environment. Annexin V is a protein with high affinity for PS that can serve as a sensitive probe for flow cytometric analysis of cells undergoing early apoptosis. Being accompanied with the membrane impermeant PI dye, this assay can aid in identifying different apoptosis stages. Early apoptosis can be identified through PI-negative and Annexin V-positive flow cytometric analysis, whereas late apoptosis would normally show both PI and Annexin V-positive reading. Cells that are negative to both dyes are alive and not undergoing apoptosis.

The two tested AML cell lines were treated with 0.1% DMSO or 0.5 μ M of ST1926. In order to set up the compensation and the quadrants by flow cytometry, three controls were generated and optimized for this experiment. Two positive controls for Annexin V and PI dyes were exclusively required. They were obtained by fixing the cells in 80% ethanol for an hour followed by vigorous vortexing and addition of the dyes. Figure 17 shows the controls generated for this experiment with a general principle of the protocol. The plots represent the spread of the cells with respect to their green fluorescence absorbance. Figure 17A represents the stained DMSO treated THP-1 control cells, where the flow analysis indicated negative reading for both dyes. Figure 17B represents the AnnexinV-positive control where most cells stained positive for FITC Annexin V, whereas Figure 17C represents PI and Annexin V-positive control where most cells stained positive for both PI and FITC Annexin V. Same controls were tested for MOLM-13 which showed similar trend (data not shown).

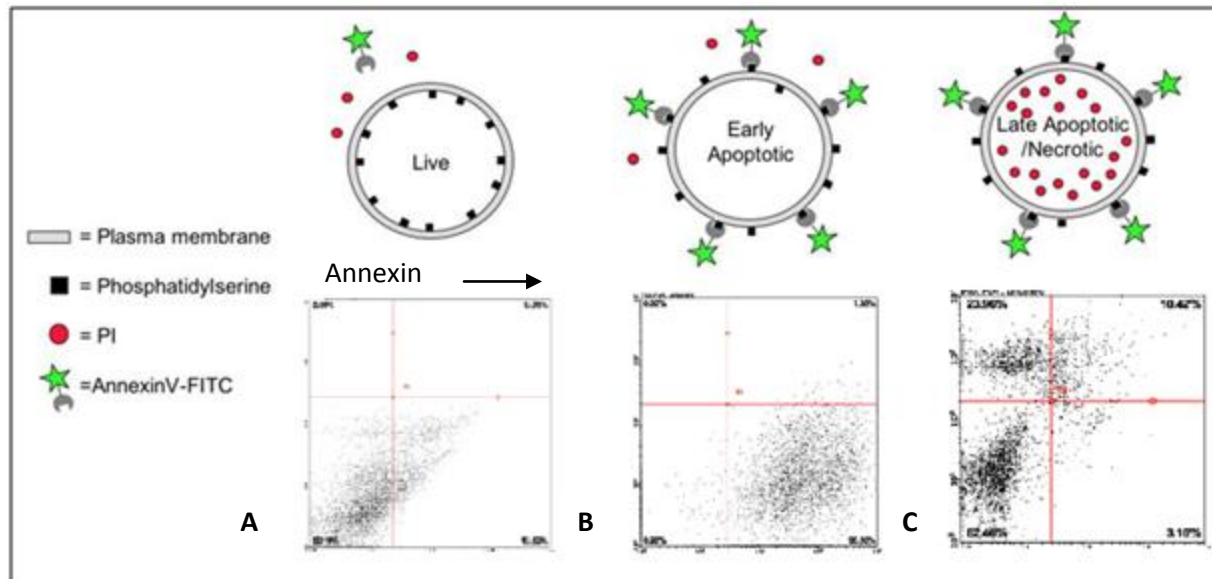


Figure 17. Annexin V/PI compensation controls. THP-1 cells were seeded at a concentration of 2×10^5 cells/ml treated with 0.1% DMSO. Cells were then collected after 12 hours and the pellet was divided into three controls, two of which were fixed in ethanol for an hour. Cells were then incubated in Annexin V and PI. Panels represent: (A) control untreated cells, (B) Annexin V positive control (C) Annexin V and PI positive controls (C). Positive controls for Annexin V and PI dyes were obtained by fixing the cells in 80% ethanol for an hour followed by vigorous vortexing and the addition of the dyes. All controls were then analyzed by flow cytometry. Electronic compensation was done using the controls to exclude overlapping of the two emission spectra of both dyes.

We then investigated early apoptosis in 0.5 μ M ST1926 treated-AML. A 30% FITC Annexin V positive shift in THP-1 was seen 12 hours post-treatment and increased to 50% after 24 hours of treatment (Figure 18). Similarly, MOLM-13 cells showed a 15% FITC Annexin V positive at 12 hours, and doubled to 30% 24 hours post-treatment (Figure 19).

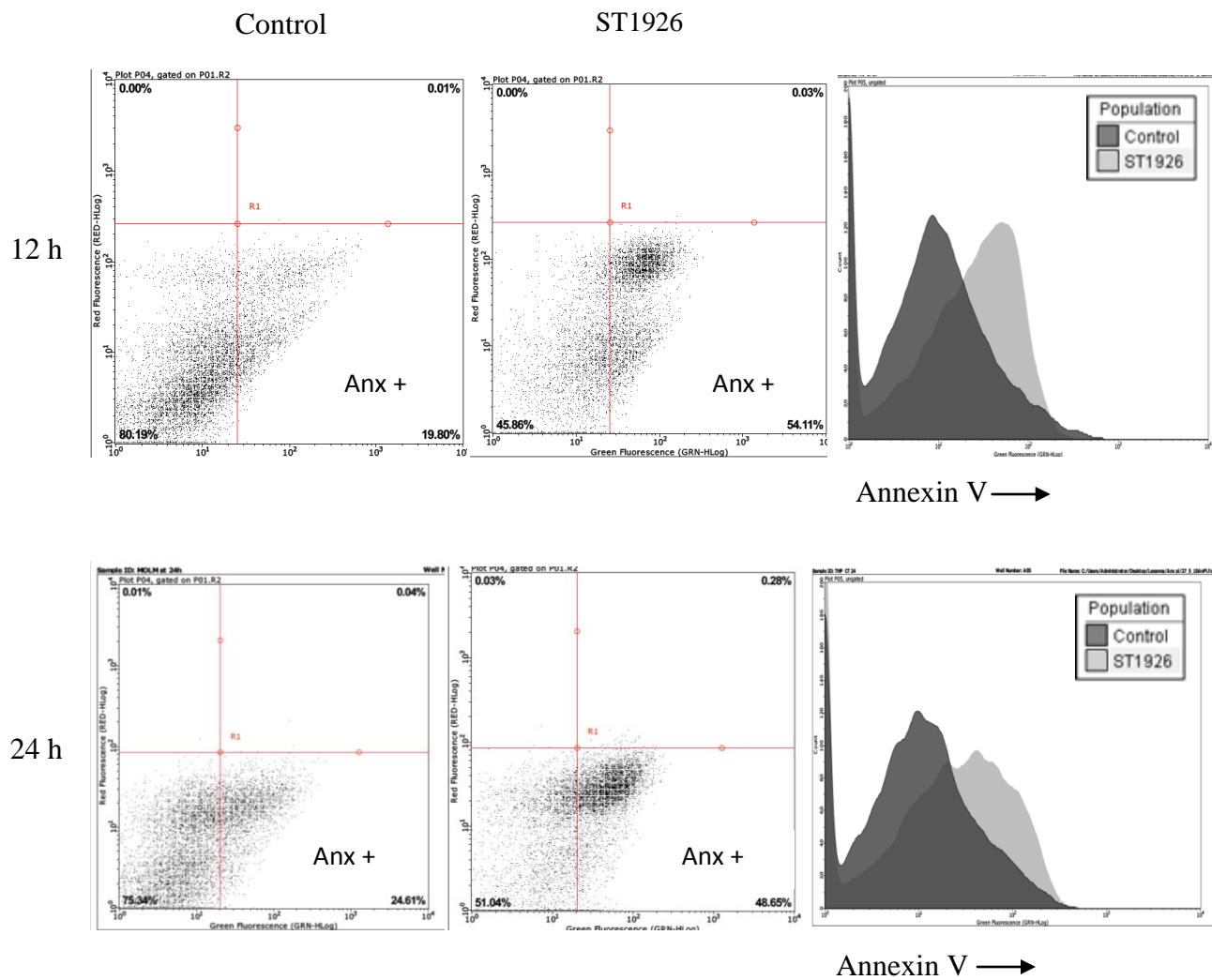


Figure 18. Early apoptosis induction in ST1926 treated THP-1 cells as evident by the Annexin V FITC-positivity using flow cytometry. THP-1 cells were seeded at a concentration of 2×10^5 cells/ml treated with 0.1% DMSO (control) or 0.5 μ M ST1926 up to 24 hours. Cells were then collected after 12 or 24 hours and exposed to Annexin V (Anx) and PI dyes for 15 min in the dark. The cells were then analyzed by flow cytometry. The results shown are representative of two independent experiments and the histograms expressing an overlay of the treated cell (light grey) compared to their respective controls (dark grey).

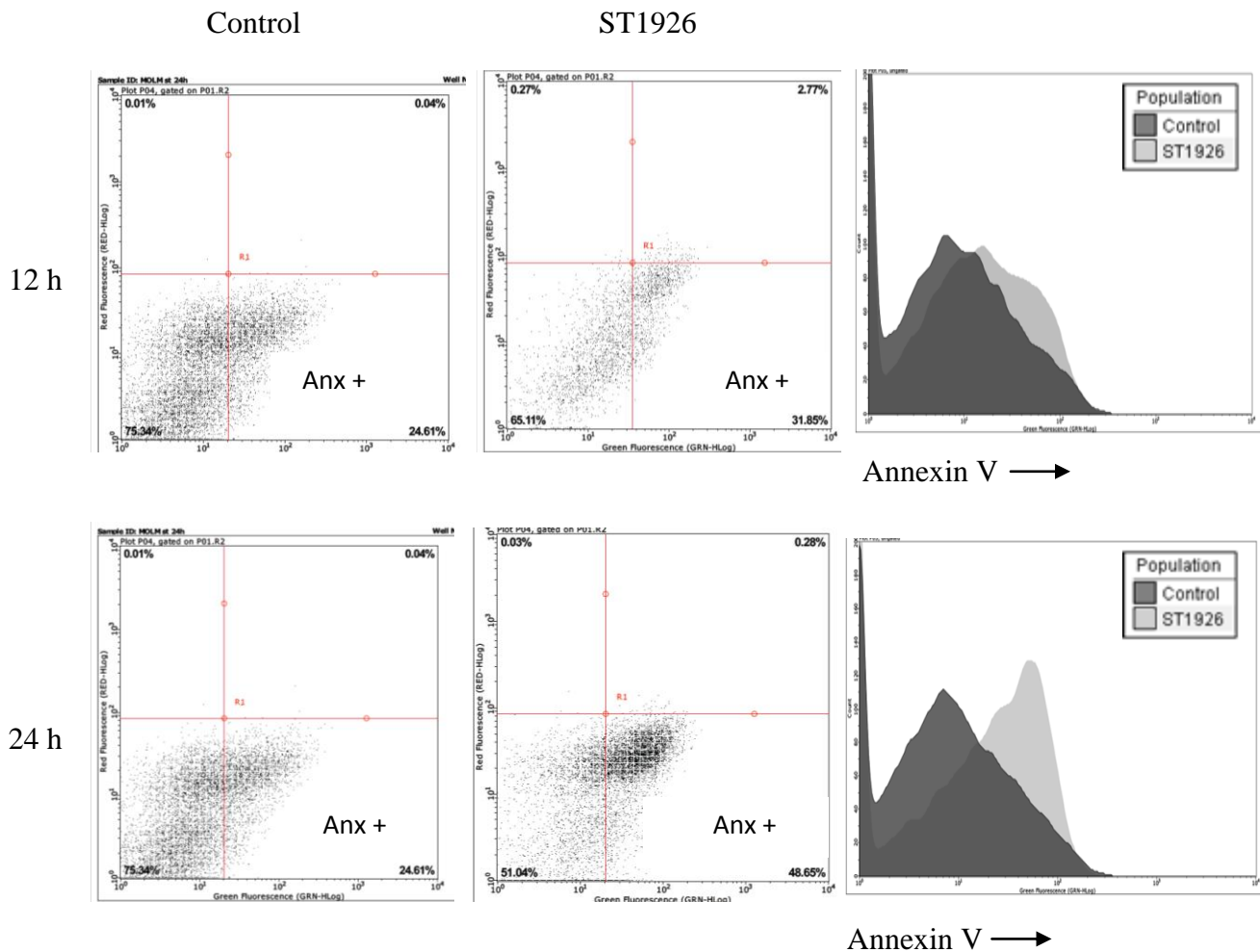


Figure 19. Early apoptosis induction in ST1926 treated- MOLM-13 cells as evident by the Annexin V FITC positivity using flow cytometry. MOLM-13 cells were seeded at a concentration of 2×10^5 cells/ml treated with 0.1% DMSO (control) or 0.5 μ M ST1926 up to 24 hours. Cells were then collected after 12 or 24 hours and exposed to Annexin V and PI dyes for 15 min in the dark. The cells were then analyzed by flow cytometry. Results shown are representative of two independent experiments and the histograms expressing an overlay of the treated cell (light grey) compared to their respective controls (dark grey).

3. ST1926 treatment of AML cells results in loss of mitochondrial membrane potential as assessed by Rhodamine-123 efflux

In many systems, apoptosis is associated with the loss of the mitochondrial membrane potential and signals through intrinsic apoptotic pathways (Desagher 2000). Accordingly, we aimed to further decipher the ST1926-induced apoptosis in AML cells through investigating its effect on the mitochondrial potential. Using Rhodamine-123 efflux assay, the mitochondrial membrane potential was monitored in the two chosen AML representative cell lines, THP-1 and MOLM-13. Rhodamine-123 is a cell permeable cationic dye that enters the mitochondria and settles there, and any depolarization of the mitochondrial potential results in the loss of Rhodamine from the mitochondria leading to a drop in the intracellular fluorescence.

AML cells were treated with 0.1% DMSO or 0.5 μ M of ST1926 for up to 48 hours and then incubated with Rhodamine-123 dye. Using flow cytometry based analysis, our results show that the intracellular fluorescence of Rhodamine-123 dye decreased significantly by 40% in THP-1 cells, one day post-treatment, and by 53% at day 2 (Figure 20). Similarly, there was a significant decrease in the intracellular Rhodamine dye in MOLM-13 cells from 25% on day 1 to 50% on day 2 post-ST1926 treatment (Figure 20). Figure 21 shows representative results from three independent experiments after flow cytometric analysis, where we display an overlay of the mitochondrial membrane dissipation of Rhodamine dye in the treated cells as compared to their respective controls for THP-1 and MOLM-13 cells. These results show the loss of mitochondrial potential upon ST1926 treatment of AML cells.

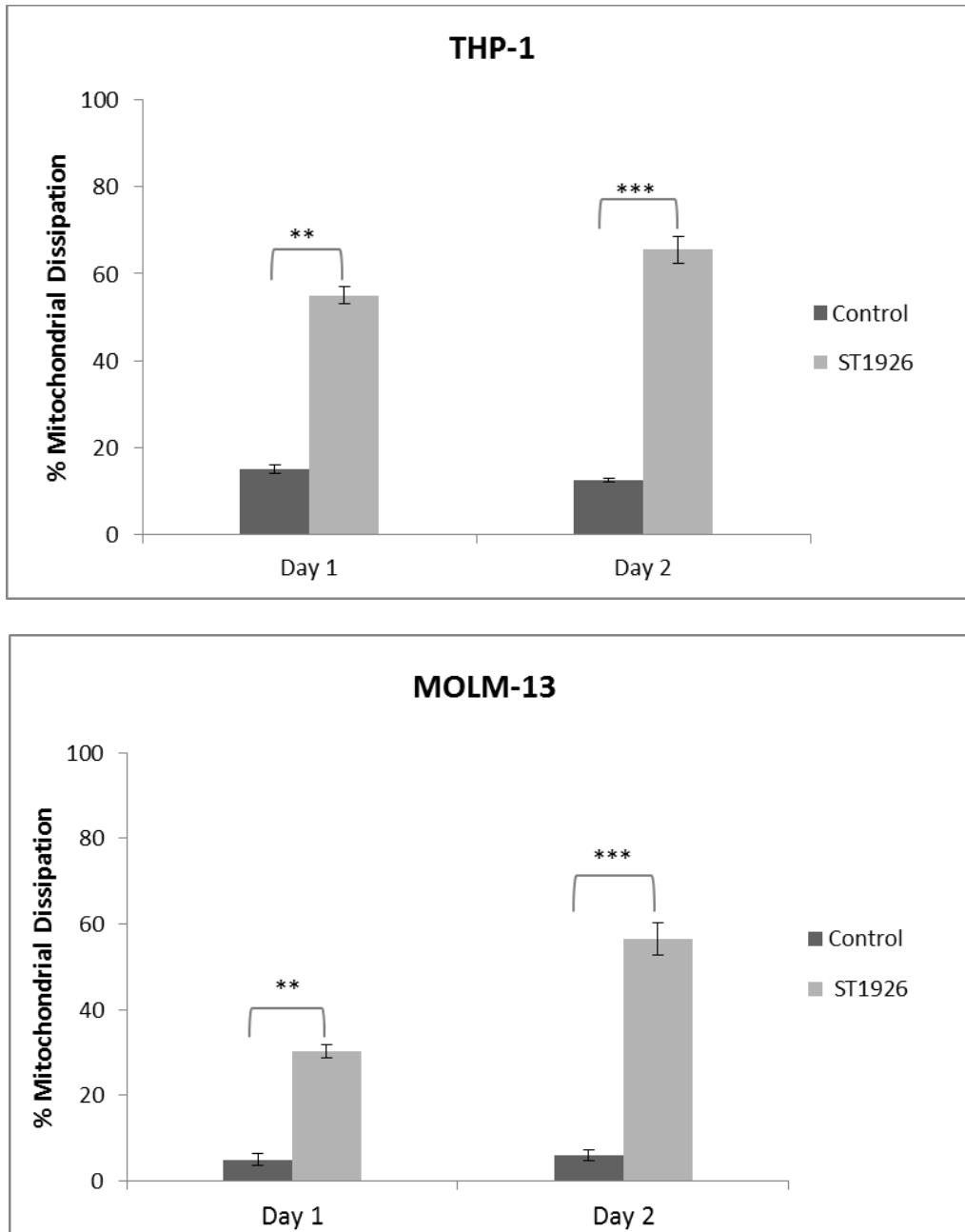


Figure 20. The percentage change in the mitochondrial membrane dissipation in ST1926-treated AML cells. THP-1 and MOLM-13 were seeded at a concentration of 2×10^5 cells/ml and treated with $0.5 \mu\text{M}$ ST1926 for up to 2 days. Cells were then exposed to $1 \mu\text{M}$ of Rhodamine-123 for 1 hour at 37°C . Then, the intracellular accumulation of Rhodamine dye was measured through FACScan flow cytometer. The change in the mitochondrial Rhodamine dye in the control to the treated cells was calculated and plotted. Results are reported as mean \pm SE and are an average of three independent experiments (*, $P < 0.05$; **, $P < 0.01$; *** $P < 0.001$).

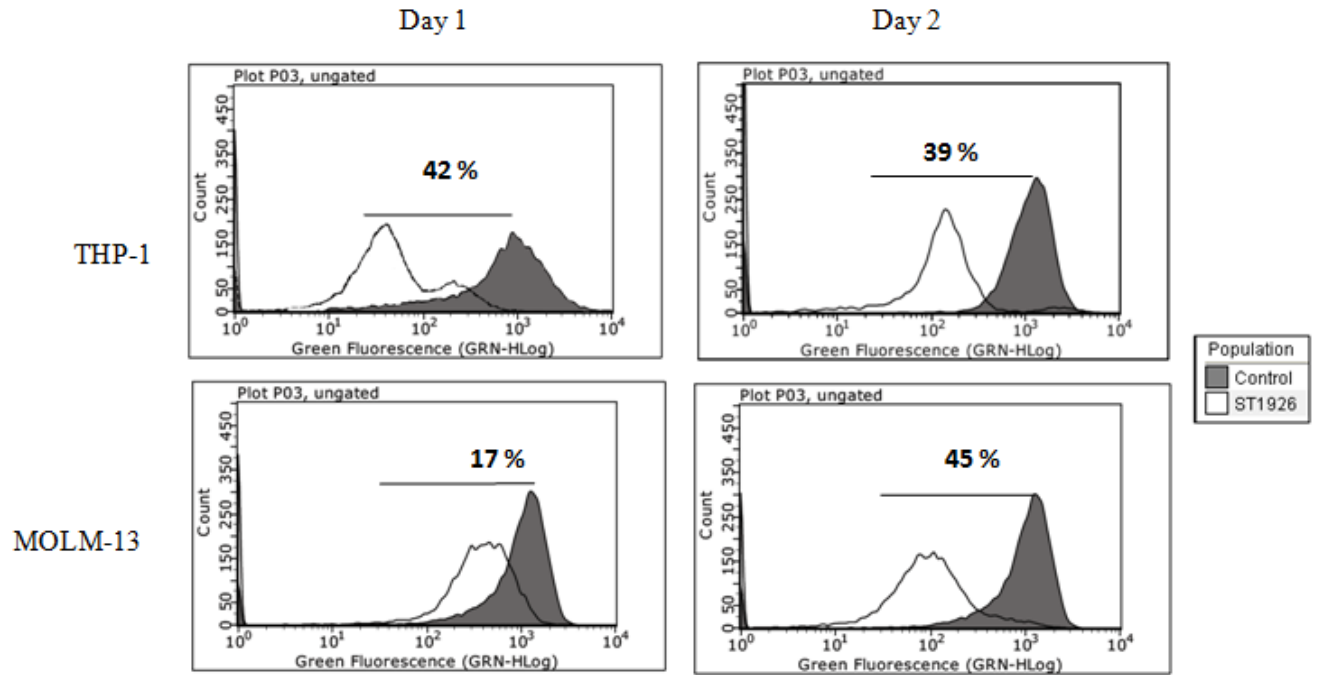


Figure 21. Loss of the mitochondrial membrane potential after ST1926 treatment of AML cells. THP-1 and MOLM-13 were seeded at a concentration of 2×10^5 cells/ml and treated with $0.5 \mu\text{M}$ ST1926 up to 48 hours. Cells were then exposed to $1 \mu\text{M}$ of Rhodamine-123 for 1 hour at 37°C . Histograms represent flow cytometry-based analysis of Rhodamine-123 fluorescence (x-axis) over cell counts (y-axis), and the panels represent an overlay of ST1926-treated cells (white) over control cells (dark grey). The results shown are representative of at least three independent experiments.

4. ST1926 induces PARP cleavage in AML-treated cells

During the execution phase of apoptosis, and upon subsequent mitochondrial membrane dissipation, several downstream signals are activated including caspases; leading to the cleavage of a 113 kDa PARP to an 89-kDa death associated fragment. Cleavage of PARP is considered to be a hallmark of apoptosis (Kaufmann 1993).

To confirm this, PARP antibody was probed on the membranes of whole cell lysates of cells treated with 0.1% DMSO or 0.5 μ M of ST1926 up to 48 hours. Our results show, that in all of the four tested AML cells; THP-1, KG1-a, MOLM-13 and ML-2, PARP cleavage was detected in the treated cells as early as 24 hours post-treatment and was pronounced after 48 hours of treatment (Figure 22).

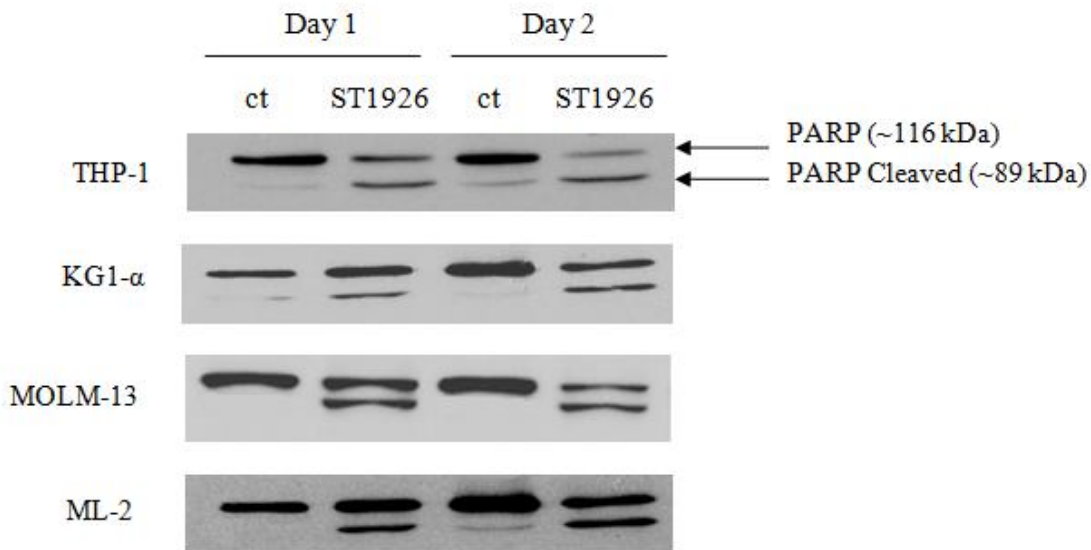


Figure 22. Induction of PARP cleavage after ST1926 treatment in AML cells. THP-1, KG1- α , MOLM-13 and ML-2 were seeded at a concentration of 2×10^5 cells/ml and treated with 0.1% DMSO (ct) or 0.5 μ M of ST1926. Cells were then collected 1 or 2 days post-treatment and the protein lysates (50 μ g/ml) were prepared and immunoblotted against PARP antibody. Results shown are representative of at least three independent experiments.

5. ST1926 treatment in AML cells increases total p53 protein levels

Another early marker of apoptosis is the initial fragmentation of genomic DNA leading to its damage and subsequent activation and upregulation of the tumor suppressor protein p53 (Leroy 2014; Muller 2014). Under normal and unstressed conditions, p53 remains undetected intracellularly due to its short half-life. Hence, overexpression of p53 can be an early detector of apoptosis, which can also be mediated through mitochondrial membrane dissipation (Muller 2014).

Under this section, we are using cell lines that further reflect the heterogeneity of AML disease in regards of *p53* status. Whilst ML-2 and MOLM-13 exhibit a wild type *p53* profile, THP-1 has a heterozygous *p53* mutation, whereas both KG1- α and HEL exhibit a homozygous mutation in *p53* (Table 3). Regardless of the status of *p53*, our results show that ST1926 manifests a potent apoptotic effect in all the tested AML cells. In fact, previous studies have already demonstrated that ST1926 induces its antitumor effects on several cancerous cells through p53-independent mechanisms (Cincinelli 2003; El Hajj 2014).

Nevertheless, we wanted to investigate the effect of ST1926 on total p53 protein levels in the AML cells that express a wild type status of the protein. Therefore, total p53 antibody was probed on the membranes of whole cell lysates of ML-2 and MOLM-13 cells, treated with 0.1% DMSO or 0.5 μ M of ST1926 up to 2 days. Our results show a remarkable increase in the expression of p53 at 24 hours post-ST1926 treatment. This increase remained notable after 48 hours in both cell lines, when compared to their respective DMSO-treated controls.

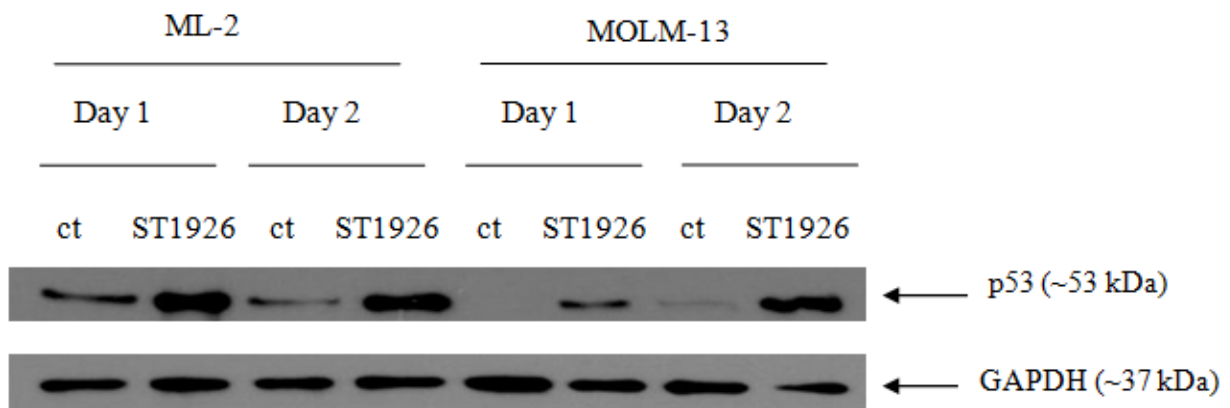


Figure 23. Increase of total p53 protein levels after ST1926 treatment of AML cells. THP-1 and MOLM-13 cells were seeded at a concentration of 2×10^5 cells/ml treated with 0.1% DMSO (ct) or 0.5 μ M of ST1926. Cells were then collected up to 2 days post-treatment and the protein lysates (50 μ g/ml) were prepared and immunoblotted against p53 antibody. Blots were also probed with GAPDH antibody to ensure equal protein loading. The results shown are representative of two independent experiments.

6. ST1926 treatment of AML cells induces early accumulation of γ H₂AX, an indication of DNA damage

One of the early triggers of p53 upregulation is DNA damage which if not repaired can ultimately lead to cellular apoptosis (Muller 2014). ST1926 has been previously characterized as a genotoxic drug that causes early DNA damage in various types of tumor cells (Valli 2008; El Hajj 2014).

Upon DNA damage, many double-stranded breaks (DSBs) are generated which is followed by a prompt phosphorylation of the histone H₂AX to γ H₂AX (Turinetto 2015). Because this phosphorylation is rapid, abundant and correlates well with each DSB, it has been considered as a sensitive marker that can be used to examine cellular DNA damage produced and its subsequent repair (Sharma 2012). Accordingly, γ H₂AX antibody was probed on the membranes of whole cell lysates of THP-1 and MOLM-13 cells, treated with 0.1% DMSO or 0.5 μ M of ST1926 for up to 12 hours. Our results show an early accumulation of γ H₂AX in both cell

lines, as early as 30 min post-treatment in MOLM-13 cells and as early as 2 hours in THP-1 cells (Figure 23).

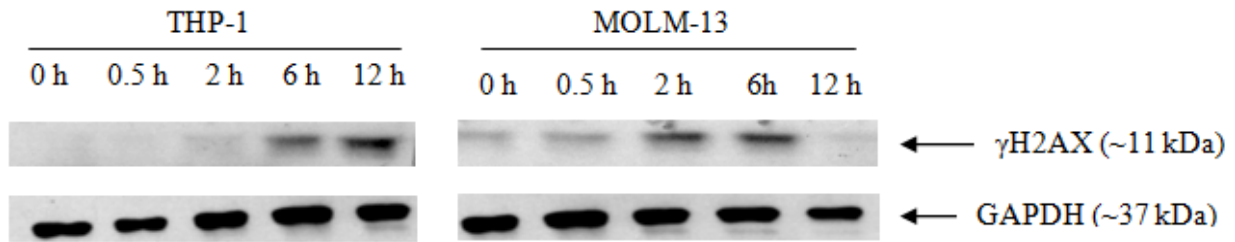


Figure 24. Early accumulation of γ H2AX following ST1926 treatment of AML cells. THP-1 and MOLM-13 cells were seeded at a concentration of 2×10^5 cells/ml treated with 0.1% DMSO or 0.5 μ M of ST1926. Cells were then collected at the indicated time points and the protein lysates (50 μ g/ml) were prepared and immunoblotted against γ H2AX antibody. Blots were also probed with GAPDH antibody to ensure equal protein loading. Results shown are representative of at least three independent experiments.

F. ST1926 induced growth-inhibitory effect on AML cells is reversed by the DNA damage inhibitor Caffeine

To further investigate the role of ST1926-induced DNA damage, Caffeine, was used in combination with ST1926 in AML cells. Caffeine is known to inhibit the ATM and ATR kinases necessary for activation of DNA damage response pathway (Sarkaria 1999). It has recently been shown that Caffeine mitigated the S-phase arrest induced by ST1926 in rhabdomyosarcoma cells and resulted in a decrease in the protein expression levels of CDK1, a key player in the cell cycle regulation and DNA damage response (Basma 2015). In our studies, the effect of ST1926 on THP-1 and MOLM-13 cells was significantly altered upon co-treating the cells with Caffeine. Treatment of ST1926 alone in THP-1 and MOLM-13 resulted in a 63% and 55% decrease in the cell growth, respectively; when the cells were co-treated with both ST1926 and Caffeine, cell growth was significantly increased to 80% and 110% of control

values, respectively (Figure 25). These results confer the genotoxic role of ST1926 in AML cell lines.

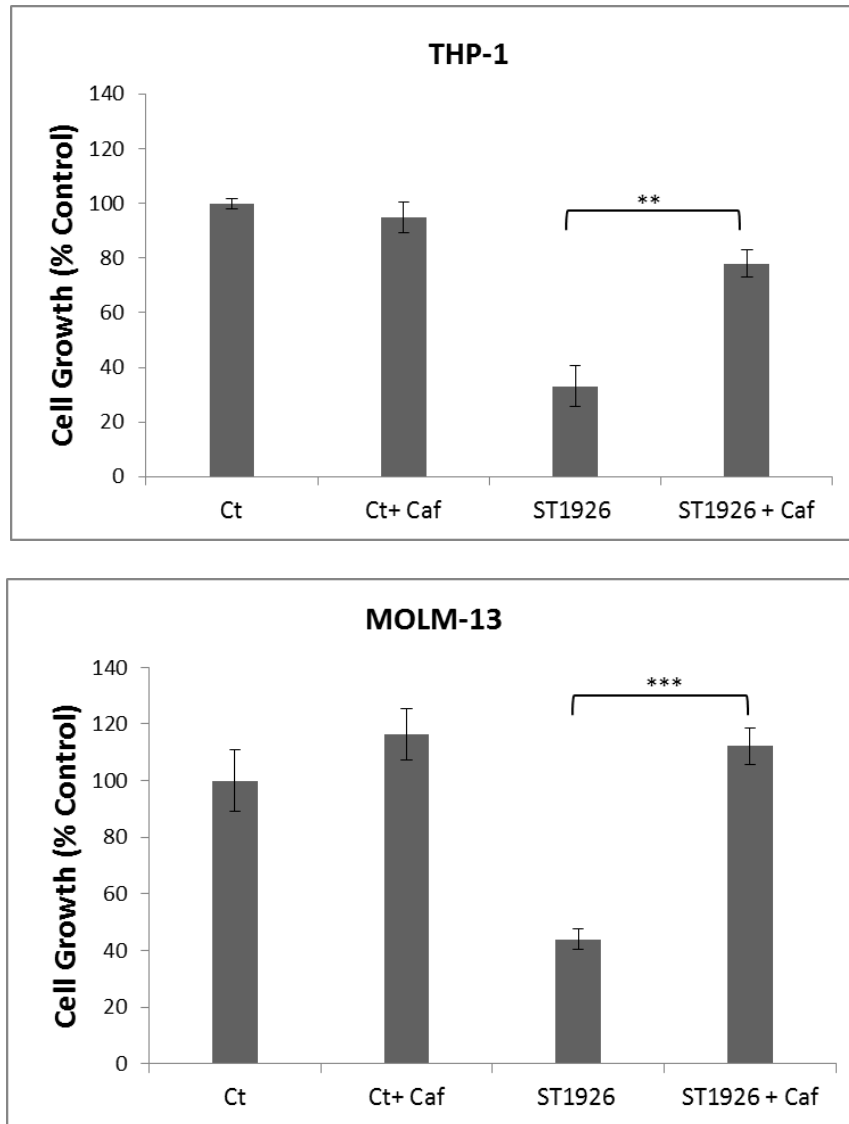


Figure 25. ST1926-induced growth inhibition in AML cells is reversed upon the abrogation of DNA damage. THP-1 and MOLM-13 were seeded at a density of 2×10^5 cells/ml. Cells were pretreated with $2 \mu\text{M}$ Caffeine for 24 hours then treated with 0.1% DMSO, $2 \mu\text{M}$ Caffeine (Caf) alone, $0.5 \mu\text{M}$ of ST1926 alone, or both ST1926 and Caffeine for up to 48 hours. Cell growth was assessed in triplicate wells using CellTiter non-radioactive cell MTT proliferation assay. The results are expressed as percentage of their control (0.1% DMSO) and are an average of two independent experiments (\pm SE) (*, $P < 0.05$; **, $P < 0.01$; *** $P < 0.001$).

G. ST1926 treatment of AML cells results in RAR γ and RXR α downregulation

Whilst ATRA is known to mediate its effect through retinoic acid signaling pathway (Altucci 2001), we wanted to first investigate the effect of ST1926 on the expression levels of some retinoic acid receptors in AML cells, where it has been shown that their downregulation can be correlated with apoptosis or cellular differentiation (Kam 2012). Therefore, RAR γ and RXR α were probed on the membranes of whole cell lysates (100 μ g) of THP-1 and MOLM-13 cells treated with 0.1% DMSO or 0.5 μ M of ST1926 up to 48 hours. Our results show a decrease in the protein expression levels of both receptors at 24 hours post-ST1926 treatment. This decrease persisted after 48 hours of the treatment (Figure 26).

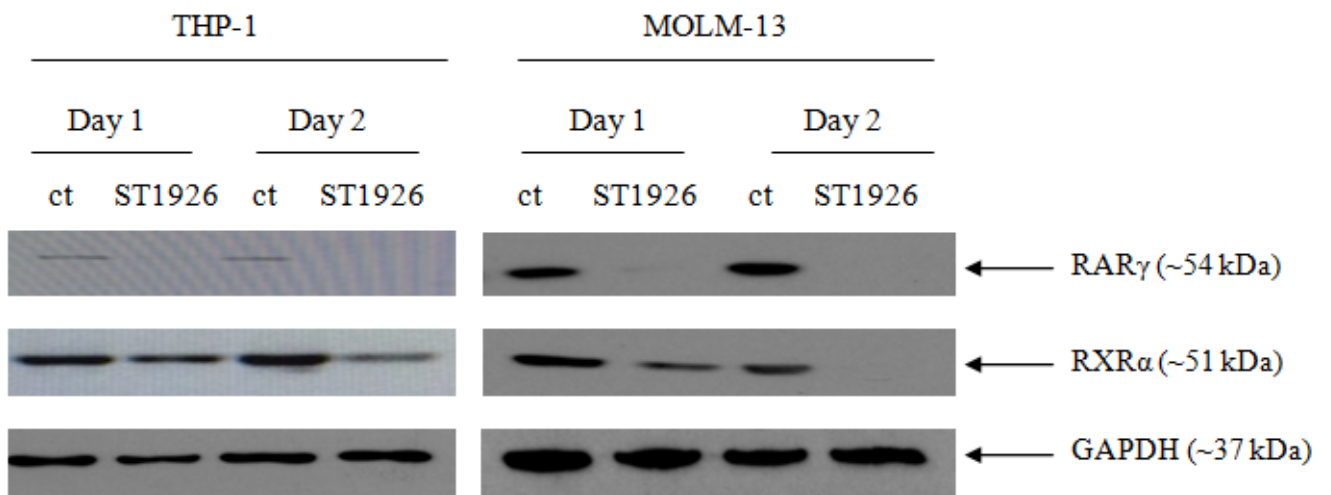


Figure 26. RAR γ and RXR α downregulation following ST1926 treatment of AML cells . THP-1 and MOLM-13 cells were seeded at a concentration of 2×10^5 cells/ml treated with 0.1% DMSO (ct) or 0.5 μ M of ST1926. Cells were then collected up to 48 hours post-treatment and the protein lysates (100 μ g/ml) were prepared and immunoblotted against RAR γ and RXR α antibody. Blots were also probed with GAPDH antibody to ensure equal protein loading. Results shown are representative of two independent experiments.

H. ST1926 growth-inhibitory effect is independent of the RAR signaling pathways

The decrease in expression levels of the retinoid receptors upon ST1926 treatment evoked us to further investigate the dependency of ST1926 on this pathway. It has been previously shown in our laboratory that ST1926 anti-growth effect is not mediated through the retinoic acid receptors pathway in CML lines (Hmadi MS AUB 2013). To verify whether ST1926 effect in AML cell lines is independent on the retinoid receptors signaling pathways, THP-1 and MOLM-13 were treated with the pan-RAR inverse agonist, BMS493. Blocking RARs abrogates the whole retinoid-receptor signaling pathway including RXR, since they cannot modulate their target genes in the absence of RARs bound ligands (Altucci 2001). Accordingly, AML cells were pre-treated with 1 μ M BMS493 for 20 min, then cells were treated with 0.1% DMSO or 0.5 or 1 μ M concentrations of ST1926. Using MTT assay, we found that ST1926-induced growth inhibition in the tested AML cells were not affected in the presence of BMS493 (Figure 27).

C8166 ATL cell line was used as a positive control for BMS493. C8166 is sensitive to ATRA, where 3 μ M ATRA was shown to reduce 70% of cell growth, 72 hours post-treatment (Darwiche 2001, Darwiche 2004). Therefore, we reproduced the data by treating C8166 cells with 3 μ M ATRA up to 3 days in the presence and absence of BMS493. Our results show that BMS493 reversed ATRA-induced growth inhibition in C8166 cells after 72 hours of treatment, from 80% to 30% (Figure 28). These results confirm that ATRA-induced growth inhibition in C8166 cells is retinoid-receptor dependent and that BMS493 is blocking RARs, abrogating the retinoid-receptor signaling pathway.

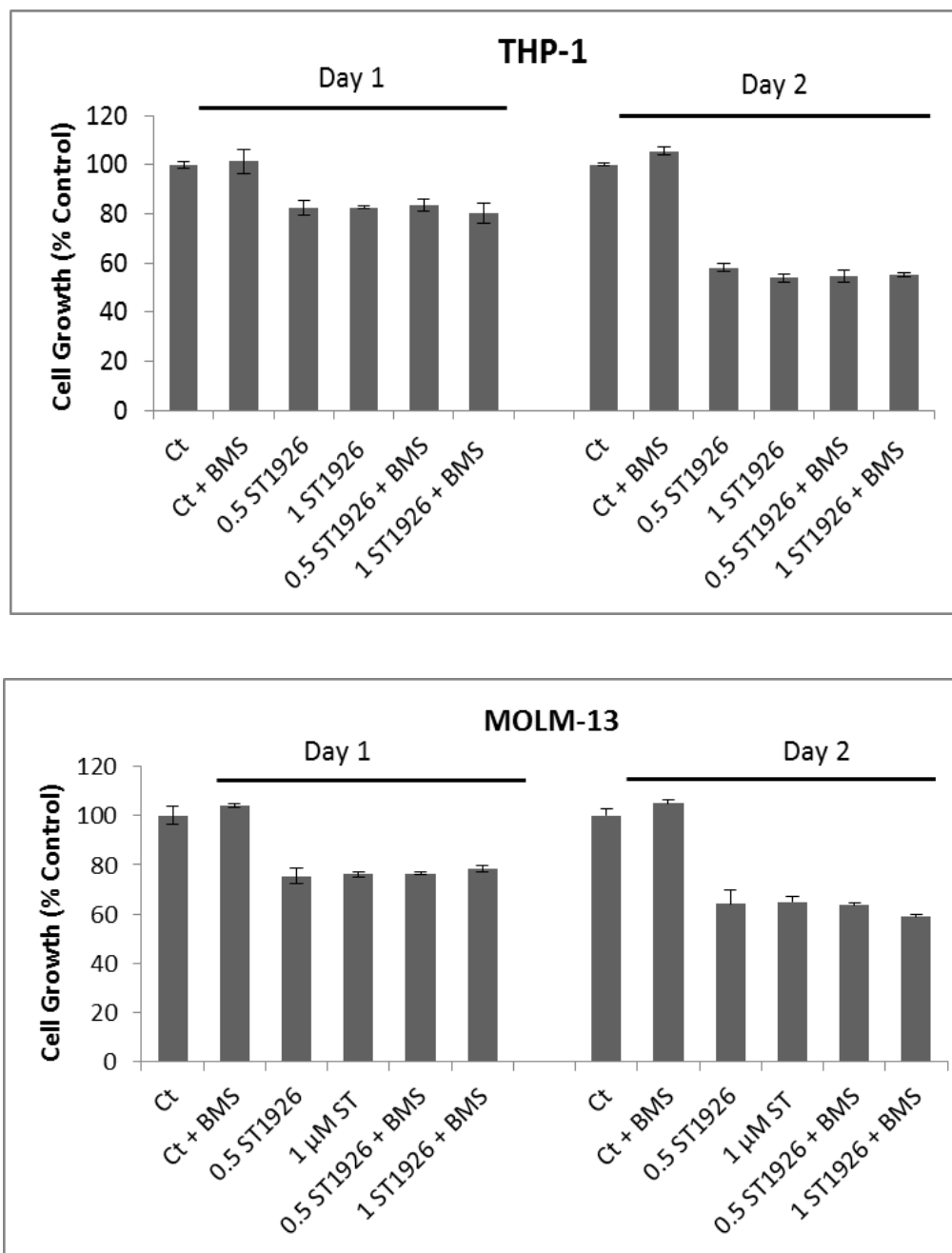


Figure 27. ST1926-induced growth inhibition effect is independent of the retinoid receptor signaling pathway. THP-1 and MOLM-13 were seeded at a density of 2×10^5 cells/ml. Cells were pretreated with $1 \mu\text{M}$ BMS493 (BMS) for 20 min then treated with 0.1% DMSO (ct), 0.5 or $1 \mu\text{M}$ ST1926 for up 48 hours. Cell growth was assayed in triplicate wells using CellTiter non-radioactive cell MTT proliferation assay. Results are expressed as percentage of control (0.1% DMSO) and are an average of two independent experiments (\pm SE).

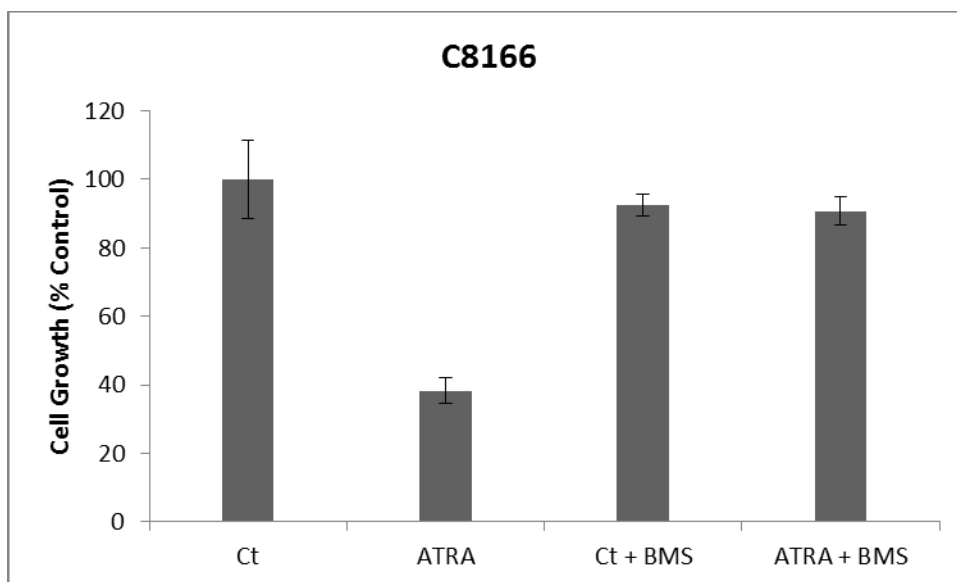


Figure 28. ATRA-induced growth inhibition in the C8166 is reversed by the pan-RAR inverse agonist BMS493. C8166 cells were seeded at a density of 2×10^5 cells/ml. C8166 cells were treated with 0.1 % DMSO, 1 μ M BMS493 (BMS), or pre-treated with 1 μ M BMS493 for 20 min then treated with 3 μ M ATRA up to 72 hours. Cell growth was assayed in triplicate wells using CellTiter non-radioactive cell MTT proliferation assay. Results are expressed as percentage of control (0.1% DMSO) and are an average of two independent experiments (\pm SE).

I. ST1926 at sub-micromolar concentrations re-sensitize ATRA-resistant THP-1 to ATRA

As mentioned previously, the tested AML cell lines used are all ATRA-resistant cells. ST1926 was found to be a genotoxic drug that causes DNA damage and mediates its effect through RAR independent mechanisms in the tested AML cells. Therefore, we wanted to investigate whether co-treatment of the AML cells with ST1926 and ATRA would re-sensitize the cells to ATRA. Subsequently, THP-1 cells were treated with varying concentrations of ATRA (0.5, 1, or 3 μ M) in the presence or the absence of ST1926. The concentrations of ST1926 used were as low as 0.05 and 0.075 μ M, and these concentrations have shown to have no or minimum effect on the growth of AML cells upon single treatment. Interestingly, our preliminary results show that, after 72 hours of treatment, and at 0.05 μ M concentrations of

ST1926, the percentage growth of THP-1 cells dropped to 60%, 40%, and 25% at ATRA concentrations of 0.5, 1 and 3 μM , respectively (Figure). Notably, the same concentrations of ATRA or ST1926 used as single treatments had no or minimal effect on THP-1 cells.

Similarly, at 0.075 μM concentrations of ST1926, the percentage growth of THP-1 cells dropped to 40%, 45%, and 15% at ATRA concentrations of 0.5, 1 and 3 μM , respectively (Figure 29). Moreover, the same concentrations of ATRA or ST1926 alone had no or minimal effect on THP-1 cells. These results highlight a potential role of ST1926 in re-sensitizing ATRA resistant cells to ATRA that can have a significant implications in future clinical research.

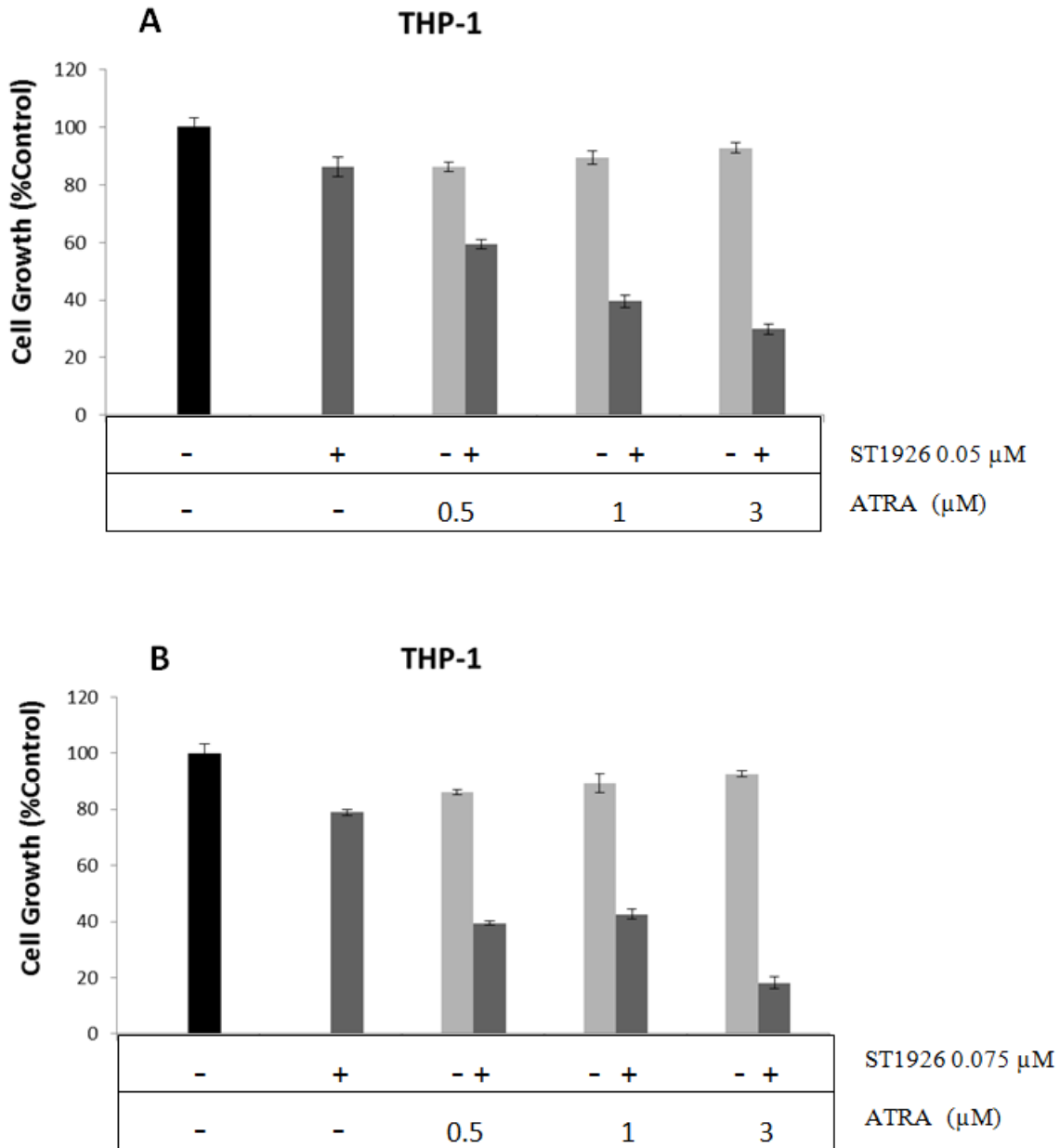


Figure 29. ST1926 at sub-micromolar concentrations re-sensitize ATRA-resistant AML cells. THP-1 cells were seeded at a density of 2×10^5 cell/ml. Cells were treated with 0.1% DMSO (-), ATRA alone at the indicated concentrations, 0.05 μM (A) or 0.075 μM (B) ST1926 alone, or both ST1926 and ATRA for up to 3 days. Cell growth was assayed in triplicate wells using CellTiter non-radioactive cell MTT proliferation assay at 72 hours. The results are expressed as percentage of their control (0.1% DMSO) (\pm SD).

J. Nanoparticle formulation of ST1926

It is important to note that solubility and bioavailability problems are both major reasons for many drug candidates to fail in preclinical development, and appropriate measures should be taken to address these issues. ST1926 is a highly hydrophobic drug that was found to undergo major glucuro-conjugation leading to its poor bioavailability and rapid excretion by the liver (Sala 2009). Therefore, to prolong the ST1926 plasma half-life before testing it *in vivo*, we generated polymer coated ST1926 nanoparticles using Flash Nanoprecipitation technique (Liu 2008). ST1926 was formulated into nanoparticles with a drug to polymer mass ratio of 1:5. 5 mg of ST1926 and 25 mg of polystyrene-*b*-poly(ethylene oxide) block copolymer (PS1.5-PEO2.4) with a polystyrene hydrophobic block. The resulting solution was mixed at an optimized rate using the MIVM mixer. We determined the nanoparticle size using DLS apparatus, which correlated the frequency shift in the Brownian motion of the particles to their size. ST1926 formulated nanoparticles size was 230 nm, and remained stable at room temperature even after 24 hours (Figure 30).

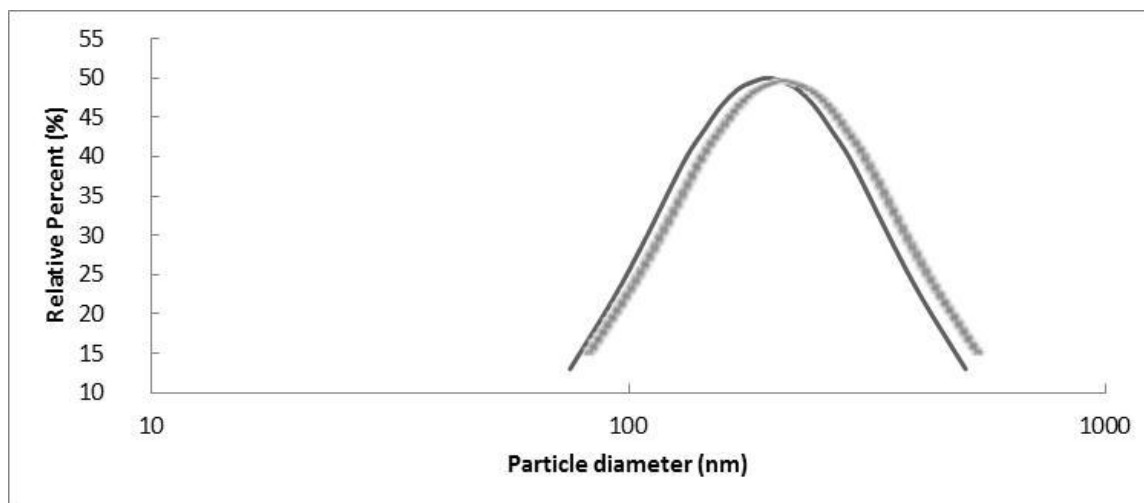


Figure 30. Intensity-based particle size distribution of the formulated ST1926 nanoparticles. The size of the polymer-coated ST1926 was as obtained by the DLS initially (black) and 24 hours (grey) time points using number-weighted particle size distribution. The mean ST1926 nanoparticle was 230 nm, and remained stable at room temperature beyond 24 hours.

K. ST1926 exhibited similar growth-inhibitory effect in AML cells as its nanoparticle formulation

To test whether formulating the drug as nanoparticles can influence the efficacy of ST1926 *in vitro*, THP-1 and MOLM-13 cells were treated with the same concentrations of ST1926 and its formulated nanoparticle (ST1926-NP) and their cell growth was assayed using MTT proliferation assay. The concentrations of ST1926 and ST1926-NP used ranged from 0.05 to 5 μM . Interestingly, cell growth inhibition by ST1926 wasn't affected by nanoparticle formulation. In fact, ST1926 exhibited similar growth-inhibitory effect as its nanoparticle formulation with an estimated IC_{50} of 0.5 μM at 48 hours for both treatments, and in both cell lines (Figure 31).

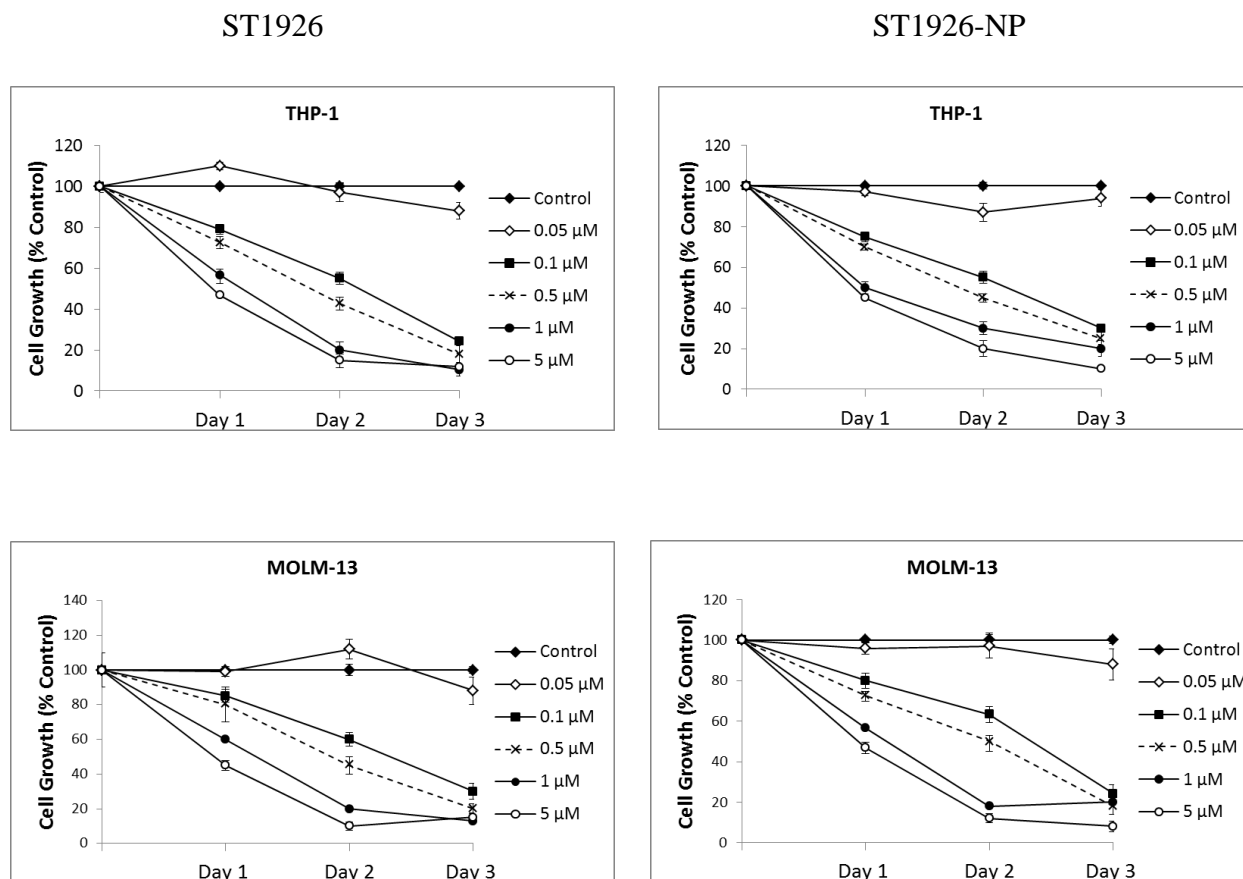


Figure 31. Effect of ST1926 and its nanoparticle formulation on the proliferation of AML cells using MTT assay. THP-1 and MOLM-13 cells were seeded at a concentration of 2×10^5 cells/ml and treated with 0.1% DMSO or indicated concentrations of ST1926 or its nanoparticle formulation (ST1926-NP) for up to 72 hours. Cell growth was assessed in triplicate wells using CellTiter non-radioactive cell MTT proliferation assay. The results are expressed as a percentage of control (0.1% DMSO) and they represent an average of two independent experiments (\pm SE).

L. Generation of AML xenograft mouse model

Using *in vitro* human cell lines is a valid tool for drug screening. However, its limitations reside at the genotypic level, where it fails to engage the microenvironment that has a significant role in cancer progression. As such, *in vitro* models are not sufficient for predicting the drug's mode of action in patients. Hence, in order for us to confirm the results obtained *in vitro*, we reproduced two AML xenograft mouse models (Shen 2007; Moore 2012), to further be used in future *in vivo* treatments.

First of all, the protocol was approved by the Institutional Animal Care and Utilization Committee (IACUC) of the American University of Beirut. Subsequently, NOD-*scid* IL2 γ ^{null} mice were intraperitoneally injected with 5×10^6 MOLM-13 or THP-1 AML cells (5 mice for MOLM-13 and 3 for THP-1, due to the mice availability). The health status of the mice and the possible nodules formation around the abdominal region were monitored every other day, over the period of 4 weeks. Nodules around the abdominal region were observed as early as two weeks in both AML xenograft mouse models. The survival of both mice over the course of a month is shown in Figure 32 and will be used as a standard in future therapy experiments. Xenografted animals started dying 25 days post-injection of the AML cells, where they all died by day 35 (Figure 32).

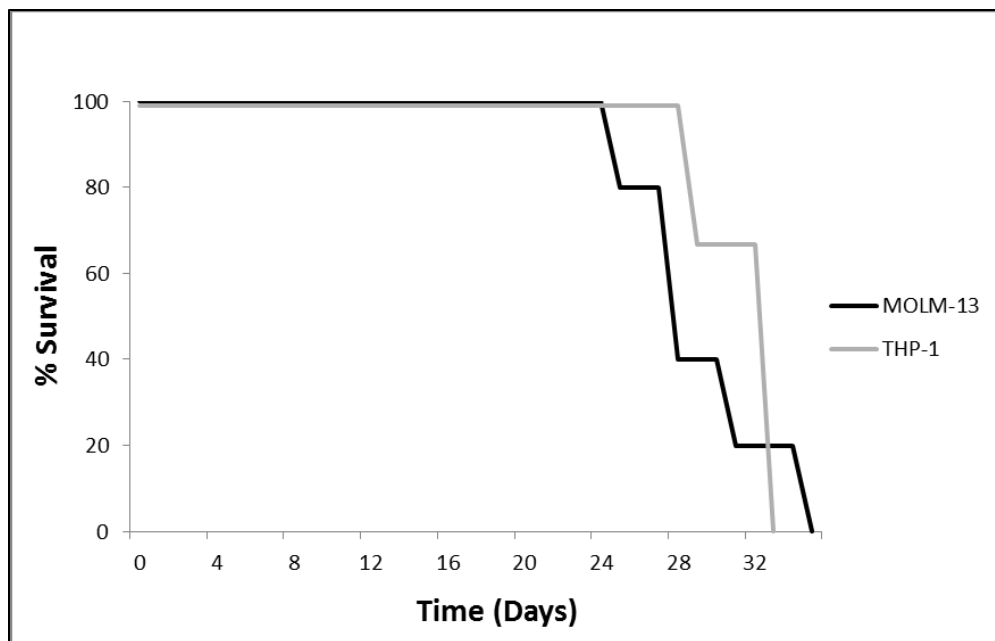


Figure 32. Survival graph of the generated AML xenografted mouse models.

NOD-*scid* IL2 γ^{null} mice were intraperitoneally injected with 5×10^6 MOLM-13 or THP-1 AML cell lines. Overall survival of the mice was recorded and plotted, and will be used as a standard for later experiments.

CHAPTER IV

DISCUSSION

Acute myeloid leukemia is the most common form of acute leukemias among adults and accounts for the largest number of annual deaths due to blood malignancies in the USA (Siegl 2015). It is a highly heterogeneous and clonal disorder with a very complex and big diversity of karyotypes among the patients (Martens 2010) dictating a difference in treatment regimens and yet a high still occurring number of deaths. Even though treatments of AML have improved over the past 30 years, more than 50% of young adults and 90% of older patients still die of the disease (Estey 2006).

Retinoic acid is a biologically active metabolite of vitamin A that regulates the growth and differentiation of a wide variety of cell types (Gudas 2012). ATRA is the most potent available derivative of RA and is established as the treatment of choice for patients suffering from APL (de Thé 2010), an AML M3 subtype accounting for around 5–10% of cases of AML. ATRA induces promyelocytes with PML-RAR α to differentiate into mature granulocytes, and its combination with arsenic induces degradation of PML-RARA α , curing APL in mice (Ablain 2014; Lallemand-Breitenbach 1999; Nasr 2008) and patients (Lo-Coco 2013; Ravandi 2009; Shen 2004).

However, in non-APL AML patients, ATRA is only effective on those presenting with *NPM-1* mutations but not the other subtypes (Glasow 2005). In fact, even in APL, several intrinsic mechanisms of ATRA resistance have been recently identified, ultimately leading to disease relapse (di Masi 2015). Clinical strategies aiming to overcome this resistance and to

target all AML subtypes include efforts to reduce toxicity, retain bioavailability, and develop effective combination regimens. One of the approaches includes the use of synthetic, non-classical retinoids that have retinoid receptor-independent properties, or that would bypass RAR signalling pathway repression. Of the promising synthetic retinoids with anti-neoplastic activities, increased bioavailability, and reduced toxicity, the adamantyl retinoid ST1926 presents all these properties (Cincinelli 2003; Basma 2015).

ST1926 showed significant antitumor potential in APL models (Grattini 2004; Fratelli 2013). However, to the best of our knowledge, no reports have been published to date about ST1926 effect in non-APL AML subtypes which accounts for ~90% of the disease. Hence, this is the first study to elucidate the anti-neoplastic properties and mechanism of action of ST192 in non-APL AML models.

To represent the heterogeneity and genetic complexity of the disease, we selected five ATRA-resistant AML cells harboring different genetic mutations and corresponding to many AML karyotypes. We found that ST1926 significantly inhibited the cell proliferation and viability of all tested AML cells at sub- μ M concentrations through activation of DNA damage pathways, resulting in mitochondrial-mediated apoptosis and inhibition of the cell cycle progression. This ST1926 mechanism of action was shown to be similar to other previously tested hematological malignancies (Grattini 2004; Fratelli 2013; El Hajj 2014; Nasr 2015) and solid tumors (Zuco 2004; Di Francesco 2007; Milli 2011; Basma 2015).

Importantly, and in addition to ST1926 -inhibited cell proliferation and viability of all tested AML cells, ST1926 exerted the same inhibitory effect on primary derived cells from two AML patients, at sub- μ M concentrations even as low as 0.1 μ M, while sparing normal resting, and activated lymphocytes (El Hajj 2014). This growth-inhibitory effect of ST1926 was

irreversible even three days post-drug removal, which is in agreement with several other reports (Zuco 2005; our unpublished data). We noted that ST1926 mostly induced the accumulation of the cells in the pre-G₁ phase of the cell cycle with a minor G₀/G₁ phase arrest in KG1- α , MOLM-13, and ML-2; and a minor S-phase arrest in the THP-1, after one day of treatment. Pre-G₁ cell accumulation presumably indicates cell death by apoptosis (Kandeel 2015). The pro-apoptotic efficacy of ST1926 on the treated AML cells was confirmed through Annexin V/PI assay that revealed early apoptosis induction. Furthermore, we observed a loss in the mitochondrial membrane potential post-ST1926 treatment of the tested AML cells as assessed by Rhodamine efflux assay. Similar results were observed upon ST1926 treatment of CML cells (Nasr 2015).

Upon mitochondrial membrane dissipation, several downstream signals are activated including caspases, which lead to a subsequent cleavage of a PARP to its death associated fragment that is considered to be a hallmark of cancer (Kaufmann 1993). Our results show that ST1926 treatment induced PARP cleavage in the tested AML cells, suggesting a caspase-dependant mechanism of apoptosis. It has been previously shown that ST1926-induced apoptosis is partially caspase-dependent in ATL and CML treated models (El Hajj 2014; Nasr 2015). Additional studies are planned to confirm the involvement of caspase in ST1926-induced apoptosis using the pan-caspase inhibitor z-VAD.

Another early and substantial marker for apoptosis is the initial activation and upregulation of the tumor suppressor p53 (Leroy 2014; Muller 2014). In AML, p53 mutations are less common; however, they occur at higher frequency in older patients or with patients in relapse (Stirewalt, 2001). We found that regardless of p53 status, ST1926 manifests a potent apoptotic effect in all tested AML cells. In fact, previous studies have demonstrated that ST1926 induces its antitumor effects in several cancerous cells through p53-independent mechanisms

(Cincinelli 2003; El Hajj 2014). Nevertheless, when investigated, ST1926 was shown to increase the expression of total p53 levels in AML cells with wild type *p53* status. Hence, the importance of ST1926 lies in its antitumor efficacy irrespective of *p53* status, which is important for treatment of relapsed and resistant tumors where p53 signaling pathway may be compromised.

Furthermore, one of the early triggers of p53 upregulation is DNA damage that ultimately leads to cellular apoptosis (Muller 2015). ST1926 has been previously characterized as a genotoxic drug that causes early DNA damage in various types of tumor cells (Zuco 2005; Fratelli 2013; Valli 2008; El Hajj 2014). H₂AX phosphorylation to γ H₂AX is considered as a sensitive marker that can be used to examine cellular DNA damage produced and its subsequent repair (Sharma 2012). Our results show an early accumulation of γ H₂AX in the ST1926-treated AML cells indicating early DNA damage. To further investigate the role of ST1926-induced DNA damage, AML cells were treated with ST1926 in combination with Caffeine, a DNA damage inhibitor. Caffeine was recently shown to attenuate the S-phase arrest induced by ST1926 in rhabdomyosarcoma cells and resulted in a decrease in the protein expression levels of the cyclin dependent kinase 1 (CDK1), a key player in the cell cycle regulation and DNA damage responses (Basma 2015). Similarly, we showed that upon co-treatment of ST1926 with Caffeine, the anti-growth effect of ST1926 was reversed. These results confirm the potential antitumor role of ST1926 in early DNA damage induction and its subsequent repair.

All the tested ATRA-resistant AML cells were shown to be sensitive to ST1926 regardless of their mutational status. Knowing that ATRA mediates its activity primarily by targeting members of the RAR subfamily, namely RAR α , RAR β and RAR γ (di Masi 2015), we

wanted to investigate the effect of ST1926 on the expression levels of some retinoid receptors in AML cells, where it has been shown that their downregulation can be correlated with apoptosis or cellular differentiation (Kam 2012). We showed that ST1926 decreased the protein expression levels of RAR γ and RXR α in the treated AML cells. Such results evoked us to further investigate the dependency of ST1926 on the RAR signaling pathway in AML cells by pre-treating the cells with the pan-RAR inverse agonist, BMS493. Blocking RARs abrogates the whole retinoid-receptor signaling pathway including RXR, since they cannot modulate their target genes in the absence of RARs bound ligands (Altucci 2001). We found that ST1926-induced growth inhibition in the tested AML cells is independent of the retinoid receptor signaling pathway. These results are in agreement with our previous studies where ST1926-induced growth inhibition in CML cells was shown to be independent of retinoid receptor signaling pathway (Hmadi MS AUB 2013). Recently, the non-genomic effects of ATRA have been highlighted, where it has been shown to activate multiple kinase signaling pathways leading to transcriptional effects independent of nucleolar RARs *via* transcription factors that lie at the end of these signaling cascades (Schenk 2014). It remains to be investigated whether ST1926 also regulated, similar to ATRA, several non-genomic pathways, and independent of the classical mechanism of nuclear receptor action.

ATRA in APL has been the paradigm of targeted therapy for oncogenic transcription factors, where the effective differentiation of APL cells by ATRA is only observed in cells that harbor the PML-RAR α fusion gene (de Thé 2010). However, in spite of its success in achieving CR, APL patients receiving ATRA treatment alone do not achieve definite cure of the disease (Arteaga 2013). Although refined APL treatment regimens in combination with anthracycline-based chemotherapy or arsenic result in 90% of initial CR, a significant proportion of patients

still relapse and are resistant to the treatment with 3 years overall survival in second remission of only around 50% (Sanz and Lo-Coco, 2011). Also, while the success of ATRA treatment in APL sets the stage for targeted therapy of oncogenic transcription factors, it is only effective in non-APL AML patients presenting with *NPM-1* mutations but not the other subtypes, where arsenic and ATRA combinations were shown to synergistically induce proteasome-mediated degradation of mutant NPM-1, resulting in differentiation, growth arrest and apoptosis (El Hajj 2015; Martelli 2013). However, this drug combination was found to improve the disease but not cure it (El Hajj 2015). This is because targeted cancer therapy usually does not yield a sustained tumor eradication, where few drug-resistant cancerous clones can eventually lead to disease relapse. Therefore, the use of multiple drugs to target several deregulated signaling pathways in the tumor can trigger synergetic effects and sustained antitumor response.

In this study, we showed that combining sub- μ M concentrations of ATRA and ST1926, that do not have any effect as a single treatment, displayed a synergetic growth inhibitory effect in the tested AML cells. These findings provide important molecular insights into ATRA response and a promising venue for overcoming ATRA resistance. Additional experiments will be performed in the future to test whether ST1926 is activating ATRA-driven differentiation pathways in AML ATRA-resistant cells.

Therefore, ST1926 was shown to inhibit the growth of all the tested ATRA-resistant AML cells, regardless of the complex and diverse mutational status they harbor, in contrast to ATRA which exerts its effects only on NMP- 1-mutant AML subtypes.

Even though no major toxicities were encountered when ST1926 was tested in a Phase I trial for patients with ovarian cancer, it was found to undergo major glucuro-conjugation on its

phenolic hydroxyl group leading to its poor bioavailability and rapid excretion by the liver (Sala 2009). However, in recent pharmacokinetic studies, ST1926 was shown to achieve adequate plasma concentration levels and to exert significant extravascular distribution in rhabdomyosarcoma xenografted mouse models, contributing to its antitumor activities *in vivo* (Basma 2015). Lately, there has been a sharp decline in the number of new drug approvals in the pharmaceutical industry, where only 15% of molecules entering clinical trials receive marketing approvals (Curry 2008), where it has been shown that poor pharmacokinetic profile of the drugs majorly contributed to their withdrawal from clinical development (Kerns 2015). Estimates of 40% of approved drugs are poorly soluble intravenously, and undergo metabolism leading to their rapid excretion (Loftsson 2010). In our case, there have been multiple efforts in synthesizing derivatives of ST1926 to reduce its glucuronidation (Giannini 2012). One of these derivatives, namely ST5589 showed antitumor activity in lymphoma pre-clinical models, phenocopying the preclinical activity of ST1926; however it was shown to revert fast to its parental drug (Bernasconi 2015).

Fortuitously, several novel technologies are being recently deployed to address drug solubility and bioavailability issues. The use of nanotechnology in medicine is an emerging tool for addressing these challenges where it is expected to change the landscape of pharmaceutical and biotechnological industries in the foreseeable future (Bhattacharyya 2009; Lamba 2006; Malakar 2012). Encapsulating the drugs in nanoparticles can increase their efficacy, prolong their half-life, and improve their targeting to tumor cells (Basavara 2014). The tumor vasculature is more porous than the normal cells and this allows the concentration of the nano drug carriers at the tumor sites. This process is regarded as EPR, and is considered to be a passive targeting of the drugs in cancer treatment (Danhier 2010).

In an attempt to prolong the ST1926 plasma half-life of AML cells before testing it *in vivo*, we generated polymer-stabilized ST1926 nanoparticle formulations of the drug using FNP (Liu 2008). The hydrophilic block used was PEG, where it has been shown to prolong the nanoparticles circulation time *in vivo* (Zhang 2008). We showed that that native ST1926 and its nanoparticle formulation had comparable antitumor activities and IC₅₀ values in the tested AML cells. We intend to monitor and optimize ST1926-NP formulations stability over time through DLS and HPLC. Additionally, ST1926-NP will be further characterized in order to quantify drug loading content and encapsulation efficiency. These properties will then be optimized based on further biological assays' results. In particular, we are interested in monitoring cellular intake behavior through the use of isotopes or fluorescent tagging. This will allow us to further compare structure-function relationships to explain enhanced drug effect.

Several studies have highlighted the use of passive targeting of nanoparticle-encapsulated drugs in enhancing their therapeutic efficacy and bioavailability (Basavaraj 2014). Doxil, the PEGylated liposome encapsulated formulation, was the first nanodrug used to treat metastatic ovarian cancer and Kaposi's sarcoma (Barenholz 2012). The nanoparticle formulation was shown to prolong the drug's half-life, where 90% of the drug remained in the liposomes during the circulation till it reached the tumor site, and this diminished the repeated administration of drug and showed reduced clinical cardiotoxicity (Safra 2000; Hofheinz 2005). In addition, preclinical studies in mice revealed that the concentrations of paclitaxel in tumor for micelle formulation were higher than naked paclitaxel (Kim 2001).

Native ST1926 and its nanoparticle formulation will be further evaluated in AML xenografted animal models with an aim of providing enhanced bioavailability of the drug. Animal models have been used as the front line in predicting efficacy and finding toxicities for

cancer chemotherapeutic agents before reaching the clinic (Cheon 2011). In our study, we have successfully reproduced and optimized an AML xenografted mouse model using NOD-*scid* IL2 γ^{null} mice. We aim to assess the plasma retention time of ST1926 and its nanoparticle formulation *in vivo*. In addition, histological characteristics of the tumors, including volume, morphology, cell proliferation, apoptotic markers, and vascularization will be monitored over time before and during the treatment.

In conclusion, ST1926 was previously tested on several tumor models and has shown promising antitumor properties in hematological (Grattini 2004; Fratelli 2013; El Hajj 2014; Nasr 2015) and solid tumors (Zuco 2004; Di Francesco 2007; Milli 2011; Basma 2015). Our results show a great promise of the antitumor effect of ST1926 in ATRA-resistant AML cells, and deciphering its mechanism of action will help us understand how ST1926 is killing blast cells while sparing the normal ones. Additionally, we highlighted the use of ST1926 and its nanoparticle formulation as promising anticancer drug candidates for further preclinical investigation in AML therapy, where the AML xenografted mouse model was successfully reproduced and optimized.

Nonetheless, while the search for the “magic bullet” is irresistible, the heterogeneity of AML at the molecular and pathogenic level suggest that combination therapy may remain superior to any single agent. Cancer stem cells (CSCs) are the underlying factor of tumor relapse and metastasis (Clevers 2011). In particular, targeting AML leukemic stem cells (LSCs) is a pressing need which governs the development of future clinical trials. Whilst ST1926 may be initially targeting leukemic cells and eradicating them, some LSCs might be developing resistance to therapy, undergoing self-renewal, and eventually causing an aggressive disease

relapse (Ding 2012). LSCs are mostly quiescent in the G_0 phase of the cell cycle and are protected from apoptosis (Guzman 2001) they are, therefore, only minimally impacted by conventional chemotherapy that targets dividing cells (Pollyea 2014). In CML, it has been shown that treatment with ST1926 significantly prolonged the longevity and reduced tumor burden of primary CML mice, however it did not eradicate LSCs (Nasr 2015). Nevertheless, preliminary results from our lab have shown that ST1926 might be endowed with anti-CSCs properties in breast, prostate, and colon cancer models (unpublished data). The effect of ST1926 on LSCs in AML remains to be determined.

Finally, the heterogeneity of AML and LSCs presents formidable challenge in pre-clinical and clinical trials. One way to overcome drug resistance and disease relapse in AML is through combining several drugs that target different signaling pathways. These compounds might include inhibitors that target critical cellular signaling substrates specific to LSCs. The self-renewal properties of LSCs, which depend on the activation of pathways such as WNT/ β -catenin, NOTCH and Hedgehog, may represent such targets (Pollyea 2014). We propose to formulate ST1926 in combination with the indicated agents in nano carriers for enhanced drug efficacy and bioavailability in AML therapy.

REFERENCES

- Al Tanoury, Z., Piskunov, A., & Rochette-Egly, C. (2013). Vitamin A and retinoid signaling: genomic and nongenomic effects Thematic Review Series: Fat-Soluble Vitamins: Vitamin A. *Journal of Lipid Research*, *54*(7), 1761-1775.
- Alizadeh, F., Bolhassani, A., Khavari, A., Bathaie, S. Z., Naji, T., & Bidgoli, S. A. (2014). Retinoids and their biological effects against cancer. *International Immunopharmacology*, *18*(1), 43-49.
- Altucci, L., & Gronemeyer, H. (2001). The promise of retinoids to fight against cancer. *Nature Reviews Cancer*, *1*(3), 181-193.
- Arteaga, M. F., Mikesch, J. H., Qiu, J., Christensen, J., Helin, K., Kogan, S. C., ... & So, C. W. E. (2013). The histone demethylase PHF8 governs retinoic acid response in acute promyelocytic leukemia. *Cancer Cell*, *23*(3), 376-389.
- Asson-Batres, M. A., & Rochette-Egly, C. (Eds.). (2014). *The Biochemistry of Retinoic Acid Receptors I: Structure, Activation, and Function at the Molecular Level* (Vol. 70). Springer.
- Bain, B. J. (2010). *Leukaemia Diagnosis*. John Wiley & Sons.
- Barenholz, Y. C. (2012). Doxil®—the first FDA-approved nano-drug: lessons learned. *Journal of Controlled Release*, *160*(2), 117-134.
- Basavaraj, S., & Betageri, G. V. (2014). Can formulation and drug delivery reduce attrition during drug discovery and development—review of feasibility, benefits and challenges. *Acta Pharmaceutica Sinica B*, *4*(1), 3-17.
- Basma, H., Ghayad, S. E., Rammal, G., Mancinelli, A., Harajly, M., Ghamloush, F., ... & Saab, R. (2015). The synthetic retinoid ST1926 as a novel therapeutic agent in rhabdomyosarcoma. *International Journal of Cancer*. *In press*.
- Bennett JM, Catovsky D, Daniel MT, et al. Proposals for the classification of the acute leukaemias. French-American-British (FAB) co-operative group. *Br J Haematol* 1976;*33*(4):451-458.
- Bernasconi, E., Gaudio, E., Kwee, I., Rinaldi, A., Cascione, L., Tarantelli, C., ... & Bertoni, F. (2015). The novel atypical retinoid ST5589 down-regulates Aurora Kinase A and has anti-tumour activity in lymphoma pre-clinical models. *British Journal of Haematology*, *171*(3), 378-386.
- Brannon-Peppas, L., & Blanchette, J. O. (2012). Nanoparticle and targeted systems for cancer therapy. *Advanced Drug Delivery Reviews*, *64*, 206-212.

- Breitman, T. R., Selonick, S. E., & Collins, S. J. (1980). Induction of differentiation of the human promyelocytic leukemia cell line (HL-60) by retinoic acid. *Proceedings of the National Academy of Sciences*, 77(5), 2936-2940.
- Burnett, A. K., Hills, R. K., Milligan, D. W., Goldstone, A. H., Prentice, A. G., McMullin, M. F., ... & Wheatley, K. (2010). Attempts to optimize induction and consolidation treatment in acute myeloid leukemia: results of the MRC AML12 trial. *Journal of clinical Oncology*, 28(4), 586-595.
- Cassinat, B., & Chomienne, C. (2001, January). Future perspectives for acute promyelocytic leukemia therapy. In *Seminars in Hematology* (Vol. 38, No. 1, pp. 86-91). WB Saunders.
- Cassinat, B., Chevret, S., Zassadowski, F., Balitrand, N., Guillemot, I., Menot, M. L., ... & Chomienne, C. (2001). In vitro all-trans retinoic acid sensitivity of acute promyelocytic leukemia blasts: a novel indicator of poor patient outcome. *Blood*, 98(9), 2862-2864.
- Cassinat, B., Chevret, S., Zassadowski, F., Balitrand, N., Guillemot, I., Menot, M. L., ... & Chomienne, C. (2001). In vitro all-trans retinoic acid sensitivity of acute promyelocytic leukemia blasts: a novel indicator of poor patient outcome. *Blood*, 98(9), 2862-2864.
- Cheon, D. J., & Orsulic, S. (2011). Mouse models of cancer.
- Chow, G. M., & Noskova, N. I. (Eds.). (2012). *Nanostructured Materials: Science & Technology* (Vol. 50). Springer Science & Business Media.
- Cincinelli, R., Dallavalle, S., Merlini, L., Penco, S., Pisano, C., Carminati, P., ... & Zunino, F. (2003). A novel atypical retinoid endowed with proapoptotic and antitumor activity. *Journal of Medicinal Chemistry*, 46(6), 909-912.
- Clevers, H. (2011). The cancer stem cell: premises, promises and challenges. *Nature Medicine*, 313-319.
- Collins, S. J. (2002). The role of retinoids and retinoic acid receptors in normal hematopoiesis. *Leukemia*, 16(10), 1896-1905.
- Cooper, G. M. (1993). *The cancer book: a guide to understanding the causes, prevention, and treatment of cancer*. Jones & Bartlett Learning.
- Curry, S. H. (2008). Translational science: past, present, and future. *Biotechniques*, 44(2), 2-8.
- Danhier, F., Feron, O., & Pr at, V. (2010). To exploit the tumor microenvironment: passive and active tumor targeting of nanocarriers for anti-cancer drug delivery. *Journal of Controlled Release*, 148(2), 135-146.
- Darwiche, N., Abdel-Samad, R., Hmadi, R., El-Sabban, M., Muhtasib, H., & Pisano, C. (2014). 846: Antitumor activity of the synthetic retinoid ST1926 in colorectal cancer cells: involvement of DNA damage. *European Journal of Cancer*, (50), S206.

- Darwiche, N., Hatoum, A., Dbaibo, G., Kadara, H., Nasr, R., Abou-Lteif, G., ... & Bazarbachi, A. (2004). N-(4-hydroxyphenyl) retinamide induces growth arrest and apoptosis in HTLV-I-transformed cells. *Leukemia*, *18*(3), 607-615.
- Darwiche, N., Scita, G., Jones, C., Rutberg, S., Greenwald, E., Tennenbaum, T., ... & Yuspa, S. H. (1996). Loss of retinoic acid receptors in mouse skin and skin tumors is associated with activation of the rasHa oncogene and high risk for premalignant progression. *Cancer Research*, *56*(21), 4942-4949.
- Dawson, M. I., Chao, W. R., Hobbs, P. D., & Zhang, X. K. (1998). Effects of trans-retinoic acid, 9-cis-retinoic acid, 1 α , 25-(dihydroxy) vitamin D 3 and a novel apoptosis-inducing retinoid on breast cancer and endothelial cell growth. *Cancer Letters*, *133*(1), 1-8.
- Degos, L., & Wang, Z. Y. (2001). All trans retinoic acid in acute promyelocytic leukemia. *Oncogene*, *20*(49), 7140-7145.
- Desagher, S., & Martinou, J. C. (2000). Mitochondria as the central control point of apoptosis. *Trends in Cell Biology*, *10*(9), 369-377.
- DeSantis, C, Siegel, R., Bandi, P., and Jemal A. (2011). Breast cancer statistics 2011. *CA: A Cancer Journal for Clinicians* *61*, no. 6: 408-418
- Ding, L., Ley, T. J., Larson, D. E., Miller, C. A., Koboldt, D. C., Welch, J. S., ... & DiPersio, J. F. (2012). Clonal evolution in relapsed acute myeloid leukaemia revealed by whole-genome sequencing. *Nature*, *481*(7382), 506-510.
- Döhner, H., Weisdorf, D. J., & Bloomfield, C. D. (2015). Acute Myeloid Leukemia. *New England Journal of Medicine*, *373*(12), 1136-1152.
- Drexler, K. E., (1987). *Engines of Creation -The Coming Era of Nanotechnology*. Anchor, Reprint edition, New York.
- El Hajj, H., Khalil, B., Ghandour, B., Nasr, R., Shahine, S., Ghantous, A., ... & Darwiche, N. (2014). Preclinical efficacy of the synthetic retinoid ST1926 for treating adult T-cell leukemia/lymphoma. *Blood*, *124*(13), 2072-2080.
- Estey, E., & Döhner, H. (2006). Acute myeloid leukaemia. *The Lancet*, *368*(9550), 1894-1907.
- Fenaux, P., Chastang, C., Chevret, S., Sanz, M., Dombret, H., Archimbaud, E., ... & Degos, L. (1999). A randomized comparison of all transretinoic acid (ATRA) followed by chemotherapy and ATRA plus chemotherapy and the role of maintenance therapy in newly diagnosed acute promyelocytic leukemia. *Blood*, *94*(4), 1192-1200.

- Fenaux, P., Chomienne, C., & Degos, L. (2001, January). All-trans retinoic acid and chemotherapy in the treatment of acute promyelocytic leukemia. In *Seminars in hematology* (Vol. 38, No. 1, pp. 13-25). WB Saunders.
- Fenaux, P., Chomienne, C., & Degos, L. (2001, January). All-trans retinoic acid and chemotherapy in the treatment of acute promyelocytic leukemia. In *Seminars in hematology* (Vol. 38, No. 1, pp. 13-25). WB Saunders.
- Fernandez, H. F., Sun, Z., Yao, X., Litzow, M. R., Luger, S. M., Paietta, E. M., ... & Tallman, M. S. (2009). Anthracycline dose intensification in acute myeloid leukemia. *New England Journal of Medicine*, *361*(13), 1249-1259.
- Fontana, J. A., & Rishi, A. K. (2002). Classical and novel retinoids: their targets in cancer therapy. *Leukemia*, *16*(4), 463-472.
- Frankel, S. R., Eardley, A., Lauwers, G., Weiss, M., & Warrell, R. P. (1992). The retinoic acid syndrome in acute promyelocytic leukemia. *Annals of Internal Medicine*, *117*(4), 292-296. de The H. Altered retinoic acid receptors. *FASEB* *10*(9): 955-960,1996
- Fratelli, M., Fisher, J. N., Paroni, G., Di Francesco, A. M., Pierri, F., Pisano, C., ... & Garattini, E. (2013). New insights into the molecular mechanisms underlying sensitivity/resistance to the atypical retinoid ST1926 in acute myeloid leukaemia cells: The role of histone H2A, Z, cAMP-dependent protein kinase A and the proteasome. *European Journal of Cancer*, *49*(6), 1491-1500.
- Garattini, E., Gianni, M., & Terao, M. (2004). Retinoid related molecules an emerging class of apoptotic agents with promising therapeutic potential in oncology: pharmacological activity and mechanisms of action. *Current Pharmaceutical Design*, *10*(4), 433-448.
- Giannini, G., Brunetti, T., Battistuzzi, G., Alloatti, D., Quattrociochi, G., Cima, M. G., ... & Cabri, W. (2012). New retinoid derivatives as back-ups of Adarotene. *Bioorganic & Medicinal Chemistry*, *20*(7), 2405-2415.
- Glasow, A., Prodromou, N., Xu, K., von Lindern, M., & Zelent, A. (2005). Retinoids and myelomonocytic growth factors cooperatively activate RAR α and induce human myeloid leukemia cell differentiation via MAP kinase pathways. *Blood*, *105*(1), 341-349.
- Goodell, M. (2015). Introduction to a review series on hematopoietic stem cells. *Blood*, *125*(17), 2587-2587.
- Grimwade, D., Walker, H., Oliver, F., Wheatley, K., Harrison, C., Harrison, G., ... & Goldstone, A. (1998). The importance of diagnostic cytogenetics on outcome in AML: analysis of 1,612 patients entered into the MRC AML 10 trial. *Blood*, *92*(7), 2322-2333.
- Griseri, T., McKenzie, B. S., Schiering, C., & Powrie, F. (2012). Dysregulated hematopoietic stem and progenitor cell activity promotes interleukin-23-driven chronic intestinal inflammation. *Immunity*, *37*(6), 1116-1129.

- Gudas, L. J. (2012). Emerging roles for retinoids in regeneration and differentiation in normal and disease states. *Biochimica et Biophysica Acta (BBA)-Molecular and Cell Biology of Lipids*, 1821(1), 213-221.
- Guzman, M. L., Neering, S. J., Upchurch, D., Grimes, B., Howard, D. S., Rizzieri, D. A., ... & Jordan, C. T. (2001). Nuclear factor-kappaB is constitutively activated in primitive human acute myelogenous leukemia cells. *Blood-New York-*, 98(8), 2301-2307.
- Hanahan, D., & Weinberg, R. A. (2000). The hallmarks of cancer. *Cell*, 100(1), 57-70.
- Hanahan, D., & Weinberg, R. A. (2011). Hallmarks of cancer: the next generation. *Cell*, 144(5), 646-674.
- Hoffbrand, V., & Moss, P. (2011). *Essential Haematology* (Vol. 39). John Wiley & Sons.
- Hofheinz, R. D., Gnad-Vogt, S. U., Beyer, U., & Hochhaus, A. (2005). Liposomal encapsulated anti-cancer drugs. *Anti-Cancer Drugs*, 16(7), 691-707.
- Horton, S. J., & Huntly, B. J. (2012). Recent advances in acute myeloid leukemia stem cell biology. *Haematologica*, 97(7), 966-974.
- Huang, M. E., Ye, Y. C., & Zhao, L. (1987). Treatment of acute promyelocytic leukemia by retinoic acid with or without low dose cytosine arabinoside: report of 4 cases. *Zhonghua Nei Ke Za Zhi*, 26(6), 330.
- Huang, X., Cho, S., & Spangrude, G. J. (2007). Hematopoietic stem cells: generation and self-renewal. *Cell Death & Differentiation*, 14(11), 1851-1859.
- Jaffe, E. S. (Ed.). (2001). *Pathology and genetics of tumours of haematopoietic and lymphoid tissues* (Vol. 3). IARC.
- Kandeel, M. M., Refaat, H. M., Kassab, A. E., Shahin, I. G., & Abdelghany, T. M. (2015). Synthesis, anticancer activity and effects on cell cycle profile and apoptosis of novel thieno [2, 3-d] pyrimidine and thieno [3, 2-e] triazolo [4, 3-c] pyrimidine derivatives. *European Journal of Medicinal Chemistry*, 90, 620-632.
- Kerns, E. H. (2013). Pharmaceutical Profiling Case Study in Disruption. *ACS Medicinal Chemistry Letters*, 4(2), 150-152.
- Kim, S. C., Kim, D. W., Shim, Y. H., Bang, J. S., Oh, H. S., Kim, S. W., & Seo, M. H. (2001). In vivo evaluation of polymeric micellar paclitaxel formulation: toxicity and efficacy. *Journal of Controlled Release*, 72(1), 191-202.
- Lee, M. O., Han, S. Y., Jiang, S., Park, J. H., & Kim, S. J. (2000). Differential effects of retinoic acid on growth and apoptosis in human colon cancer cell lines associated with the induction of retinoic acid receptor β . *Biochemical Pharmacology*, 59(5), 485-496.

- Leroy, B., Anderson, M., & Soussi, T. (2014). TP53 mutations in human cancer: database reassessment and prospects for the next decade. *Human Mutation*, 35(6), 672-688.
- Levis, M., & Small, D. (2003). FLT3: ITDoes matter in leukemia. *Leukemia*, 17(9), 1738-1752.
- Lippman, S. M., & Lotan, R. (2000). Advances in the development of retinoids as chemopreventive agents. *The Journal of Nutrition*, 130(2), 479S-482S.
- Lo-Coco, F., Avvisati, G., Vignetti, M., Thiede, C., Orlando, S. M., Iacobelli, S., ... & Platzbecker, U. (2013). Retinoic acid and arsenic trioxide for acute promyelocytic leukemia. *New England Journal of Medicine*, 369(2), 111-121.
- Loftsson, T., & Brewster, M. E. (2010). Pharmaceutical applications of cyclodextrins: basic science and product development. *Journal of Pharmacy and Pharmacology*, 62(11), 1607-1621.
- Lowenberg, B., Downing, J. R., & Burnett, A. (1999). Acute myeloid leukemia. *New England Journal of Medicine*, 341(14), 1051-1062.
- Maeda, Y., Miyatake, J., Sono, H., Sumimoto, Y., Matsuda, M., Horiuchi, F., ... & Horiuchi, A. (1996). New therapeutic effects of retinoid for adult T-cell leukemia [letter]. *Blood*, 88(12), 4726-4727.
- Maeda, Y., Miyatake, J., Sono, H., Sumimoto, Y., Matsuda, M., Horiuchi, F., ... & Horiuchi, A. (1996). New therapeutic effects of retinoid for adult T-cell leukemia [letter]. *Blood*, 88(12), 4726-4727.
- Maeda, Y., Yamaguchi, T., Hijikata, Y., Tanaka, M., Hirase, C., Takai, S., ... & Kanamaru, A. (2008). Clinical efficacy of all-trans retinoic acid for treating adult T cell leukemia. *Journal of Cancer Research and Clinical Oncology*, 134(6), 673-677.
- Martens, J. H., & Stunnenberg, H. G. (2010). The molecular signature of oncofusion proteins in acute myeloid leukemia. *FEBS letters*, 584(12), 2662-2669.
- Martelli, M. P., Gionfriddo, I., Mezzasoma, F., Milano, F., Pierangeli, S., Mulas, F., ... & Vetro, C. (2015). Arsenic trioxide and all-trans retinoic acid target NPM1 mutant oncoprotein levels and induce apoptosis in NPM1-mutated AML cells. *Blood*, 125(22), 3455-3465.
- Mandelli, F., Vignetti, M., Suci, S., Stasi, R., Petti, M. C., Meloni, G., ... & de Witte, T. (2009). Daunorubicin versus mitoxantrone versus idarubicin as induction and consolidation chemotherapy for adults with acute myeloid leukemia: the EORTC and GIMEMA Groups Study AML-10. *Journal of Clinical Oncology*, 27(32), 5397-5403.
- McPherson, R. A., & Pincus, M. R. (2011). *Henry's clinical diagnosis and management by laboratory methods*. Elsevier Health Sciences.
- Milli, A., Perego, P., Beretta, G. L., Corvo, A., Righetti, P. G., Carenini, N., ... & Cecconi, D. (2010). Proteomic analysis of cellular response to novel proapoptotic agents related to atypical retinoids in human IGROV-1 ovarian carcinoma cells. *Journal of Proteome Research*, 10(3), 1191-1207.

- Miyatake, J. I., & Maeda, Y. (1997). Inhibition of proliferation and CD25 down-regulation by retinoic acid in human adult T cell leukemia cells. *Leukemia*, *11*(3), 401-407.
- Moore, A. S., Faisal, A., de Castro, D. G., Bavetsias, V., Sun, C., Atrash, B., ... & Linardopoulos, S. (2012). Selective FLT3 inhibition of FLT3-ITD+ acute myeloid leukaemia resulting in secondary D835Y mutation: a model for emerging clinical resistance patterns. *Leukemia*, *26*(7), 1462-1470.
- Muller, P. A., & Vousden, K. H. (2014). Mutant p53 in cancer: new functions and therapeutic opportunities. *Cancer Cell*, *25*(3), 304-317.
- Nakanishi, M., Tanaka, K., Shintani, T., Takahashi, T., & Kamada, N. (1999). Chromosomal instability in acute myelocytic leukemia and myelodysplastic syndrome patients among atomic bomb survivors. *Journal of Radiation Research*, *40*(2), 159-167
- Nasr, R., Guillemain, M. C., Ferhi, O., Soilihi, H., Peres, L., Berthier, C., ... & de Thé, H. (2008). Eradication of acute promyelocytic leukemia-initiating cells through PML-RARA degradation. *Nature Medicine*, *14*(12), 1333-1342.
- Nasr, R., Lallemand-Breitenbach, V., Zhu, J., & Guillemain, M. C. (2009). Therapy-induced PML/RARA proteolysis and acute promyelocytic leukemia cure. *Clinical Cancer Research*, *15*(20), 6321-6326.
- O'Donnell, M. R., Abboud, C. N., Altman, J., Appelbaum, F. R., Arber, D. A., Attar, E., ... & Gregory, K. M. (2012). Acute myeloid leukemia. *Journal of the National Comprehensive Cancer Network*, *10*(8), 984-1021.
- Parrella, E., Gianni, M., Fratelli, M., Barzago, M. M., Raska, I., Diomede, L., ... & Garattini, E. (2006). Antitumor activity of the retinoid-related molecules (E)-3-(4'-hydroxy-3'-adamantylbiphenyl-4-yl) acrylic acid (ST1926) and 6-[3-(1-adamantyl)-4-hydroxyphenyl]-2-naphthalene carboxylic acid (CD437) in F9 teratocarcinoma: role of retinoic acid receptor γ and retinoid-independent pathways. *Molecular Pharmacology*, *70*(3), 909-924.
- Pisano, C., Vesci, L., Fodera, R., Ferrara, F. F., Rossi, C., De Cesare, M., ... & Zunino, F. (2007). Antitumor activity of the combination of synthetic retinoid ST1926 and cisplatin in ovarian carcinoma models. *Annals of Oncology*, *18*(9), 1500-1505.
- Pollyea, D. A., Gutman, J. A., Gore, L., Smith, C. A., & Jordan, C. T. (2014). Targeting acute myeloid leukemia stem cells: a review and principles for the development of clinical trials. *Haematologica*, *99*(8), 1277-1284.
- Pustulka, K. M., Wohl, A. R., Lee, H. S., Michel, A. R., Han, J., Hoye, T. R., ... & Macosko, C. W. (2013). Flash nanoprecipitation: particle structure and stability. *Molecular Pharmaceutics*, *10*(11), 4367-4377.

- Robertson, K. A., Emami, B., & Collins, S. J. (1992). Retinoic acid-resistant HL-60R cells harbor a point mutation in the retinoic acid receptor ligand-binding domain that confers dominant negative activity. *Blood*, *80*(8), 1885-1889.
- Roco, M. C. (2007). National nanotechnology initiative-past, present, future. *Handbook on Nanoscience, Engineering and Technology*, *2*.
- Safra, T., Muggia, F., Jeffers, S., Tsao-Wei, D. D., Groshen, S., Lyass, O., ... & Gabizon, A. (2000). Pegylated liposomal doxorubicin (doxil): reduced clinical cardiotoxicity in patients reaching or exceeding cumulative doses of 500 mg/m². *Annals of Oncology*, *11*(8), 1029-1033.
- Sala, F., Zucchetti, M., Bagnati, R., D'Incalci, M., Pace, S., Capocasa, F., & Marangon, E. (2009). Development and validation of a liquid chromatography–tandem mass spectrometry method for the determination of ST1926, a novel oral antitumor agent, adamantyl retinoid derivative, in plasma of patients in a Phase I study. *Journal of Chromatography B*, *877*(27), 3118-3126.
- Sarkaria, J. N., Busby, E. C., Tibbetts, R. S., Roos, P., Taya, Y., Karnitz, L. M., & Abraham, R. T. (1999). Inhibition of ATM and ATR kinase activities by the radiosensitizing agent, caffeine. *Cancer Research*, *59*(17), 4375-4382.
- Schenk, T., Stengel, S., & Zelent, A. (2014). Unlocking the potential of retinoic acid in anticancer therapy. *British Journal of Cancer*, *111*(11), 2039-2045.
- Sharma, S., Kelly, T. K., & Jones, P. A. (2010). Epigenetics in cancer. *Carcinogenesis*, *31*(1), 27-36.
- Shen, J., Tai, Y. C., Zhou, J., Wong, C. H. S., Cheang, P. T. S., Wong, W. S. F., ... & Chen, C. S. (2007). Synergistic antileukemia effect of genistein and chemotherapy in mouse xenograft model and potential mechanism through MAPK signaling. *Experimental Hematology*, *35*(1), 75-e1.
- Siegel, R. L., Miller, K. D., & Jemal, A. (2015). Cancer Statistics, 2015. *CA: A Cancer Journal for Clinicians*, *65*(1), 5-29.
- Siegel, R., Ma, J., Zou, Z., & Jemal, A. (2014). Cancer statistics, 2014. *CA: A Cancer Journal for Clinicians*, *64*(1), 9-29.
- Slovak, M. L., Kopecky, K. J., Cassileth, P. A., Harrington, D. H., Theil, K. S., Mohamed, A., ... & Appelbaum, F. R. (2000). Karyotypic analysis predicts outcome of preremission and postremission therapy in adult acute myeloid leukemia: a Southwest Oncology Group/Eastern Cooperative Oncology Group Study. *Blood*, *96*(13), 4075-4083.
- Smith, C. (2003). Hematopoietic stem cells and hematopoiesis. *Cancer Control*, *10*(1), 9-16.
- Smith, D. A. (2015). A new phase of drug discovery? The rise of PK/PD means extremely challenging work at the coalface. *Bioanalysis*, *7*(12), 1415-1417.

- Smith, R. A., Manassaram-Baptiste, D., Brooks, D., Doroshenk, M., Fedewa, S., Saslow, D., ... & Wender, R. (2015). Cancer screening in the United States, 2015: a review of current American Cancer Society guidelines and current issues in cancer screening. *CA: A Cancer Journal for Clinicians*, 65(1), 30-54.
- Stirewalt, D. L., Kopecky, K. J., Meshinchi, S., Appelbaum, F. R., Slovak, M. L., Willman, C. L., & Radich, J. P. (2001). FLT3, RAS, and TP53 mutations in elderly patients with acute myeloid leukemia. *Blood*, 97(11), 3589-3595.
- Svenson, S., & Prud'homme, R. K. (2012). *Multifunctional nanoparticles for drug delivery applications: imaging, targeting, and delivery*. Springer Science & Business Media.
- Tang, X. H., & Gudas, L. J. (2011). Retinoids, retinoic acid receptors, and cancer. *Annual Review of Pathology: Mechanisms of Disease*, 6, 345-364.
- Torchilin, V. (2011). Tumor delivery of macromolecular drugs based on the EPR effect. *Advanced Drug Delivery Reviews*, 63(3), 131-135..
- Turinetto, V., & Giachino, C. (2015). Multiple facets of histone variant H2AX: a DNA double-strand-break marker with several biological functions. *Nucleic Acids Research*, gkv061.
- Valli, C., Paroni, G., Di Francesco, A. M., Riccardi, R., Tavecchio, M., Erba, E., ... & Garattini, E. (2008). Atypical retinoids ST1926 and CD437 are S-phase-specific agents causing DNA double-strand breaks: significance for the cytotoxic and antiproliferative activity. *Molecular Cancer Therapeutics*, 7(9), 2941-2954.
- Vardiman, J. W., Harris, N. L., & Brunning, R. D. (2002). The World Health Organization (WHO) classification of the myeloid neoplasms. *Blood*, 100(7), 2292-2302.
- Venditti, A., Buccisano, F., Del Poeta, G., Maurillo, L., Tamburini, A., Cox, C., ... & Amadori, S. (2000). Level of minimal residual disease after consolidation therapy predicts outcome in acute myeloid leukemia Presented in part at the 41st Annual Meeting of the American Society of Hematology, December 3-7, 1999, New Orleans, LA. *Blood*, 96(12), 3948-3952.
- Vogelstein, B., & Kinzler, K. W. (2004). Cancer genes and the pathways they control. *Nature Medicine*, 10(8), 789-799.
- Vogelstein, B., Papadopoulos, N., Velculescu, V. E., Zhou, S., Diaz, L. A., & Kinzler, K. W. (2013). Cancer genome landscapes. *Science*, 339(6127), 1546-1558.
- Walker, T. (2013). FDA approves late-stage pancreatic cancer injectable.
- Yokota, S., Kiyoi, H., Nakao, M., Iwai, T., Misawa, S., Okuda, T., ... & Naoe, T. (1997). Internal tandem duplication of the FLT3 gene is preferentially seen in acute myeloid leukemia and myelodysplastic syndrome among various hematological malignancies. A study on a large series of patients and cell lines. *Leukemia*, 11(10), 1605-1609.